To the Graduate Council:

I am submitting herewith a dissertation written by Zhensheng Chen entitled "Diagenesis of Upper Cambrian Mount Simon Sandstone in the Illinois Basin – Microscale Investigation of Basinal Fluid Migration and Mass Transfer." I have examined the final copy of this dissertation for form and content and recommend that it be accepted in partial fulfillment of the requirements for the degree of Doctor of Philosophy, with a major in Geology.

Claudia I. Mora, Major Professor

We have read this dissertation
and recommend its acceptance:

Lee R. Riciputi

Steven G. Driese

Michael E. Essington

Accepted for the Council:

Vice Provost and Dean of Graduate Studies

DIAGENESIS OF UPPER CAMBRIAN MOUNT SIMON SANDSTONE IN THE ILLINOIS BASIN – MICROSCALE INVESTIGATION OF BASINAL FLUID MIGRATION AND MASS TRANSFER

A Dissertation
Presented for the
Doctor of Philosophy
Degree
The University of Tennessee, Knoxville

Zhensheng Chen
December 2001

Acknowledgments

This research was sponsored by the Division of Chemical Sciences, Geosciences and Biosciences, Office of Basic Energy Science, U.S. Department of Energy, under contract DE-AC05-00OR22725 with Oak Ridge National Laboratory, managed by UT-Battelle, LLC, with supports from research funding to Dr. Lee R. Riciputi of Oak Ridge National Laboratory. Additional funding provided by Carden research funds to Dr. Claudia I. Mora from the University of Tennessee, a GSA Research Grant-in-Aid and a Sarif Scholarship to ZC.

I would like to express my gratitude to the Department of Geological Sciences, University of Tennessee for granting me graduate teaching and research assistantships. Special thanks go to Drs. Claudia I. Mora, Lee R. Riciputi, Steven G. Driese, and Michael E. Essington who served on my committee and generously offered me all the help I asked for. I am grateful to Drs. Mostafa Fayak and Otto Kopp, and Mr. Allen Patchen at UTK for their assistance in SIMS and CL analyses. Dr. Neil S. Fishman of the U.S. Geological Survey in Denver provided a series of Mount Simon Sandstone borehole samples and informative reviews of my manuscripts. Dr. Steven Driese provided outcrop samples of the Mount Simon Sandstone from Wisconsin. I thank Drs. Robert J. Bodnar at Virginia Polytechnic Institute, Lawrence A. Taylor at University of Tennessee, and Kip V. Hodges and William Olszewski in Massachusetts Institute of Technology for allowing me access to their analytical laboratories. I am grateful for constructive reviews of part of this dissertation by Drs. S. Diehl, M. Goldhaber, and M. Henry.

I would like to express my gratitude to all faculty members and graduate students in our department. For more than 1,500 days at UT, I have received countless help and all kinds of greetings from them.

Finally, I am grateful to my wife, Hanshen, for taking care of me through all these years at the University of Tennessee.

Abstract

A series of investigations were conducted to evaluate microscale evidence for basinal fluid migration in the Illinois basin during diagenesis of the Upper Cambrian Mount Simon Sandstone. Samples were examined using transmitted light and cathodoluminescence (CL) petrography, fluid inclusion analysis, and Secondary Ion Mass Spectrometry (SIMS) analysis of $^{18}O/^{16}O$ ratios and trace element compositions. Preliminary investigation of *in situ* laser ablation ^{40}Ar-^{39}Ar age dating techniques on authigenic K-feldspar overgrowths was also completed.

Two major generations of quartz overgrowths are observed, on the basis of transmitted light and CL petrography and fluid inclusion studies. High-resolution (100 μm x 100 μm), gray-scale images of CL in authigenic quartz overgrowths were acquired using the electron microprobe. Generation 1 quartz overgrowths have low intensity, medium- to dark- gray CL and are associated with fluid inclusion homogenization temperatures (T*h*) of 60 – 95 °C. Generation 2 quartz overgrowths have light-gray CL and are related to fluid inclusion T*h* of 100 – 145 °C. T*h* decreases from the southern part of the basin towards the north. Burial temperatures estimated by stratigraphic reconstruction and thermal history modeling did not exceed 60 - 90 °C, thus, passage of at least two generations of basinal fluid flow, at temperatures similar to or slightly elevated relative to burial temperature (T*h* = 60 – 145 °C) through the Mount Simon Sandstone are indicated. Salinities of these Na-Ca-K-Mg-Cl-H_2O fluids vary from 18 wt% to 25 wt% NaCl equivalent, suggesting that both diagenetic fluids were highly saline basinal brines.

Ion-microprobe oxygen isotope analyses of authigenic K-feldspar and quartz reveal a south-to-north-increasing trend in $\delta^{18}O$ values. Average K-feldspar $\delta^{18}O$ (V-

SMOW) values increase systematically from +14 ± 1‰ in the southernmost and deepest borehole samples from Illinois to +24 ± 2‰ in the northernmost outcrop samples in Wisconsin. A similar south-to-north trend was observed for quartz overgrowths (22 ± 2‰ to 28 ± 2‰). Within-sample $\delta^{18}O$ variations of up to 9‰ are much greater than analytical precision of the ion probe. This may be, in part, the result of sampling different generations of cements, as supported by CL and fluid inclusion studies in quartz. CL zones within quartz overgrowths were analyzed to evaluate $\delta^{18}O$ values in different generations of quartz cements. Generation 1 quartz cements have $\delta^{18}O$ values that are equal to (within analytical precision) or greater than (up to 6.8‰ difference) generation 2 quartz cements. Overall, however, generation 1 cements are isotopically-enriched relative to generation 2 cements. Constraints on fluid compositions using fluid-inclusion temperatures that were point-matched to $\delta^{18}O$ values of quartz overgrowths containing these fluid inclusions reveal two distinct diagenetic fluids, corresponding to generation 1 ($T < 95$ °C) and generation 2 ($T > 95$ °C) fluids. The $\delta^{18}O$ values of generation 1 fluid are about -5‰ in the southern portion of the basin and increase to ~ 0‰ in the northern part of the basin; $\delta^{18}O$ values of generation 2 fluid increases from ~ +2‰ in the south to ~ +7‰ in the north. For the generation 1 diagenetic event ($T < 95$ °C), fluid temperatures are consistent with burial temperatures in the deeper part of the southern basin, where the fluid may have originated. Fluid temperatures in the northern part of the basin are lower than in the southern basin, but still higher than burial temperatures.

Ion-microprobe studies of authigenic K-feldspar and quartz reveal that Rb, Sr, Ba, Pb, Fe, Mg, B, Ti, and Cl are present in trace amounts in authigenic K-feldspar. In quartz cements, K, Al, Fe, B, Ti, Mg, and Cl were detected. Strongly covariant relationships among Sr-Ba-Pb-Rb, Na-Mg-Ca-Cl, and K-Al in authigenic cements were attributed to their similar geochemical behaviors and incorporation modes, continuous chemical changes in the fluid during migration and cement precipitation, and the requirements of solid solution charge compensation. Concentrations of Ba, Sr, Rb,Pb, Fe, Ca, and Ce in diagenetic fluids were estimated on the basis of trace element contents in authigenic K-feldspar and distribution coefficients between sanidine and hydrothermal fluids. No correlation between fluid compositions and positions in the basin (south to north) is apparent. Total K+Na+Li+Mg+Ca concentrations are significantly higher in generation 2 quartz cement, compared to generation 1 cements; B and K are both notably enriched in generation 2. These differences suggest that later brines had a different composition. The lack of regional trends indicates more local control of the physiochemical environment on trace element concentrations in authigenic minerals, compared to their oxygen isotope or fluid inclusion compositions.

Preliminary trials of *in situ* UV-laser probe $^{40}Ar/^{39}Ar$ dating of authigenic K-feldspar cements were largely unsuccessful in releasing Ar gas out of the overgrowths; rather, the UV-laser mostly shattered the grains, without melting them. Ar-laser step heating tests on areas ~ 50 x 50 μm in size released gas from both detrital and authigenic K-feldspar. An overwhelming amount of atmospheric air was also released from the ceramic adhesive, resulting in very large analytical errors related to air-compound

corrections. Procedures need to be taken to reduce air in the ceramic adhesive during thin section preparation, if this ceramic is used to substitute for epoxies..

This study demonstrates that *in situ* microscale ion probe analytical techniques have significant advantages over conventional analysis in obtaining oxygen isotope compositions and trace-element concentrations from very fine-grained authigenic minerals. High-resolution ion probe analysis, in concert with detailed CL petrography and fluid inclusion studies, may provide valuable geochemical constraints on low-temperature diagenesis and basinal fluid migration, revealing multiple events, regional flow directions, fluid compositions, and temperatures and possible fluid sources.

Table of Contents

List of Tables

List of Figures

Chapter 1

Introduction

Working Hypothesis and Objectives

There has been a long-standing hypothesis that regional-scale, basinal fluid flow in the Illinois basin resulted in mass transport of materials to the basin margin, where mineral and petroleum natural resources formed (*e.g.*, Garven and Freeze, 1984; Bethke et al., 1990; Rowan and Goldhaber, 1995; Pitman and Spötl, 1996; Fishman, 1997). Earlier studies have developed a basic understanding of the diagenetic history of the Mount Simon Sandstone in the Illinois basin and its periphery, including information on the burial history, temperature, fluid origin and evolution, fluid flow pattern and its relations with MVT deposits (*e.g.*, Hoholick et al., 1984; Bethke, 1986; Goldhaber, et al., 1990; Byrnes and Wilson, 1992; Fishman, 1997). Fishman (1997) postulated the regional migration of relatively high temperature diagenetic fluids through the Mount Simon Sandstone, leading to the formation of widespread authigenic K-feldspar and quartz cements. Large-scale mass transfers accompanying the regional migration of basinal fluids in paleoaquifers like the Mount Simon Sandstone may have left behind significant geochemical signatures in these authigenic minerals. However, very few isotopic and trace-element data are reported for authigenic cements, apart from bulk mineral or bulk rock analyses that also include detrital material (Harper et al., 1995). Acquisition of such data may significantly improve constraints on the characteristics of diagenetic fluids, and thus help elucidate the diagenetic and fluid flow history of the basin.

Characterization of the isotopic and trace element chemistry of authigenic minerals, without contamination by detrital phases, is challenging. Mechanical

separation of detrital and authigenic phases has proven tedious, and mostly incomplete (Lee and Savin, 1985; Girard and Deynoux, 1991; Girard and Onstott, 1991; Hay et al., 1992, 1993). In order to characterize the widespread authigenic K-feldspar and quartz cements in the Mount Simon Sandstone, microscale, *in situ* analytical techniques were applied to twenty-seven samples collected through the Illinois basin, in borehole and outcrop. The techniques applied in this study include *in situ* Secondary Ion Mass Spectrometry (SIMS) analysis of oxygen isotopes and trace elements, high resolution, gray-scale imaging of cathodoluminescence (CL) using the electron microprobe, fluid inclusion microthermometry, and *in situ* UV laser $^{40}Ar/^{39}Ar$ age dating.

The principle objective of this research is to evaluate Fishman's (1997) hypothesis that high temperature, regional fluid migrations in the basin were responsible for the formation of widespread authigenic K-feldspar. In particular, this dissertation addresses four major problems:

(1) Characterization of temperature and composition of different generations of diagenetic fluids based on fluid inclusion, CL, and oxygen isotope studies of authigenic K-feldspar and quartz. Possible connections of regional fluid events with Mississippi Valley type (MVT) mineralization around the periphery of the basin are considered;

(2) Characterization of basinal fluid migrations, on the basis of regional oxygen isotope variations of authigenic minerals. These studies considered the temperature and composition of diagenetic minerals and fluid flow direction;

(3) Constraints on mass transfer in the Illinois basin in association with basinal fluid migrations, on the basis of trace element studies; and

(4) Refinement of diagenetic age information on K-feldspar cements in the Mount Simon Sandstone to better constrain the timing of potassic diagenesis in the U.S. Midcontinent, based on *in situ*, laser $^{40}Ar/^{39}Ar$ dating of authigenic K-feldspar.

Geologic Setting

Illinois Basin

The Illinois basin covers part of the states of Illinois, Indiana, Kentucky and Tennessee in the U.S. mid-continental region (Fig. 1-1), with an area of ~155,000 km^2 (Buschbach and Kolata, 1990). The basin is bounded to the west by the Mississippi River arch and the Ozark dome, to the east by the Cincinnati arch, to the northeast by the Kankakee arch, and to the south by the Pascola arch (Buschbach and Kolata, 1990; Fishman, 1997; Pitman et al., 1997).

The basin contains about 450,000 km^3 of Cambrian through Permian sedimentary rocks, including marine carbonates (> 50%), sandstone (25%), some shale, siltstone, chert and minor amounts of anhydrite (Buschbach and Kolata, 1990). The deepest part of the basin is in western Kentucky, where >7,000 m of sedimentary rocks are preserved (Pitman et al. 1997).

The origin of intracratonic basins is not clearly known. Numerous mechanisms have been suggested, including thermal contraction after intrusion, sediment loading, isostatic subsidence, and horizontally transmitted tectonic stress (Quinlan, 1987; Sloss, 1988; Bally, 1989; Kolata and Nelson, 1990). The Illinois basin was probably related to the development of a failed rift, the Reelfoot rift and Rough Creek graben, during the breakup of a supercontinent in Early and Middle Cambrian time (Braile et al., 1984;

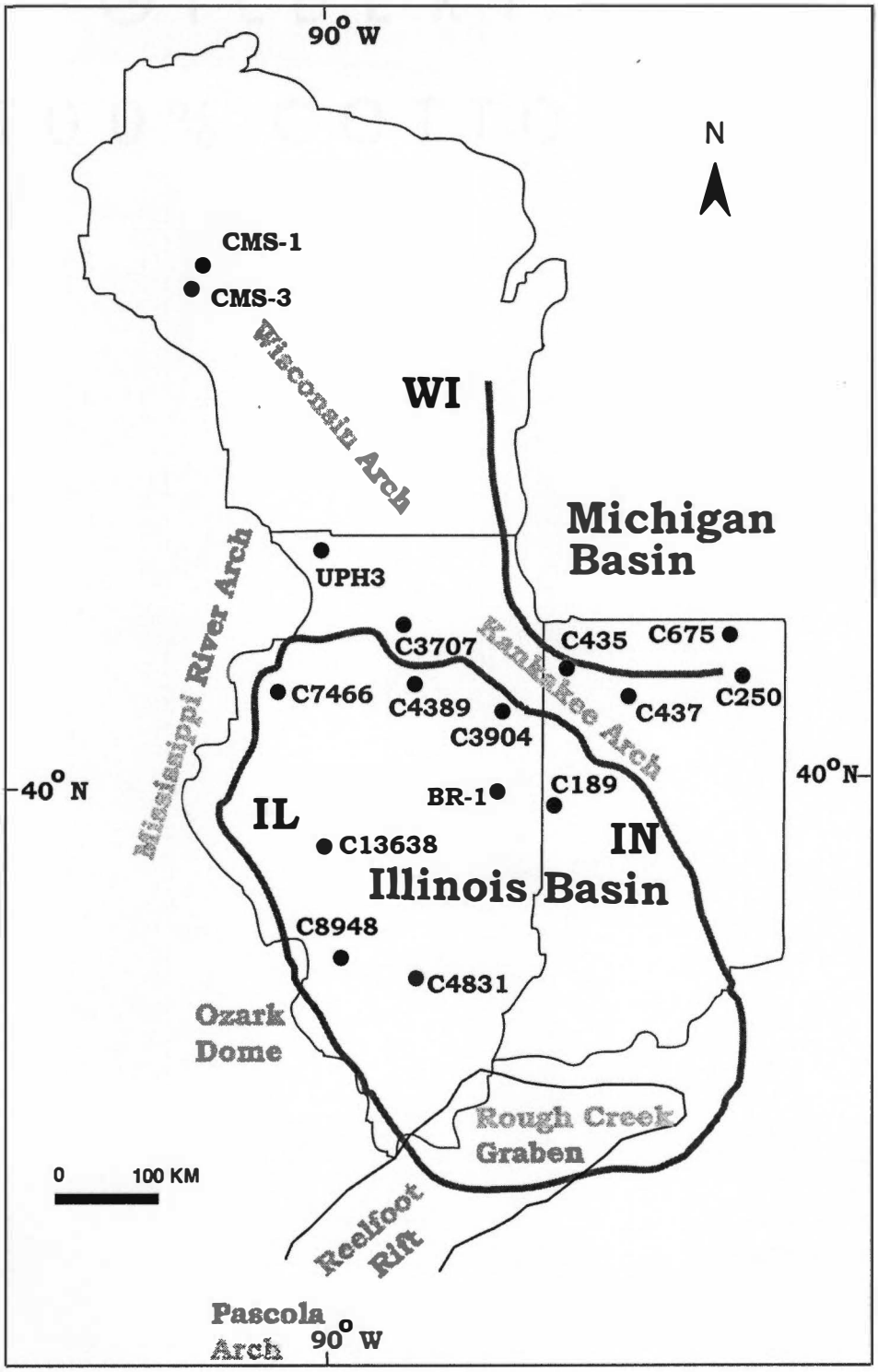

Figure 1-1 Map showing an outline of the Illinois basin and surrounding area, and core locations for samples analyzed in this study.

Leighton and Kolata, 1990). There is seismic reflection evidence of lava flows and pyroclastic units interbedded with Cambrian sedimentary rocks at the base of the rift complex (Buschbach and Kolata, 1990). Beginning in the Late Cambrian, broad regional downwarping began in the rift complex and adjacent cratonic areas, probably initiated by thermal subsidence and, subsequently, by isostatic subsidence (Leighton, 1990). Breakup of the Pangean supercontinent reactivated the rift complex at the end of the Paleozoic, followed by another round of subsidence and sedimentation in the basin (Buschbach and Kolata, 1990).

Through most of the Paleozoic, the southern end of the Illinois basin was connected to the Arkoma and BlackWarrior basins. The Late Paleozoic Ouachita and Alleghenian orogenies caused uplift of the Pascola arch, resulting in structural closure of the basin in the south (Leighton, 1990).

Mount Simon Sandstone

In the Illinois basin, the Late Cambrian Mount Simon Sandstone unconformably overlies Precambrian igneous and metamorphic basement rocks, and is overlain by the Upper Cambrian Eau Claire Formation, Knox Supergroup, and Middle Ordovician St. Peter Sandstone (Nesbitt, 1980; Driese et al., 1981; Hoholick et al., 1984; Bear, 1997; Fishman, 1997). The Mount Simon Sandstone was deposited throughout much of the Illinois basin. It is a very inhomogeneous sandstone formation, composed of yellow to white, fine- to coarse-grained arkose, subarkose, and quartzarenite (Driese et al., 1981; Hololick et al., 1984; Duffin et al., 1989). The majority of sediments were deposited in tidal-flat and shallow-marine subtidal environments (Driese et al., 1981; Fishman, 1997;

Pitman et al., 1997). The source of siliciclastics was dominantly the Precambrian shield area to the north of the intracratonic basin (Buschbach and Kolata, 1990). The Mount Simon Sandstone is a relatively thick body, typically close to a hundred meters thick, but reaching up to 790 m thick in northeastern Illinois (Hoholick et al., 1984; Fishman, 1997). The Mount Simon and St. Peter Sandstones are thought to have been important conduits through which paleofluids have migrated (Fishman, 1997).

Previous Studies of Diagenesis of the Mount Simon Sandstone

Diagenetic processes typically occur when sediments undergo physicochemical changes at temperatures below 200 ~ 300 °C, before metamorphism begins (Singer and Muller, 1979), and can extend to a depth of about 10,000 m in basin areas with a normal geothermal gradient (~ 30 °C/km). Diagenesis may begin very early in the burial history and continues during burial compaction, when primary porosity decreases with increasing sediment load (Pettijohn et al., 1987; Houseknecht; 1991). Chemical reactions between pore fluids and sediments leading to dissolution of detrital grains and precipitation of authigenic minerals are among the most important processes that affect the physiochemical properties of sedimentary rocks.

The Illinois basin is a classic study area for investigation of sedimentary-rock diagenesis and basin-scale fluid flow. Previous studies, summarized in the following sections, include investigations of porosity changes, burial reconstruction and thermal history modeling of the Mount Simon Sandstone, petrographic timing of potassic diagenetic events, and numerical modeling of the paleohydrogeology of the Illinois basin.

Porosity Change of the Mount Simon Sandstone

Primary pore space in quartzose and carbonate sands in the Illinois basin is generally > 35% (Pryor, 1972; Fishman, 1997). Porosity of the Mount Simon Sandstone in outcrop samples from Wisconsin can reach ~ 40% (this study). Previous studies of the Mount Simon Sandstone show that rock porosity in the subsurface can reach 18% at 5,000 ft (1524 m) and drops sharply to ~ 8% below 1,500 m and to <1% below 4,500 m (Hoholick et al., 1984; Cottingham, 1990). It is estimated that most of the porosity currently observed in the Mount Simon Sandstone is a result of dissolution of authigenic cements (Fishman, 1997). A decrease in porosity by compaction and cementation may directly affect permeability, consequently affecting the fluid flow rates of diagenetic fluids.

Burial History of the Mount Simon Sandstone

Burial reconstruction and thermal history modeling of the Mount Simon Sandstone in the Illinois basin indicate that from Late Cambrian time through most of the Paleozoic, the Mount Simon Sandstone was buried to increasingly greater depths (Fig. 1-2, Fishman, 1997). After peak burial, which occurred approximately between 275 and 325 Ma (Fig. 1-2), the basin was uplifted slowly until the Late Cretaceous, when it reached a level similar to present day (Fig. 1-2). Since then, the depth of burial has remained relatively unchanged. In general, the Mount Simon Sandstone was buried deeper in the southern and central part of the Illinois basin than in the northern part (Fishman, 1997). Potassic diagenesis leading to precipitation of K-feldspar cements occurred at ~ 400 Ma (Duffin et al., 1989); the timing of diagenesis is discussed in a later

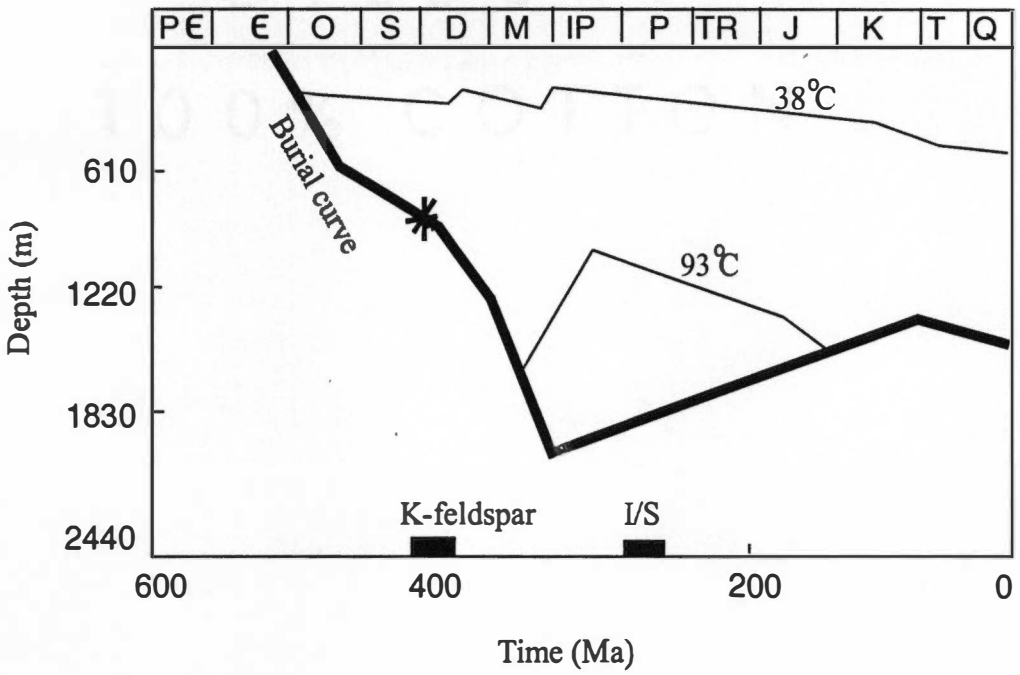

Figure 1-2 Burial history curve (bold line) of the Mount Simon Sandstone in central Illinois (between the locality of borehole C4389 and C13638, Fig. 1-1) compared to regional isotherms (light line) (from Fishman,1997). The ages of potassic diagenetic events precipitating K-feldsparand illite/smectite (I/S) are shown; see references in text.

section. Based on this burial curve and similar curve derived for a deeper portions of the basin (Fishman, 1997), diagenetic temperatures due solely to burial should be less than 90 °C in the south and 60 °C in the north (Fishman, 1997). At peak burial, burial temperatures in the deepest portions of the basin did not exceed 100 °C - 150 °C, and were significantly lower in the northern portion and periphery of the basin. Based on homogenization temperatures (100 – 130 °C) of fluid inclusions in authigenic quartz (Fishman, 1997), diagenetic temperatures of the Mount Simon Sandstone were much higher than concurrent burial geogradient temperatures (Fig. 1-2), suggesting migration of superheated fluids through the Mount Simon Sandstone. Similar implications were derived from studies of St. Peter Sandstone in the Illinois and Michigan basins (Girard and Barnes, 1995; Pitman et al., 1997). The source and driving mechanisms for these fluids are uncertain, and form a primary objective of this study.

Authigenic Minerals in the Mount Simon Sandstone

Cements in the Mount Simon Sandstone include K-feldspar and quartz overgrowths, some iron oxide (hematite), sericite, kaolinite, interstratified illite/smectite (I/S), chlorite, carbonates, and minor pyrite, anhydrite, fluorite and barite (Hoholick et al., 1984; Duffin et al., 1989; Fishman, 1997). Duffin et al. (1989) described the paragenetic sequence for major authigenic minerals in the Mount Simon Sandstone. K-feldspar (and chlorite) formed first, closely followed by quartz overgrowths, sericite, and possibly a second generation of quartz overgrowths. Fishman (1997) developed a detailed diagenetic mineral paragenesis for the Mount Simon Sandstone (Fig. 1-3). The relative precipitated sequence for major diagenetic minerals is, from early to late, (1) iron-oxides,

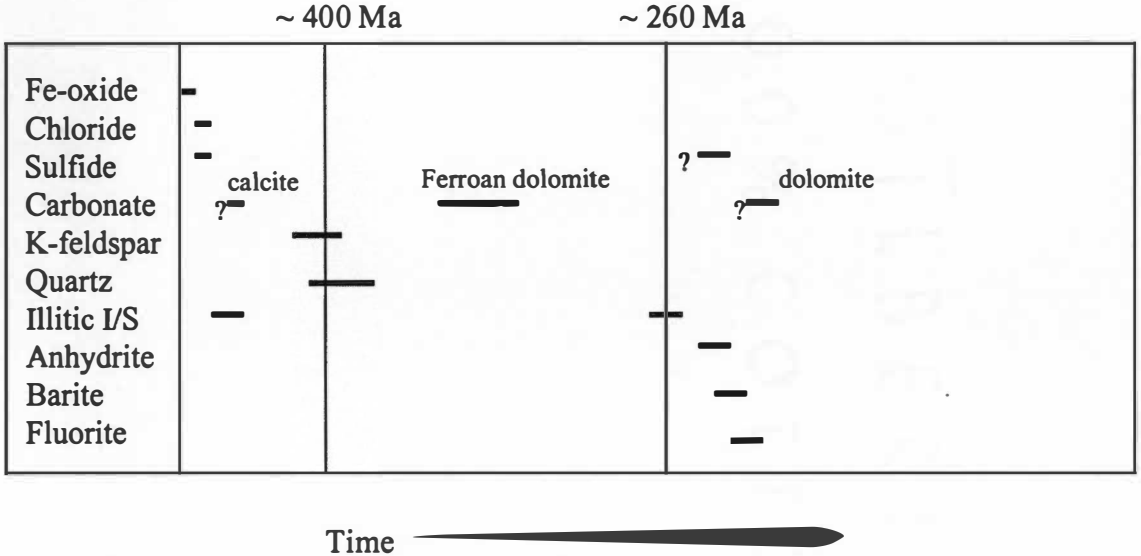

Figure 1-3 Diagram showing relative timing of alterations in the Mount Simon Sandstone (from Fishman, 1997).

(2) clay minerals, including chlorite and mixed layer illite/smectite (I/S), (3) potassium feldspar, (4) quartz, (5) dolomite, and (6) I/S. Ferric oxide and clay minerals generally appear as grain coatings; I/S of a later generation appears as both grain coatings and void fillings; carbonate is generally minor and occurs as a poikilotopic texture cementing K-feldspar and quartz grains (Duffin et al., 1989; Byrnes and Wilson, 1992; Fishman, 1997). The paragenetic sequence in the Mount Simon Sandstone is similar to the diagenetic alteration sequence of the underlying Precambrian rocks at the Precambrian-Cambrian boundary in southwestern Ontario (Harper et al., 1995). Duffin et al. (1989) suggested that alteration minerals in the near-boundary basement rocks formed during the same episode as in the Mount Simon Sandstone.

Authigenic K-feldspar comprises up to 7% by volume of the Mount Simon Sandstone (Duffin et al., 1989; Fishman, 1997). The volume of authigenic K-feldspar varies significantly over small vertical distances (Fishman, 1997). In some fine-grained, outcrop samples from Wisconsin examined in this study, K-feldspar overgrowths comprise up to 12% in rocks, with abundant detrital K-feldspar grains also present. Authigenic K-feldspar cements appear most typically as overgrowths < 40 μm in thickness on detrital K-feldspar grains. Some authigenic feldspar forms cement on detrital quartz grains (Duffin et al., 1989), indicating that authigenic K-feldspar was precipitated from Al-Si enriched solution, rather than as a replacement of detrital feldspar. Mineral inclusions of clays and oxides and minute fluid inclusions are abundant at the boundaries between detrital grains and overgrowths.

Authigenic quartz is the most abundant cement in the Mount Simon Sandstone and may reach up to 23% with an average volumetric abundance of ~ 12% (Duffin et al.

1989; Fishman 1997). Authigenic quartz overgrowths are generally thicker than K-feldspar overgrowths and occur as syntaxial overgrowths of tens of micrometers in thickness. Similarly to authigenic K-feldspar, the volume of diagenetic quartz may change significantly over small distance. Quartz and K-feldspar overgrowths are approximately coeval, based on paragenetic relationships, determined petrographically (Fishman, 1997). Based on SEM studies, Fishman (1997) suggested that some quartz overgrowths reflect multiple episodes of precipitation. Crosscutting textures in the uppermost Precambrian altered rocks indicate that quartz continued to form after the main stage of K-feldspar development (Harper et al. 1995).

Timing of Diagenesis

Potassium enrichment during diagenesis is a widespread phenomenon throughout Lower Paleozoic sediments of North American interior. Cambrian and Ordovician rocks in the Midcontinent, Appalachian region, and Mississippi Valley region are rich in authigenic K-feldspar and illite (Buyce and Friedman, 1975; Odom et al., 1979; Hearn and Sutter, 1985; Elliott and Aronson, 1987; Hay et al., 1988; Duffin et al., 1989; Bethke and Marshak, 1990; Aleinikoff et al., 1993; Diehl and Goldhaber, 1995; Harper et al., 1995).

Previous studies report on the ages of authigenic minerals in the Mount Simon Sandstone. Duffin et al. (1989) report dates from a sample which did not contain detrital feldspar. The 2 – 74 μm whole rock fraction yielded a K-Ar age of 395 ± 6 Ma. Different size fractions (< 0.2μm, <1.0μm, and 0.2 – 2μm) of I/S from sample areas rich in authigenic K-feldspar or I/S yield K-Ar ages of 214 – 271 ± 5 Ma (Duffin et al., 1989),

with slightly younger ages in the smaller-size fractions. Hay et al. (1992; 1993) reported K-Ar, $^{40}Ar/^{39}Ar$, Rb-Sr, and K-Ca ages of 375 ~ 448 Ma for authigenic K-feldspar from veins present in the alteration profile at the Precambrian-Cambrian unconformity, from a diabase replaced by K-feldspar, and from a tuff consisting of >85% authigenic K-feldspar. Replacement K-feldspar and K-feldspar from fracture fillings at the Precambrian-Cambrian boundary in southwestern Ontario yielded K-Ar ages of 412 – 453 Ma and Rb-Sr model ages of 394 – 482 Ma (mostly 431 – 454 Ma) (Harper et al., 1995). K-Ar ages of authigenic illite from St. Peter Sandstone in Michigan basin range from 322 Ma to 367 Ma (Girard and Barnes, 1995). As can be seen, the timing of diagenesis is poorly constrained, owing mostly to the difficulty of obtaining clean authigenic mineral separates for dating. Most data suggest two potassic events, a K-feldspar forming event at ~ 400 Ma and an I/S forming event at ~270 Ma.

Geochemistry of Authigenic Minerals

It has been long recognized that low-temperature authigenic K-feldspars are rather pure in terms of their chemical compositions (Kastner and Siever, 1979; Wadleigh et al., 1990; Spötl et al., 1996). Electron microprobe analyses reveal that authigenic K-feldspars from the Mount Simon Sandstone in the Illinois basin and from the Precambrian-Cambrian boundary profile in southwestern Ontario have near end-member orthoclase compositions, with minor (mostly < 0.1%) to non-detectable amounts of Na, Ca, Ba, Fe and Sr (this study; Duffin et al., 1989; Wadleigh et al., 1990; Harper et al., 1995).

Numerous studies of the oxygen isotope compositions of authigenic minerals in

Paleozoic sandstone aquifers and samples at the Precambrian-Cambrian boundary have been performed. Oxygen isotope compositions of K-feldspar from the Precambrian-Cambrian unconformity in western Wisconsin and Missouri range from 19.8 to 22.2‰, with an average value of 21.4‰ (Hay et al., 1992). Replacement K-feldspar from the Precambrian-Cambrian boundary unconformity in southwestern Ontario has $\delta^{18}O$ values ranging from 15.4 to 21.4‰ (Harper et al., 1995). These values were obtained from K-feldspar mineral separates and analyzed by conventional techniques; no attempt has made to separate the authigenic materials. Thus, they may contain a component of detrital K-feldspar or clay minerals, in addition to authigenic K-feldspar.

Reported $\delta^{18}O$ values of authigenic quartz from the Precambrian – Cambrian boundary in southwestern Ontario vary from 19.2 to 23.1‰ (Harper et al., 1995). Ion microprobe analyses of authigenic quartz in the St. Peter Sandstone from the Wisconsin arch and Michigan basin reveal $\delta^{18}O$ values ranging from 15 to 32‰ (Girard and Barnes, 1995; Graham et al., 1996). Sericites in the Mount Simon Sandstone and the basement rocks have $\delta^{18}O$ values ranging from 17.7 to 18.9‰ (Duffin et al., 1989). $\delta^{18}O$ values of illite from the St. Peter Sandstone range from 12.7 to 16.9‰ (Girard and Barnes, 1995). The large variations in these data may arise from mixtures of authigenic and detrital phases or reflect multiple generations of authigenic cements and a complex diagenetic history.

Diagenetic Fluids

Previous fluid-inclusion studies suggest that authigenic quartz and K-feldspar in the Mount Simon Sandstone were precipitated from relatively high temperature (100 –

130 °C), saline (salinity > 20 wt% NaCl equivalent) brines (Fishman, 1997). The hot brines probably originated deeper in the basin (Spirakis, 1995; Fishman, 1997). There is no evidence, such as significant variations in fluid salinity, for mixing of meteoric water with hot brines. Fluid temperatures from authigenic quartz in the overlying St. Peter Sandstone may reach up to 170 °C (70 – 170 °C), with fluid salinities of 15 – 20 wt% NaCl equivalent (Girard and Barnes, 1995; Pitman et al., 1997). Homogenization temperatures of fluid inclusions from authigenic quartz in the Precambrian – Cambrian boundary in southwestern Ontario are 65 – 115 °C, with an average of 101 °C (Harper et al., 1995). In all cases, these temperatures greatly exceed those estimated from burial history, suggesting the migration of hot brines through the rocks (Harper et al., 1995; Fishman, 1997).

Basinal Fluid Migration

Bethke and Marshak (1990) discussed the relationship between the long-range brine migration and diagenesis in the Midcontinent. Their calculations predict precipitation of authigenic K-feldspar and dolomite at the expense of quartz, calcite, and muscovite. The estimated high water-rock ratio (> 100 by volume) supports the hypothesis of large quantities of migrating brines in the Midcontinent. Oliver (1986) suggested that long-range migration of crustal fluids is a general phenomenon, occurring especially during periods of tectonic deformation along the plate margins. A number of models, summarized below, have been proposed to explain fluid migration in the Illinois basin. These include (1) compaction-driven flow, (2) topography-driven flow, (3) seismic-pumping, and (4) density-driven flow (e.g., Garven and Freeze, 1984; Bethke,

1985, 1986; Oliver, 1986; Clendenin and Duane, 1990; Sverjensky and Garven, 1992; Person and Garven, 1994; Bachu, 1995). These models provide a framework for evaluating the results of this study.

Flows driven by sediment compaction – Primary depositional pore space in quartzose and carbonate sands in the Illinois basin is estimated to have ranged from 40% to 60%, whereas typical sandstone and limestone reservoirs have porosities ranging from 8% to 20%, and averaging ~ 16% (Pryor, 1972). Loss of primary porosity begins contemporaneously with deposition. Compaction and grain rotation contribute to the reduction of primary pore space, generally during early burial stages (Houseknecht, 1991). Fluid flow generated by subsidence and compaction is either small in volume or short-lived (Sverjensky and Garven, 1992). The flow rate (V) due to compaction and small excess pressures is proportional to sedimentation rate (R) with a correlation of V = 0.5R (Deming, 1994). Modeling results of sediment compaction in the Illinois basin indicate a flow system characterized by slow fluid velocities ($< 2.4 \times 10^{-3}$ meters/year) and pore pressures that remained near hydrostatic (Bethke et al., 1990). Compaction-related flow velocities resulting from the slow subsidence of the Illinois basin would be slow compared to flow in overpressured basins, such as the Gulf of Mexico, where deposition and subsidence rates are high. Compaction overpressures probably did not develop in the Illinois basin because of the low burial rate, low shale content (< 10%), and widespread sandstone aquifers in the basin (Bethke et al., 1990).

Flow driven by tectonic compression – Oliver (1986) proposed that tectonic compression could be the driving force of basinal fluid flow ("squeegee tectonics"), with pore waters expelled from deep strata during orogenesis migrating to the shallow basin

margin. Other researchers have argued that the flow rate associated with orogenesis would be very low (< 0.1meters/year) because of the slow deformation rate (Bethke and Marshak, 1990; Sverjensky and Garven, 1992). Concentrated or preferential flow within aquifers, such as the Mount Simon Sandstone, may increase the flow rate significantly (Bethke and Marshak, 1990).

Flow driven by gravity or topographic relief – Basin-wide, saline fluid migration in response to raised topography is proposed to be related to the widespread formation of Mississippi Valley-type (MVT) deposits along the margins of many Mindcontinent basins (Garven and Freeze, 1984; Sverjensky and Garven, 1992). Bethke et al. (1990) and Bethke and Marshak (1990) attributed large-scale Mesozoic brine migrations in the Illinois basin to uplift (the late Paleozoic Alleghenian-Ouachita orogeny) along the southern basin margin. Tectonic uplift in the southern part of the Illinois basin during the Mesozoic may have caused lateral migration of basinal fluid. Topographic relief is estimated to have driven fluids at rates of about 1-2 meters/year through the deep aquifer complex in Cambrian and Ordovician strata (Bethke et al., 1990), several orders of magnitude more rapidly than those predicted for compaction driven flow (< 2.4×10^{-3} meters/year). Spirakis (1995) pointed out that topography-driven flow might not completely account for the relatively high fluid temperatures related to the precipitation of MVT deposits (60 – 190 °C).

Flow driven by seismic activity – Seismic activity may generate fluid flow along regional faults (Clendenin and Duane, 1990; Sverjensky and Garven, 1992; Clendenin et al., 1994). Activation of major, regional faults, connected to secondary fault networks, provides channels for movement of the reactive, focused fluids. There is a possible

correlation between the New Madrid seismic zone and the moderate seismicity of the southern Illinois basin (McBride, 1998). Seismic pumping may have triggered some local-scale and preferential flow along the faults, however, widespread and pervasive geochemical and thermal alteration in several Midcontinent basins is difficult to explain solely by seismic pumping (Sverjensky and Garven, 1992).

Flow driven by density gradients in the formation fluid – Buoyancy differences related to significant variations in formation water density are expected to drive limited-scale convection flow in many sedimentary basins (Deming, 1994; Bachu, 1995). Fluid salinity and temperature are two major controls on fluid density. As fresh water penetrates into deep strata, its temperature is raised. The warm, low-density, fresh water may buoy up along permeable strata or other paths, driving out highly saline brines residing in pore spaces toward the shallow basin edge (Bachu, 1995).

Potential Relationships Between Basinal Fluid Migration and the Formation of Mississippi Valley-Type Mineral Deposits

Mississippi Valley-type (MVT) Pb-Zn (-Ba-F) ore deposits are hosted in stratabound/strataform carbonate rocks, with no obvious relationship to igneous intrusion. The similarity of fluid temperatures and compositions between MVT mineralizing fluids and diagenetic fluids and the presence of MVT deposits at the periphery of sedimentary basins are strong evidence for migration of hot, basin-derived, highly saline fluids through porous media (*e.g.*, Roedder, 1977; Sverjensky, 1981, 1984; Bethke, 1986; Bethke and Marshak, 1990; Appold and Garven, 1999). Temperatures of mineralizing fluids in the Upper Mississippi Valley and central Tennessee are significantly higher than

surrounding host rocks (Sangster et al., 1994), indicating the passage of anomalously hot fluids which probably originated in the deeper basin.

Fluid inclusion homogenization temperatures (T*h*) of MVT deposits vary significantly, most commonly in the range of 80 °C to 150 °C, although T*h* may reach up to 200 °C (Bailey and Cameron, 1951; Schmidt, 1962; Roedder, 1971, 1977; Leach et al., 1975; McLimans, 1977; Leach, 1979; Long et al., 1986; Zimmerman and Kesler, 1981; Hagni, 1983; Taylor et al., 1983; Gratz and Misra, 1987). Heyl (1983) suggested that these ores were deposited from hot basinal brines that migrated through paleoaquifers such as the Cambrian (Mount Simon) and Middle Ordovician (St. Peter) Sandstones. As discussed more thoroughly in Chapter 2, the ages of these MVT deposits roughly coincide with major diagenetic episodes.

Microscale Investigation of Diagenetic Fluids and Basinal Fluid Flow in theIllinois Basin

The preceding review of geological research in the Illinois basin provides a general outline of fluid migration in the Illinois basin and its relationship to the deposition of natural resources. Microscale investigation of diagenetic fluid flow may help to resolve questions of fluid composition, temperature, and migration because of its superior ability to analytically resolve authigenic and detrital components. Microscale techniques employed in this study include optical microscopy, cathodoluminescence petrography, electron microprobe cathodoluminescence (CL), fluid-inclusion microthermometry, Secondary Ion Mass Spectrometry (SIMS) and laser Ar-Ar age dating techniques. The results of this dissertation are presented in the following chapters.

Chapter 2 presents analytical results of fluid inclusion microthermometry in authigenic quartz and CL petrography of authigenic minerals. Petrographic examination of diagenetic mineral phases in sandstone thin sections (Appendix 1) was carried out prior to geochemical analysis to provide basic information on textures and abundances of different mineral components in the Mount Simon Sandstone, including authigenic quartz and K-feldspar overgrowths and cements. Distinct CL colors and intensities proved especially useful to identify fine-grained authigenic minerals, characterize the cement stratigraphy and distinguish overgrowths from detrital grains. CL investigation, using both a conventional luminoscope and fine-scale images acquired by electron microprobe, was used to characterize and digitally map the fine authigenic minerals. Zonations within a single mineral phase may reflect differences in fluid compositions and temperatures associated with mineral precipitation.

The study of fluid inclusions associated with the formation of authigenic minerals in the Mount Simon Sandstone provides direct evidence for the temperature and composition of regional, hot brine migrations through paleoaquifers in the Illinois basin. Most fluid inclusion analytical data are from mineral ore deposits. Far fewer results are reported from diagenetic minerals in basinal paleoaquifers (Goldstein and Reynolds, 1994) due to the small size (often < 50 μm across) and sparse distribution of many authigenic minerals.

Petrographic and fluid-inclusion evidence for two major generations of quartz overgrowths are presented in this chapter. Generation 1 quartz overgrowths (medium- to dark- gray CL) are associated with fluid temperatures of 60 – 95 °C. Generation 2 quartz overgrowths (light gray CL) are related to FI T*h* of 100 – 145 °C. In each generation of

quartz, T*h* is observed to decrease slightly from the south of the basin toward the north. Salinities of these fluids vary from 20 wt% to 25 wt% NaCl equivalent suggesting that diagenetic fluids are highly saline basinal brines, however, regional trends in fluid compositions cannot be resolved.

Chapter 3 focuses on SIMS oxygen isotope analyses of authigenic K-feldspars. Oxygen isotope compositions of authigenic minerals are useful for characterizing diagenetic fluid compositions, in combination with fluid temperature data. Secondary Ion Mass Spectrometry (SIMS, also known as an ion probe) is an *in situ* microscale analytical method that requires only ~ 10^{-9} grams of material for each analysis, efficiently overcoming some tedious mineral separation procedures required for conventional analysis (Hervig et al. 1995). SIMS oxygen isotope analysis of diagenetic minerals in the Michigan basin, Illinois basin, Wisconsin, Texas, and North Sea have proved successful; these data provide important evidence for characterizing diagenetic minerals (Graham et al., 1996; Williams et al., 1997a, b; Chen et al., 2000, 2001). The Cameca-4f SIMS at ORNL enables *in situ* analysis of mineral grains 15–30 μm in diameter on a standard thin section. The analytical error for $\delta^{18}O$ is ± 1‰ (1σ).

Results presented in this chapter indicate that average K-feldspar $\delta^{18}O$ values increase systematically from +14 ± 1‰ in the southernmost and deepest samples in Illinois to +24 ± 2‰ in the northernmost outcrop sample in Wisconsin. A similar trend is observed for quartz overgrowths (22 ± 2‰ to 28 ± 2‰; see also Chapter 4). The results suggest that the south-to-north-increasing $\delta^{18}O$ trend resulted from the compositional modification of northward-migrating fluids. A manuscript based on the content of this chapter was submitted to GEOLOGY and has been accepted for publication.

Chapter 4 focuses on SIMS oxygen isotope compositions of quartz overgrowths having CL zonation and overgrowths containing fluid inclusions that were measured for homogenization temperatures. The results suggest that there were two generations of quartz cements precipitated at different temperatures (Chapter 2) from diagenetic fluids having different oxygen isotopic compositions (Chapter 4). Generation 2 quartz overgrowths generally have lower $\delta^{18}O$ values than generation 1 quartz overgrowths. Using temperatures estimated by fluid inclusions matched point-to-point with oxygen isotope analyses, generation 2 quartz cements precipitated from a more evolved (higher $\delta^{18}O$) fluid than the earlier generation. Both generations of diagenetic fluids show a northward increase in $\delta^{18}O$ values.

Chapter 5 focuses on trace elements in authigenic K-feldspar and quartz cements. Potentially, one of the most direct ways to monitor mass transfers in the basin is to evaluate the variation of trace element contents in authigenic minerals precipitated from diagenetic fluids. Spatial variations in trace elements may be associated with fluid migration and evolution, however, interpretation of these data is complicated by poorly constrained distribution coefficients for trace elements between authigenic minerals and low temperature fluids. Concentrations of trace elements in authigenic quartz and K-feldspar were analyzed using SIMS.

Authigenic K-feldspar contained >1 ppm of Rb, Sr, Ba, Pb, Fe, Mg, B, Ti, and Cl. K, Al, Fe, B, Ti, Mg, and Cl were detected in quartz cements. Strong positive correlations were observed among Sr-Ba-Pb-Rb, K-Na-Mg-Ca-Cl, and K-Al in authigenic cements. Trace-element concentrations of Ba, Sr, Rb,Pb, Fe, Ca, and Ce in diagenetic fluids were estimated based on trace element contents in authigenic K-feldspar cements and available

distribution coefficients between sanidine and hydrothermal fluids. There is no convincing correlation between fluid compositions and position (south-to-north) in the basin. Trace element contents (Na + K + Li + Mg + Ca) of generation 2 authigenic quartz are elevated relative to generation 1 cements suggesting different fluid compositions and/or temperatures, however, no regional trend is apparent. The intrasample variability of trace elements suggests local heterogeneity and local-scale control on trace element content and obscures any possible regional trend.

Chapter 6 focuses on a preliminary *in situ* $^{40}Ar/^{39}Ar$ dating approach to age acquisition on authigenic K-feldspar. The absolute age(s) of authigenic K-feldspar in the Mount Simon Sandstone occurring in locations and depths in the basin is extremely important to understanding the diagenetic history. Ages of diagenetic events may constrain basinal fluid flow mechanisms and flow patterns, and help to establish any association between the diagenetic fluids and the formations of energy and mineral resources in the surrounding areas of the basin (Hearn and Sutter, 1985; Girard and Onstott, 1991; Hay et al., 1992; Aleinikoff et al., 1993; Friedman, 1993; Kunk et al., 1995; Spötl et al., 1996; Warnock et al., 1996). Conventional K-Ar and $^{40}Ar/^{39}Ar$ analysis requires a pure separate of authigenic K-feldspar, which to date cannot be obtained. Our preliminary study indicates that microscale, UV-laser, *in situ* $^{40}Ar/^{39}Ar$ age dating of authigenic K-feldspar overgrowths is presently precluded by shattering of the grain up on beam impact. An Ar-laser step-heating technique yielded mixed ages of detrital and authigenic K-feldspar, and suffered from air released by mounting ceramic.

Chapter 7 briefly discusses possible future research directions related to elucidating diagenesis and basinal fluid flow in the Mount Simon Sandstone of the Illinois basin.

Chapter 2

Fluid Inclusions and Cathodoluminescence of Authigenic Quartz in the Mount Simon Sandstone, Illinois Basin: Two Episodes of Basinal Brine Migration and their Relationship to the Formation of MVT Mineral Deposits

Abstract

Two major generations of diagenetic quartz cements are recognized in the Mount Simon Sandstone based on studies of cathodoluminescence and fluid inclusion microthermometry. Fluid inclusion homogenization temperatures (T*h*) range from 60 to 145 °C, with a bimodal distribution of 60 – 95 °C and 100 – 145 °C. Cathodoluminescence studies reveal an earlier generation of quartz cements having darker CL that correlate with the lower-temperature diagenetic fluid. A later generation of quartz cement has brighter CL and is associated with the higher-temperature fluid. Homogenization temperatures in both quartz generations weakly define temperature trends that decrease from south-to-north within the basin. Fluids inclusions associated with both generations of cements contain highly evolved basinal brines with 20 to 26 wt% NaCl equivalent salinities and a Ca-Mg-Na-(± K) model composition and support a long-standing hypothesis of hot brine migration in the Illinois basin. Previously reported ages for diagenetic minerals in the Illinois basin fall into two ranges, Silurian to Devonian and Pennsylvanian to Permian, each of which is possibly associated with distinct basinal brine migration in response to regional geologic and tectonic activities. The results of this CL and fluid inclusion study suggest that quartz cements record these two major

events. Regional fluid migrations of approximately the same age are also associated with precipitation of MVT ore deposits in the U.S. Midcontinent.

Introduction

Migrating basinal brines may react chemically and thermally with country rocks, leaving diagenetic signatures on the mineralogy and geochemistry of sedimentary rocks (Bethke and Marshak, 1990). Evidence for regional migration of superheated, highly saline fluids through sedimentary basins includes anomalous thermal histories for shallowly buried sediments, widespread potassic diagenesis in the U.S. Midcontinent, correlations of source rocks with displaced petroleum fields, correlated timing between tectonic deformation and MVT mineral deposition, and similar compositions and temperatures between diagenetic fluids and the mineralizing fluids (*e.g.*, Sverjensky, 1984; Bethke, 1985; Leach and Rowan, 1986; Bethke and Marshak, 1990; Goldhaber et al., 1990; Brannon et al., 1992; Chesley et al., 1994; Fishman, 1997; Pitman et al., 1997; Appold and Garven, 1999). The fluid inclusion temperatures of mineralizing fluids for MVT deposits (50-190 °C) within the U.S. Midcontinent typically exceed temperatures predicted from the geothermal gradients of 20 - 35 °C/km (e.g. Bailey and Cameron, 1951; Erickson, 1965; Roedder, 1971; Leach et al., 1975; Sverjensky, 1981; Hagni, 1983; Rowan and Leach, 1989; Plumlee et al., 1994). Current hypotheses invoke northward migration of huge volumes of hot, basin-derived, highly saline fluids through Midcontinent sedimentary basins (*e.g.* Noble, 1963; Roedder, 1977; Sverjensky, 1981, 1984; Bethke, 1986; Sangster et al., 1994). Evidence for the migration direction includes the northward-decreasing average temperatures of mineralizing fluids through the U.S.

Midcontinent (Leach and Rowan, 1986), the regional, northward-increasing potassium content in saline fluids (Viets and Leach, 1990; Plumlee et al., 1994), and the temporal relationship between the Appalachian-Ouachita orogenies and the formation of MVT deposits (Brannon et al., 1992, 1996; Chesley et al., 1994).

Most previous studies focus only on the immediate vicinity of the ore deposits. Far fewer studies address fluid flow in paleoaquifers within the sedimentary basins, where authigenic minerals precipitated in response to fluid migrations may record regional-scale fluid flow. Regional aquifers, such as the Mount Simon Sandstone and St. Peter Sandstone in the Illinois basin, may have served as conduits for large-scale, lateral migration of basinal brines (e.g. Heyl, 1983; Oliver, 1986; Bethke and Marshak, 1990; Fishman, 1997) in response to sedimentary compaction, orogenic uplift, or seismic activities (e.g., Garven and Freeze, 1984; Bethke, 1985, 1986; Clendenin and Duane, 1990; Sverjensky and Garven, 1992; Person and Garven, 1994). Burial curves suggest that at the time of authigenic K-feldspar precipitation (~ 400 Ma, Duffin et al., 1989), the maximum burial depth of the Mount Simon Sandstone in the Illinois basin did not exceed ~ 1500m, and maximum temperatures due to the basement heat-flow-controlled geothermal gradient would have been < 90 °C (Fishman, 1997). However, a preliminary study of fluid inclusions (18 measurements) indicated the involvement of hot (100 – 130 °C), saline (> 20 wt% NaCl equivalent) brines in the diagenesis of the Mount Simon Sandstone (Fishman, 1997). The inconsistency between fluid inclusion temperatures (100 – 130 °C) and burial temperatures obtained from burial history curves at ~ 400 Ma (< 90 °C) was attributed to regional migration of warm, saline brines through the Mount Simon Sandstone (Fishman, 1997). Similarly, fluid-inclusion temperatures in authigenic

quartz from the overlying Ordovician St. Peter Sandstone in the Illinois basin may reach up to 170 °C (Girard and Barnes, 1995; Pitman et al., 1997), and fluid inclusion temperatures in authigenic quartz occurring in the Precambrian-Cambrian boundary up to 115 °C (Harper et al., 1995).

The objective of this study is to characterize authigenic quartz cements in the Mount Simon Sandstone in the Illinois basin using CL and to make a more comprehensive study of fluid inclusion microthermometry than the more-limited results presented by Fishman (1997). Regional variations in CL and average T*h* may be useful to test the hypothesis of anomalously high-temperature, diagenetic fluid flow in the Mount Simon Sandstone and to identify fluid temperature and compositional gradients.

Geologic Setting

The Upper Cambrian Mount Simon Sandstone occurs in the intracratonic Illinois basin and its adjacent areas. It is one of the oldest siliciclastic sequences in the U.S. Midcontinent. It overlies unconformably Precambrian, dominantly igneous basement rocks and Lower Cambrian sedimentary rocks throughout much of the Illinois basin and contiguous areas (Bear, 1997), and is overlain conformably by the Upper Cambrian Eau Claire Formation (Hoholick et al., 1984; Bear, 1997; Fishman, 1997). The widespread formation reaches a thickness of up to 790 m in northeastern Illinois. It was more deeply buried in the southern part of the Illinois basin than in the northern part of the basin as a result of tectonic compression and orogenies (Taconic, Acadian and Appalachian-Ouachita orogenies) after the Late Cambrian time (Fishman, 1997). Figure 2-1 shows outline of the Illinois basin and the locations of borehole samples used in this study.

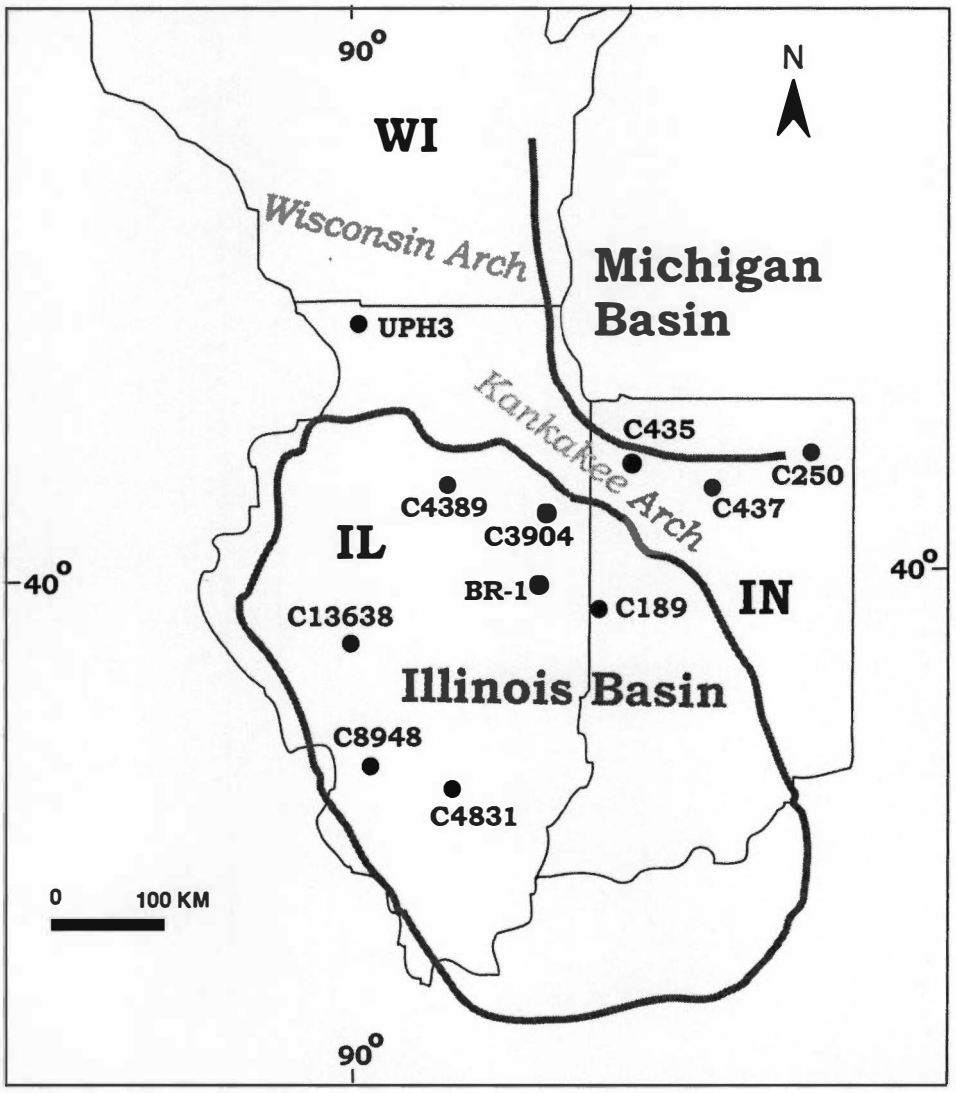

Figure 2-1 Outline of Illinois basin and locations of core samples used for fluid inclusion and cathodoluminescence study.

The Mount Simon Sandstone is a very inhomogeneous sandstone formation due to variations in wave energy during deposition, and is composed of fine- to coarse-grained arkoses, subarkoses, and quartzarenites (Driese et al., 1981; Hoholick et al., 1984; Duffin et al., 1989). The lower part is more arkosic than the upper part, and most rocks are moderately- to well- sorted. This unit shows an overall decline in porosity with depth. Cements in the Mount Simon Sandstone include predominantly quartz and K-feldspar, with lesser amounts of iron oxide, sericite, I/S, kaolinite, chlorite and carbonates, and minor pyrite, anhydrite, fluorite, and barite (Hoholick et al., 1984; Duffin et al., 1989; Fishman, 1997).

Methodologies

Cathodoluminescence

Authigenic cements were identified by transmitted light petrography on standard petrographic thin sections. Preliminary evaluation of authigenic cements was carried out at the University of Tennessee-Knoxville (UTK) with a CiTl cathodoluminescence microscope using an electron beam current of ~ 150 μA and an accelerating voltage of ~ 12 keV.

High-resolution CL analyses were performed at UTK using a Cameca SX50 electron microprobe with a Cameca CL detector designed to be equally sensitivity to all wavelengths from ultraviolet to infrared lights. Carbon-coated thin sections and chips from thin sections were examined in a sample chamber under high vacuum (~10^{-6} torr), using an electron beam with a 30 nA current and a 15 keV accelerating voltage. Clean imaging of areas 150 – 200 μm across made this micro-scaled, high-resolution CL study

at least ten times more sensitive to variations in CL than our conventional luminoscope. Gray-scaled back-scattering electron (BSE) images and CL images were obtained simultaneously.

Fluid Inclusion

Thirty-seven samples with well-developed quartz and/or K-feldspar overgrowths were selected for fluid inclusion studies. Doubly-polished fluid inclusion sections of 30 – 100 μm thick were made in the Mineral Optics Laboratory in Wilder, Vermont, using low speed and low temperature cutting and polishing techniques.

Fluid inclusion sections were examined petrographically to search for two-phase fluid inclusions in overgrowths. Sketches of measurable fluid inclusions, along with high-magnification transmitted-light petrographic (digital) photos, were prepared. Areas with measurable fluid inclusions were cored from the sections for temperature analysis. Microthermometric data of fluid inclusions in authigenic quartz were collected at Virginia Polytechnic Institute and State University, under the direction of Dr. Robert Bodnar, using a Linkam PS-1500 fluid inclusion heating/cooling stage calibrated at -56.6 °C and 0.0 °C with synthetic fluid inclusions. A recycle-measurement technique was applied, as described by Goldstein and Reynolds (1994). Some bigger fluid inclusions (> 3 μm) were also measured for ice-melting temperatures. No data were obtained from fluid inclusions in K-feldspar overgrowths, owing to their rarity and extremely small size (< 1 μm). Homogenization temperatures are accurate to ± 2.5 °C in response to a heating interval of 5 °C; ice melting temperatures are accurate to ~ ± 1 °C.

Analytical Results

Cathodoluminescence

Using the conventional luminoscope, authigenic quartz appears nonluminescent and there are no apparent CL variations within the overgrowths. A bluish to brownish luminescence was observed in detrital feldspars and clay minerals, making them easy to distinguish from quartz grains.

Electron microprobe (EMP) CL and BSE images reveal clear grain boundaries, as well as differences in the CL intensities of different minerals and mineral zonations. CL intensities of quartz overgrowths are generally lower (i.e., they appear as darker zones) than those of the detrital quartz grains, and CL zonation is recognized in the quartz overgrowths. Authigenic K-feldspar does not exhibit CL zonation. Uniform CL intensities in authigenic K-feldspar suggests that there is only one generation of K-feldspar cement in the Mount Simon Sandstone.

Quartz overgrowths in the Mount Simon Sandstone can be categorized into three groups, based on their CL patterns:

- Quartz overgrowths having uniform CL intensity (Fig. 2-2A);

- Quartz overgrowths exhibiting patchy areas with slightly different CL intensities (Fig. 2-2B);

- Quartz overgrowths with distinct zonations: an earlier, darker zone (Qog-1, Fig. 2-2C) overlain by a brighter CL zone (Qog-2, Fig. 2-2C).

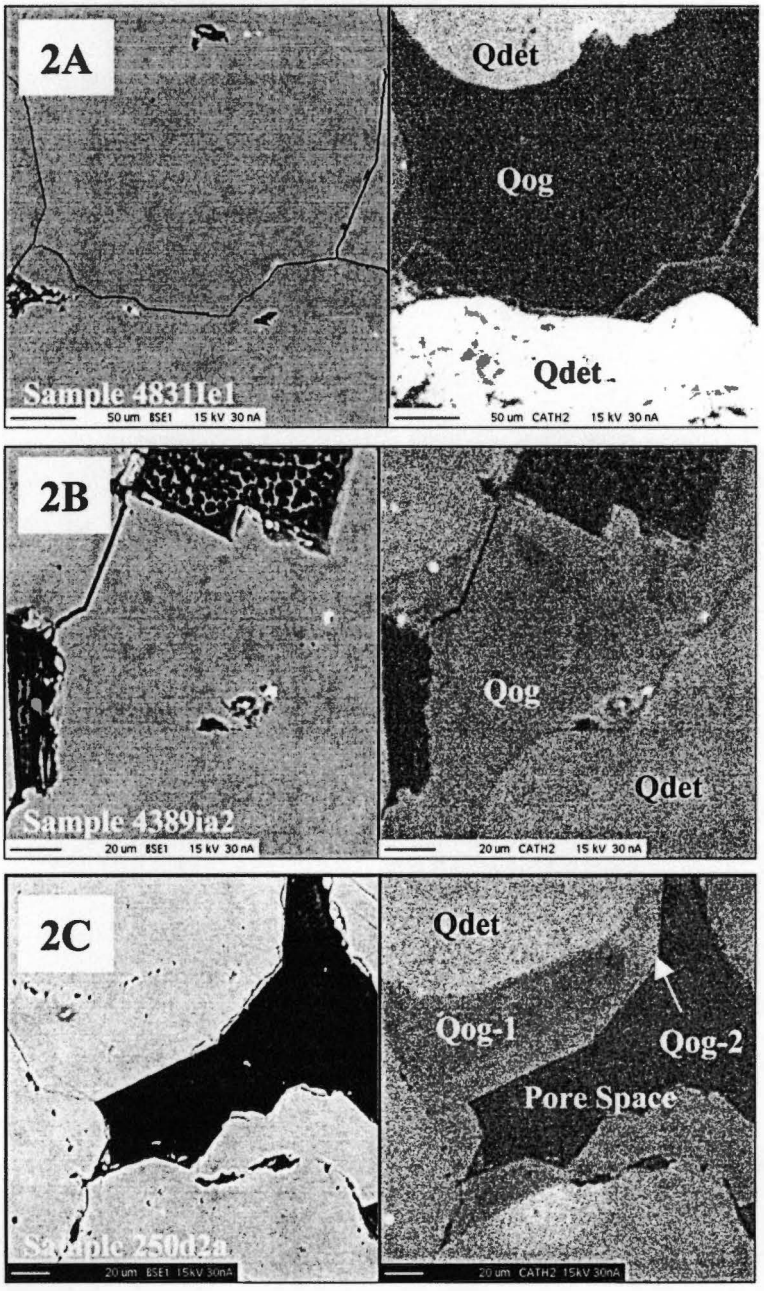

Figure 2-2 Characteristic cathodoluminescence patterns of quartz overgrowths. A – Quartz overgrowths with constant CL intensity; B – Quartz overgrowths with patchy CL intensity; C – Quartz overgrowths with two distinct CL zones.

Fluid Inclusion Microthermometry

Microscopic observation of fluid inclusion sections reveals the presence of very small (< 1 μm to ~7 μm; mostly < 3 μm) and sparse fluid inclusions in quartz overgrowths. Most fluid inclusions have round and sub-round, regular shapes and occur near the interface between the detrital grains and quartz overgrowths, but a few fluid inclusions are present within the quartz overgrowths themselves. A total of 276 fluid inclusions with visible vapor bubbles of < 10% (in volume) were analyzed for fluid inclusion temperatures (Table 2-1).

Homogenization temperatures (T*h*) of fluid inclusions from the Mount Simon Sandstone samples are shown in Fig. 2-3. Two-phase fluid inclusions homogenize to the liquid phase with T*h* ranging from 60 to 145 °C. The first ice-melting temperatures (T*e*, eutectic temperatures) of fluid inclusions range from -45 to -51°C. The final ice-melting temperatures (T*m*, freezing point depression temperatures) range from -17 to -30 °C, with most values in a narrow range of -18 to -25 °C (Table 2-2).

The T*h* data presented in this paper are not corrected for pressure differences between fluid entrapment and homogenization points. Such a correction is likely to have been quite small (Potter, 1977). At 400 Ma, when most diagenetic K-feldspar and quartz precipitated, the Mount Simon Sandstone was buried to fairly shallow depths (< 1 km) in the north of the basin and only slightly deeper (to ~ 2 km) in the south (Fishman 1997). When CH_4 or CO_2 is present, which is likely in our fluid inclusion samples, a pressure correction will be negligible (Haas, 1978; Hanor, 1980; Ravenhurst et al., 1989; Bodnar, 1990; Walgenwitz et al., 1990; McNeil et al., 1995).

Table 2-1 Frequency of homogenization temperatures of fluid inclusions in authigenic quartz

	Sample Identity										
Sample Number	UPH3	UPH3	UPH3	uph3	C675	C415	C250	C435	C437	C4389	C4389
Borehole Depth	403 m	567 m	629 m	649 m	1315 m	1196 m	1014 m	1107 m	882 m	714 m	774 m
T_h (°C)											
55-60			2	1							
60-65			11	9							
65-70			11	22				1			1
70-75		1	12	16						1	5
75-80		1	5	11						2	
80-85		2	7	5		1				1	
85-90	1	4	1	5			1	1			
90-95	1	2	1				2	3	1		
95-100			3	1			2	1			
100-105		2									
105-110		1	4	3		1		1		3	
110-115		1	1				1				
115-120		1									
120-125										1	
125-130					1						
130-135							2				
135-140		1					1				
140-145											
145-150											

Table 2-1 Continued

	Sample Identity										
Sample Number	C4389	C7466	C3904	C3904	Brl	C189	C189	C13638	C13638	C8948	C4831
Borehole Depth	797 m	796 m	995 m	1002 m	1188 m	1708 m	1762 m	1258 m	1275 m	1559 m	2561 m
T_h (°C)											
55-60											
60-65											1
65-70								1			1
70-75	1						1	1			4
75-80			1		1	3	2		2	2	3
80-85						1	1		1		5
85-90	1			1					4		4
90-95	1			1					3		5
95-100								1			4
100-105							1		1		2
105-110								2			
110-115											2
115-120											1
120-125			1						1		
125-130	1					1	1				
130-135							2	6			
135-140					1	1					1
140-145		1			1		1		1		1
145-150					1						

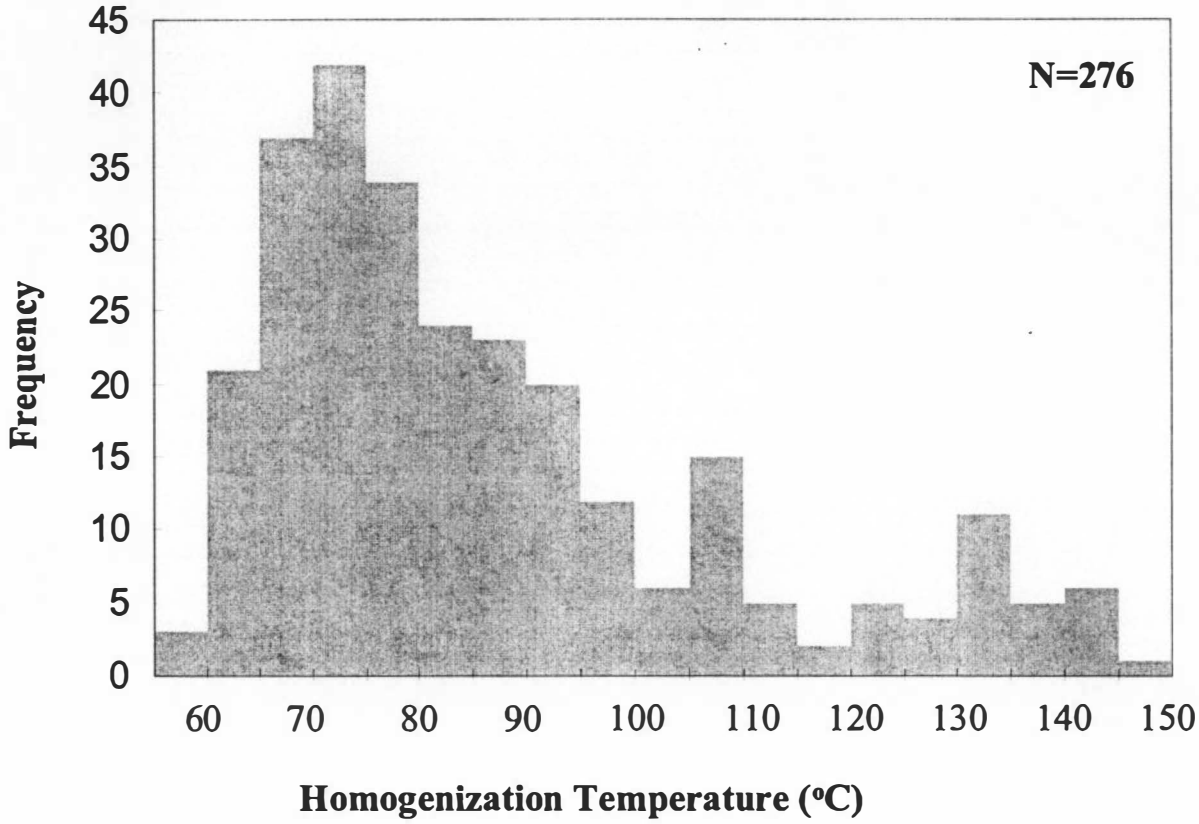

Figure 2-3 Histogram of all homogenization temperatures of fluid inclusions in quartz overgrowths obtained in this study.

Table 2-2 Homogenization temperature (T*h*), first ice-melting (T*e*) and final ice-melting temperature (T*m*) of fluid inclusions

Sample	T*h* (°C)	T*e* (°C)	T*m* (°C)
UPH3-634 m	60 to 65	-50 to -51	-19 to -20
UPH3-634 m	70 to 75	-49 to -50	-18 to -21
UPH3-634 m	80 to 85	-48 to -52	-17 to -20
UPH3-634 m	85 to 90	-45 to -46	-20 to -21
UPH3-634 m	105 to110	-48 to -49	-20 to -21
C4389-780 m	85 to 90	-48 to -51	
C189-1771 m	55 to 60	-45 to -50	-25 to -26
C4831-2581 m	70 to 75	-50 to -51	-20 to -21
C4831-2581 m	80 to 85		-20 to -25
C4831-2581 m	85 to 90	< -40	-20 to -21
C4831-2581 m	85 to 90	-50 to -52	-25 to -30
C4831-2581 m	90 to 95	-47 to -50	-18 to -19

Discussion

CL Characteristics of Authigenic Quartz

The apparent lack of luminescence from authigenic quartz using the cold cathode CiTl luminoscope can be attributed to several possible causes. Prolonged bombardment time and higher beam energy (up to 30 keV; Ramseyer et al., 1988) may be required to activate CL in authigenic quartz. The available optics (i.e., magnification) and relative instability of the scope under high kV operating conditions precluded consistent CL examination. Due to its structure and composition, only small amounts of impurities are typically incorporated into quartz and lattice defects are probably the major control on CL emissions. Ramseyer et al. (1988) reported that the cause of short-lived, green-blue luminescence (with nonluminescent areas), very common in authigenic quartz overgrowths, is associated with the presence of interstitial cations. Additionally, some luminescence may not be visible with the naked eye. Demars et al. (1996) reported that the majority of CL emissions from diagenetic quartz are in the UV-range.

CL emissions detected and recorded as gray scale maps using the EMP indicate that quartz overgrowths always have lower CL intensities than detrital grains. Gotze and Plotze (1997) reported trace element concentrations in five detrital quartz samples (from igneous and metamorphic sources). In comparison to authigenic quartz overgrowths in the Mount Simon Sandstone (chapter 5 of this thesis, Table 5-2), detrital quartz grains reported by Gotze and Plotze (1997) generally have higher trace elements contents: Al (181-704 ppm), Fe (28-534 ppm), Ti (20-87 ppm), Na (20-35 ppm), Li (3-8 ppm), Zr (20-85 ppm). It can be inferred that the higher CL intensity in detrital quartz grains is at least partly related to their higher trace element contents. However, lattice defects may still be

the most important factor for CL emission of quartz (Ramseyer et al., 1988; Ramseyer and Mullis, 1990; Perny et al., 1992, Gotze and Plotze, 1997; Watt et al., 1997). Bruhn et al. (1996) described two basic patterns of CL in quartz overgrowths, a stable brown/red/dark blue CL related to burial diagenesis and an unstable blue/green/yellow CL related to hot basinal brines. Authigenic quartz cements with orange-brown CL coincide with higher Fe concentration whereas nonluminescing cements have significantly lower Fe content (Bruhn et al., 1996). CL zonation in quartz overgrowths (i.e., Fig. 2-2C) may reflect changes in fluid temperature, pH, crystallization rate, trace element concentration, and amount of lattice defects (Miller, 1988; Ramseyer et al., 1988, 1989; Houseknecht, 1991; Watt et al., 1997; Holten et al., 2000; Hoskin, 2000). Differences in the CL of authigenic quartz (Fig. 2-2) may also be associated with pore space development.

Our work suggests that two distinct generations of quartz cement can be identified based on their CL, an early cement (Qog-1) and a later cement (Qog-2). An earlier-generation cement (i.e., Qog-1, Fig. 2-2A) has a greater likelihood to be preserved if it completely fills an open pore space, as shown in Fig. 2-2A. Partial filling of pore space permits subsequent fluid flow and cementation (e.g., Qog-2, Fig. 2-2C), or partial to complete dissolution of Qog-1 prior to the precipitation of late cements Qog-2 (Fig. 2-4 and 2-5). The inner overgrowth zone (Qog-1) in Fig. 2-4 appears partially dissolved, with the remnant preserved as a discontinuous overgrowth covering a detrital grain. This early cement, with relatively dark CL, was overlain completely by a later overgrowth having relatively bright CL (Qog-2). Partial dissolution of the first generation (Qog-1)

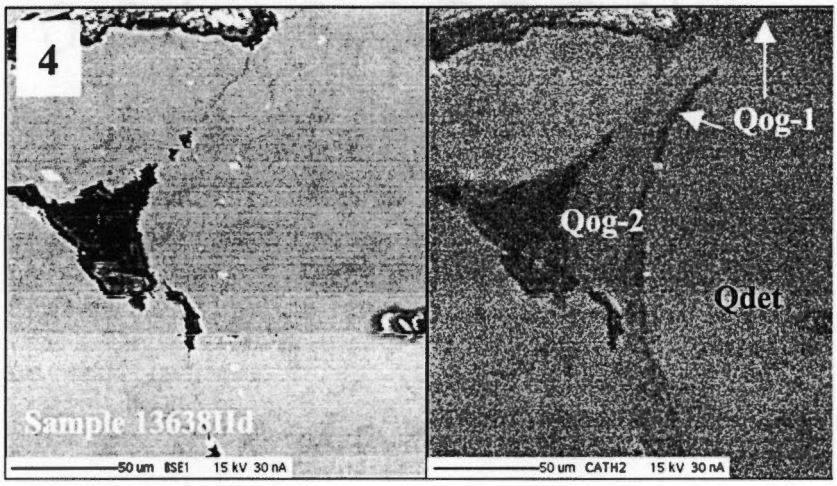

Figure 2-4 Cathodoluminescence photomicrograph showing precipitation of a generation 2 quartz overgrowth onto a partially dissolved generation 1 quartz overgrowth.

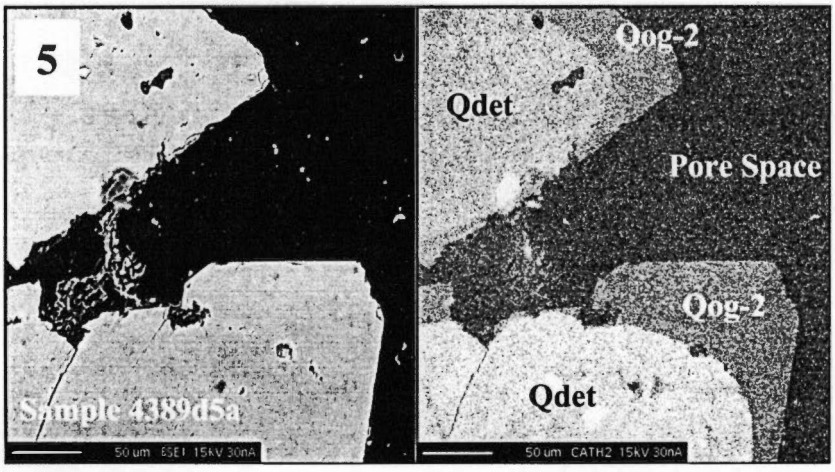

Figure 2-5 Cathodoluminescence photomicrograph showing a quartz overgrowth from the later diagenetic event, with a single CL zone and high CL intensity.

suggests there was a hiatus between precipitation of Qog-1 and Qog-2. Brighter-CL quartz overgrowths (Fig. 2-5) may occur in the absence of darker cements, and these are interpreted to be associated with the later diagenetic event (Qog-2). The euhedral morphology and brighter CL of generation 2 quartz overgrowths (Qog-2, in Fig. 2-5), is different from Qog-1 cements (Fig. 2-2A) which have a pore space morphology and a darker CL color. The over-sized pore space in Fig. 2-5 suggests that the pore space is secondary and dissolution occurred before the second-generation quartz precipitated.

CL features in quartz overgrowths suggest that there are at least two generations of diagenetic events in the Mount Simon Sandstone. Throughout the basin quartz overgrowths show predominantly two CL intensities. Quartz having relatively dark CL (Qog-1, Fig. 2-2A) was associated with an earlier diagenetic event, whereas quartz with brighter CL (Qog-2, Fig. 2-2C and Fig. 2-5) was associated with a later diagenetic event. Higher-temperature precipitation of brighter, generation 2 quartz overgrowths may accommodate incorporation of more trace elements in quartz (see Chapter 5). The solubilities of many elements decrease with decreasing fluid temperature. No simple relationship is observed between CL intensity and the concentration of any particular trace element in quartz.

Fluid Inclusion Compositions and Temperatures

The compositions and salinities of diagenetic fluids associated with authigenic quartz from the Mount Simon Sandstone were derived based on analyses of fluid inclusions. The first ice-melting temperatures (T*e*, eutectic temperatures) of these fluid inclusions range from -45 to -51°C; and the final ice-melting temperatures (T*m*, freezing

point depression temperatures) range from -17 to -30 °C, mostly falling in a narrow range of -18 to -25 °C. These ice melting temperatures suggest that authigenic quartz was precipitated from H_2O-NaCl-(KCl)-$CaCl_2$-$MgCl_2$ diagenetic fluids with high and consistent salinities, ranging from 20% to 26 wt.% NaCl equivalent, using phase diagrams of Crawford (1981), Oakes et al. (1990), and Goldstein and Reynolds (1994). The salinity range determined is concordant with results from a previous, more limited, fluid inclusion study of Mount Simon quartz overgrowths (Fishman, 1997, salinity > 20%) and confirms that diagenetic fluids in the Mount Simon Sandstone were highly saline brines.

The homogenization temperatures, T*h*, of fluid inclusions range from 60 to 145 °C (Fig. 2-3), a broader range than obtained from the previous fluid inclusion study (Fishman, 1997). Our results suggest that the fluid inclusion temperature data (T*h* = 100 – 130 °C, N=18) reported by Fishman (1997) are incomplete. The wide range of homogenization temperatures within individual thin sections (up to 40 °C difference, Fig. 2-6) indicates a complicated diagenetic history for the Mount Simon Sandstone. Several factors may have contributed to the large T*h* variation, including multiple generations of fluids, mixing of fluids, and stretching or other modifications of fluid inclusions.

Secondary modification of fluid inclusions in Mount Simon Sandstone quartz overgrowths, which would compromise the use of fluid inclusion to constrain fluid temperature and composition, is unlikely. The occurrence of post-formation modifications of primary fluid inclusions depends on fluid inclusion size, shape, salinity and host mineral nature (Larson et al. 1973; Bodnar and Bethke, 1984; Osborne and

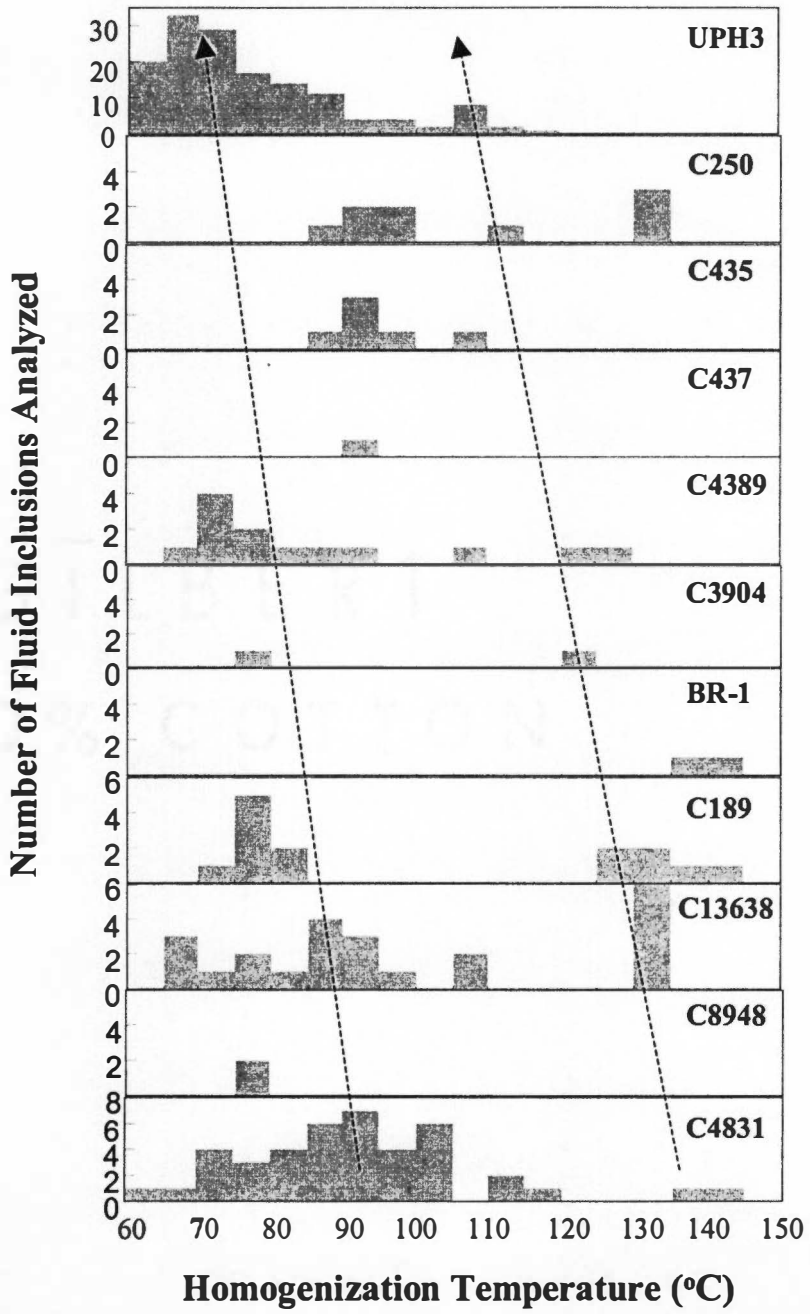

Figure 2-6 Histograms of homogenization temperatures of fluid inclusion from individual samples. From bottom up, the histograms are compiled along a roughly south to north transect. Arrows indicate at least two generations of fluid migration and temperature-decreasing trends.

Haszeldine, 1993; Goldstein and Reynolds, 1994). Bodnar and Bethke (1984) indicated that overheating by 70 °C is required for stretching to occur in a ~ 4.5 μm fluid inclusion in *fluorite*, with a confining pressure of 1 atm. Fluid inclusions in quartz in the Mount Simon Sandstone are very small, mostly < 3 μm, and quartz is mechanically stronger than fluorite. Therefore, initiation of fluid inclusion stretching in the Mount Simon quartz cements is unlikely. Overstepping of the trapping temperatures by 70 °C would have required an additional > 3 km of further burial, for which there is no evidence. In fact, samples from the northern Illinois basin and the Kankakee arch may have never been buried to > 1.5 km (Fishman, 1997), whereas fluid inclusion temperatures > 100 °C are recorded in these samples (Fig. 2-6). No correlation was identified between maximal burial depths and fluid inclusion temperatures, or between fluid inclusion size and temperature. Thus, post-formation modifications of fluid inclusion were minimal and temperature data are interpretable.

There is no evidence that mixing of fluids of different origins contributed to T*h* variability. Fluids from different origins may have noticeable differences in temperatures, chemical compositions, and salinities. Although diagenetic fluid temperatures in the Mount Simon Sandstone varied considerably, the fluid compositions and salinities are very consistent and probably originated from similar, highly evolved saline brines. At the approximate time that authigenic K-feldspar and most quartz (generation 1) are inferred to have precipitated (~ 396 Ma, Duffin et al., 1989; Fishman, 1997), the proto-Illinois basin was an open-marine cratonic embayment connected to the south with Black Warrior and Arkoma basins (Buschbach and Kolata, 1990).

The data presented here are most consistent with T*h* variations due to multiple (at least two) generations of diagenetic fluids. There appears to be a bi-modal distribution in the aggregated fluid inclusion T*h* data, with the majority (75%) between 60 and 95 °C and others between 100 and 145 °C (Fig. 2-3). Similar, bi-modal T*h* pattern are also observed in most individual samples (Fig. 2-6). The two generations of diagenetic fluids interpreted from T*h* data are consistent with other evidence documented for the Mount Simon Sandstone including transmitted light petrographic, SEM imagery, and age dating studies (Duffin et al., 1989; Fishman, 1997). Notice that temperatures from the three samples in the eastern portion of our study area, near the present Michigan basin (C250, C437, and C435, see Fig. 2-1 and Fig. 2-6), are slightly higher and offset from the two general, temperature-decreasing trends as shown in Fig. 2-6, suggesting that these samples may have been affected by somewhat different fluids emanating from the Michigan basin, with slightly difference in fluid temperatures and, perhaps, fluid compositions (Graham et al., 1996).

Although our data are limited, there appears to be a strong correlation between the bimodal distribution of fluid inclusion T*h* and the two predominant CL zonations (light and dark) observed in authigenic quartz overgrowths (Fig. 2-2, 2-3, and 2-6). We conclude that fluid inclusion homogenization temperatures in authigenic quartz overgrowths are associated with at least two generations of diagenetic fluids. These overgrowths appear to have precipitated from different pulses/generations of diagenetic fluids having similar origins (highly evolved brines) but different temperatures compositions (see trace element contents, Chapter 5). Our observations suggest that the later (outer), brighter CL zones (Qog-2, Fig. 2-2C) are associated with the higher-

temperature (100 – 145 °C, Fig. 2-6) brines, whereas darker zones (Qog-1, Fig. 2-2A) were probably associated with a lower-temperature (60 – 95 °C, Fig. 2-6) basinal brine.

Regional Fluid Migrations

Histograms of T*h* from individual fluid inclusion sections from the Illinois basin and its periphery are compiled along a roughly south to north transect in Fig. 2-6. Fluid inclusion temperatures from individual samples show a bimodal distribution, with a majority ranging from 65 to 95°C and others > 100 °C, consistent with the overall fluid inclusion bimodal T*h* distribution pattern (Fig. 2-3).

The lower-temperature fluid (60 – 95°C) is interpreted to be associated with an earlier diagenetic event, as defined by the relatively low intensity CL quartz (generation 1). Petrographic observations suggest that generation 1 quartz and authigenic K-feldspar were precipitated contemporaneously. Burial history curves suggest that the Mount Simon Sandstone was buried most deeply towards the south, with maximum burial temperature of ~ 90 °C (Fishman, 1997). This maximum burial temperature is very close to the upper limit of generation 1 fluid temperatures. On the other hand, burial temperatures in the north and along the periphery of the basin (< 60 °C, Fishman, 1997) were lower than corresponding fluid inclusion temperatures (sample UPH3, Fig. 2-7). This observation suggests that a hotter fluid passed through the formation in the northern portion of the basin. The simplest interpretation is that the generation 1 fluid originated in the deeper basin in the south (T ~ 90 °C) and migrated northward, with the northern basin seeing fluid temperatures that were slightly elevated relative to burial conditions.

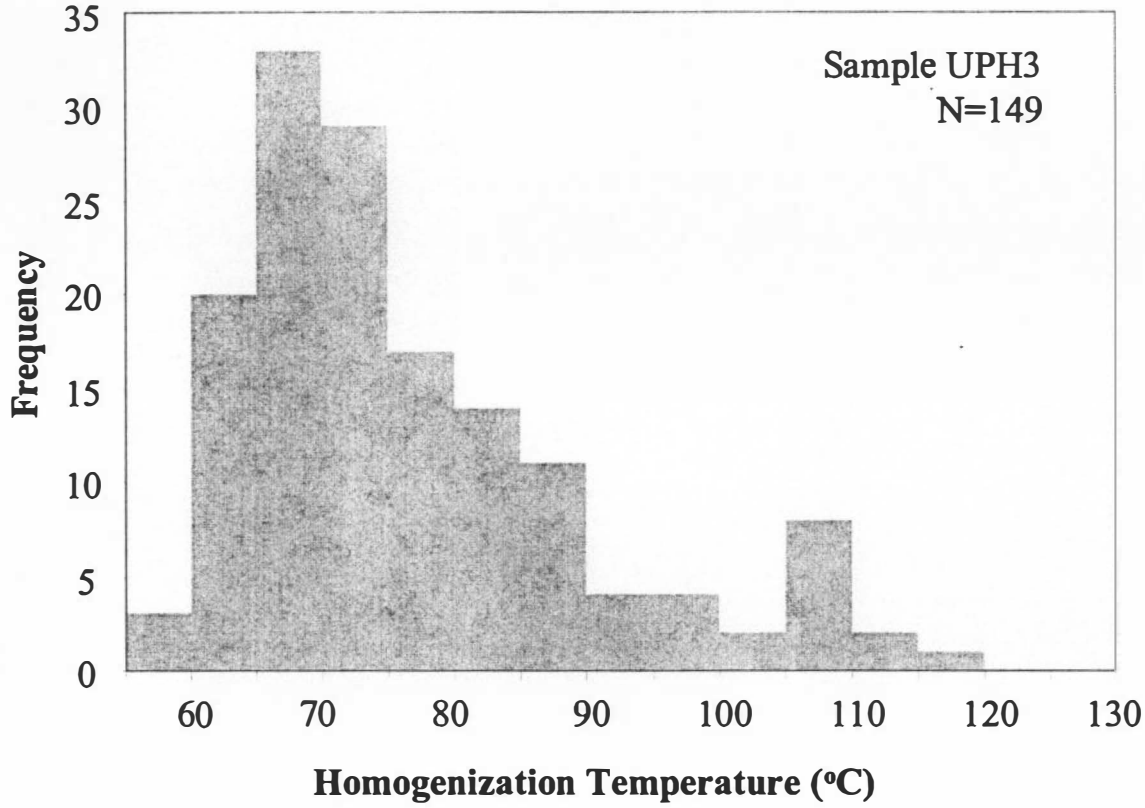

Figure 2-7 Histogram of homogenization temperatures of fluid inclusions in quartz from UPH3 bore hole samples.

Fluids associated with the higher-T*h* generation of fluid inclusions, with temperatures ranging from 100 to 145 °C, interpreted to have precipitated bright-CL quartz overgrowths (generation 2). These T*h* are similar to the previously reported T*h* of 115 – 130 °C (Fishman, 1997). As with the previous fluid T*h*, the data weakly define a trend of decreasing T*h* from south to north (Fig. 2-6), suggesting that there was a northward migration of this brine. The burial curve (Fig. 1-2) for the central Illinois basin (between borehole C13638 and C3904, Fig. 1-1) indicates further burial after the first potassic event. Therefore, fluid temperatures in the basin are expected to increase with further burial. The higher fluid temperatures associated with generation 2 quartz may indicate "superheated" fluid, but other explanations are possible. For example, if generation 2 quartz is significantly later than generation 1 quartz, or is associated with illite/smectite (I/S event at ~ 214-270 Ma), then the burial temperature have been quite a bit hotter. In fact, it could be hot enough that the second fluid also was not superheated.

Origin of Diagenetic Fluids and their Relations to MVT Deposits

Based on studies of the ages of diagenetic minerals in the Midcontinent, at least two episodes of regional diagenesis have been suggested. Diagenetic ages of authigenic minerals (K-feldspar and I/S) appear to fall into two ranges: 351 – 436 Ma and 214 – 271 Ma (Krueger and Woodward, 1972; Marshall et al., 1986; Hay et al., 1988; Duffin et al., 1989). Widespread potassic (mostly K-feldspar) diagenesis at 351 – 454 Ma in Cambrian and Ordovician strata (Hay et al., 1988, 1992, 1993; Duffin et al., 1989; Harper et al., 1995) suggests a single, lengthy, regional diagenetic event. Hay et al. (1992; 1993) reported K-Ar, $^{40}Ar/^{39}Ar$, Rb-Sr, and K-Ca ages of 375 ~ 448 Ma for authigenic K-

feldspar in Cambrian and Ordovician sandstones and tuff from the Midcontinent. Replacement K-feldspar and K-feldspar from fracture fillings in the Precambrian-Cambrian boundary in southwestern Ontario yielded K-Ar ages of 412 – 453 Ma and Rb-Sr model ages 394 – 482 Ma (mostly 431 – 454 Ma) (Harper et al., 1995). Duffin et al. (1989) reported radiometric K-Ar dating ages of ~ 395 Ma for authigenic K-feldspar and 214 – 271 Ma for authigenic illitic I/S in the Mount Simon Sandstone, suggesting two regional potassic diagenetic events in the Illinois basin. Our CL and fluid inclusion results support the existence of two distinct regional diagenetic fluid events in the Mount Simon Sandstone. The earlier event, associated with precipitation of K-feldspar, involved fluids with temperatures of 60 – 95 °C, whereas a second event, which may be associated with precipitation of I/S, involved hotter (100 – 145 °C) fluids.

Age dating of Midcontinent MVT deposits, including studies of sphalerite, fluorite, and glauconite using Rb-Sr, Sm-Nd, and Th-Pb/U-Pb techniques, reveal two major ranges of mineralizing ages. One group ranges from 347 to 392 Ma (Lange et al., 1983; Nakai et al., 1990, 1993), whereas the majority of ages range from 251 to 272 Ma (Doe et al., 1983; Brannon et al., 1992, 1996; Chesley et al., 1994). These two age groups coincide well with the regional potassic diagenetic events at ~400Ms (K-feldspar) and 214-270 Ma (I/S) (Duffin et al., 1989).

Fluid inclusion temperatures reported in this study (60 – 145 °C) are consistent with fluid inclusion temperatures reported elsewhere for Midcontinent MVT deposits. Previous fluid inclusion studies on quartz, carbonates, fluorite, and sphalerite in MVT deposits reveal fluid temperatures ranging from 50 to 190 °C (e.g. Bailey and Cameron, 1951; Erickson, 1965; Roedder, 1971; Leach et al., 1975; Sverjensky, 1981; Hagni, 1983;

Rowan and Leach, 1989; Plumlee et al., 1994; Sangster et al., 1994). In many cases, fluid inclusion temperatures of > 100 °C comprise the major proportion of the total fluid inclusion T*h* data in these deposits. By comparison with our fluid inclusion results, MVT deposits with fluid temperature > 100 °C may be closely related to the diagenetic event accompanying deepest burial of the basin. Likewise, MVT deposits with mineralizing fluid temperatures significantly < 90 °C may be affiliated with the earlier diagentic event, which involve regional migration of fluids of about the same temperature. Nakai et al. (1990) attributed the older event to fluid migrations in response to Acadian orogeny, although it appears that Acadian orogeny ceased by Devonian time. The younger event was believed to be associated with fluid migrations initiated by Alleghenian-Ouachita orogeny (Brannon et al. 1992, 1996).

Conclusions

Cathodoluminescence studies of authigenic quartz (and K-feldspar) reveal a complicated diagenetic history for the Upper Cambrian Mount Simon Sandstone in the Illinois basin. Two generations of quartz overgrowth, with distinct CL characteristics, are defined: an earlier overgrowth (generation 1) with relatively dark CL and a later generation of overgrowths (generation 2) with brighter CL. Dark-CL, generation 1 quartz cements are associated with lower fluid temperatures, whereas the brighter CL cements (generation 2 quartz) are associated with higher temperature fluid inclusions.

Fluid inclusions in quartz overgrowths are sparse and very small (mostly < 3 μm) with < 10 % vapor phase in volume. Most fluid inclusions are present at the detrital grain/overgrowth boundaries. Fluid inclusion homogenization temperatures (T*h*) range

from 60 to 145 °C, with higher T*h* more common for fluid inclusions well into overgrowths and in cements with brighter CL. There appears to be a bi-modal distribution in fluid inclusion T*h* with T*h* in the range 60 – 95 °C and 100 – 145 °C. This is consistent with the observation of two generations of quartz cements from CL studies. For each generation, weak trend of decreasing temperature towards the northern basin, from 95 → 60 °C and 145 → 100 °C, is observed. T*e* (first melting temperature) and T*m* (final melting temperature) from ice-melting analyses of some relatively larger fluid inclusions range from -45 to -52 °C and -18 to -25 °C, respectively, indicating the existence of Ca-Mg-Na-(±K) diagenetic fluids with salinities ranging from 20 to 26 wt% NaCl equivalent. Apparently the diagenetic fluids involved in both major events were evolved, highly saline basinal brines.

Two major generations of diagenesis were recognized in the Mount Simon Sandstone based on studies of cathodoluminescence and fluid inclusions in quartz overgrowths. Our study suggests that the two diagenetic events were associated with distinct basinal brines, of different temperature, migrating south to north in response to different orogenies. The earlier event is associated with precipitation of K-feldspar, dated previously at ~ 400 Ma, with fluid temperatures ranging from 60 to 95 °C. The later event is associated with fluid temperatures in the range from 100 to 145 °C. The highly saline fluid composition and temperature correlate well with fluid characteristics associated with the precipitation of MVT ore deposits in the Midcontinent, which were deposited at 347 – 392 Ma (Lange et al., 1983; Nakai et al., 1990, 1993) and 251 – 272 Ma (Doe et al., 1983; Brannon et al., 1992, 1996; Chesley et al., 1993), respectively.

Chapter 3

Regional Fluid Migration in the Illinois Basin: Evidence from *in situ* Oxygen Isotope Analysis of Authigenic K-feldspar and Quartz from the Mount Simon Sandstone

Abstract

Oxygen isotope compositions of widespread, authigenic K-feldspar and quartz overgrowths and cements in the Upper Cambrian Mount Simon Sandstone were measured by ion microprobe in 11 samples distributed across the Illinois basin and its periphery. Average K-feldspar $\delta^{18}O$ values increase systematically from +14 ± 1‰ V-SMOW in the southernmost and deepest samples in Illinois to +24 ± 2‰ in the northernmost outcrop sample in Wisconsin. A similar trend was observed for quartz overgrowths (22 ± 2‰ to 28 ± 2‰). Constant homogenization temperatures (100-130 °C) of fluid inclusions associated with quartz overgrowths throughout the basin suggest that the geographic trend in oxygen isotope compositions is a result of diagenetic modification of a south-to-north migrating basinal fluid.

Introduction

Widespread potassic alteration and diagenesis of Cambrian and Ordovician strata have been recognized throughout the Midcontinent of North America (e.g., Hay et al., 1988; Duffin et al., 1989; Diehl and Goldhaber, 1995; Harper et al., 1995; Pitman and Spötl, 1996). Potassium-argon ages of authigenic K-feldspar in Mount Simon Sandstone in the northern part of the Illinois basin suggest a regional-scale fluid flow event at 395 ±

6 Ma (Duffin et al., 1989). Regional fluid flow in sedimentary basins is commonly accompanied by abnormal thermal regimes, resulting from fluid convection or flow of relatively hot fluids from deep-basin and basement rocks; these fluids correlate well with migration of hydrocarbons and the formation of mineral deposits at basin margins (e.g., Goldhaber et al., 1990; Bethke et al., 1990; Pitman and Spötl, 1996; Fishman, 1997). Tectonism is considered to be important in mobilizing large volumes of pore fluids (e.g., Bethke, 1986a; Oliver, 1986); however, the ca. 400 Ma age of widespread authigenic K-feldspar overgrowths in the Illinois basin suggests that they precipitated between major orogenies (Taconic and Acadian). Thus, the source and nature of the fluid event responsible for the potassic alteration is uncertain.

The large oxygen isotope fractionation between authigenic K-feldspar or quartz and water is potentially a sensitive indicator of the temperature and isotopic composition of low-temperature diagenetic fluids. But the small size (<100 μm) of these cements and overgrowths and the problem of mechanically separating authigenic and detrital materials make it difficult to characterize these separate phases by using conventional isotopic methods. In contrast, secondary-ionization mass spectrometry (SIMS), with its capability for in situ analysis at a 10-30 μm spatial resolution, is ideal for characterizing the isotopic composition of fine-grained materials (Graham et al., 1996). In this paper, we present ion-microprobe results that show systematic, regional variations, across the Illinois basin, in $\delta^{18}O$ values of authigenic K-feldspar and quartz from the Mount Simon Sandstone. These data suggest that microscale analysis of authigenic minerals is useful to set limits on and refine regional-scale basin fluid-flow models.

Burial and Diagenesis of the Mount Simon Sandstone

The Upper Cambrian Mount Simon Sandstone is one of the oldest sedimentary rock sequences in the Illinois basin, unconformably overlying older Cambrian and Precambrian basement rocks (Bear, 1997). The Illinois basin developed as a broad, slowly subsiding cratonic basin, tilted and open to the south (Kolata and Nelson, 1990). Paleozoic tectonic downwarping in the southern part of the basin resulted in south-increasing depth of burial of the Mount Simon Sandstone (Fig. 3-1; Leighton and Kolata, 1990). The Mount Simon Sandstone underwent a complicated diagenetic history that precipitated authigenic quartz, K-feldspar, and illite/smectite (I/S) (Hoholick et al., 1984; Duffin et al., 1989; Fishman, 1997). Petrographic examination reveals crosscutting textures that suggest that authigenic K-feldspar and quartz formed roughly contemporaneously (Fishman, 1997), whereas I/S is paragenetically younger (Duffin et al., 1989; Fishman, 1997). This finding is consistent with relatively young ages obtained from I/S (215-271 Ma; Duffin et al., 1989) and suggests at least two distinct episodes of potassic diagenesis.

Burial curves and thermal-history modeling of Mount Simon Sandstone in the Illinois basin suggest that, at the assumed time of authigenic K-feldspar precipitation (ca. 400 Ma), maximum burial depth and temperature in the southern part of the basin did not exceed ~1500 m and 95 °C and that even lower temperatures affected the more shallowly buried northern part of the basin (Fishman, 1997). Fluid-inclusion studies in contemporaneous authigenic quartz overgrowths, however, suggest a different thermal history (Fishman, 1997). Homogenization temperatures of very small (1-3 μm), round to subround, saline (>20 wt% NaCl equivalent) fluid inclusions in quartz overgrowths

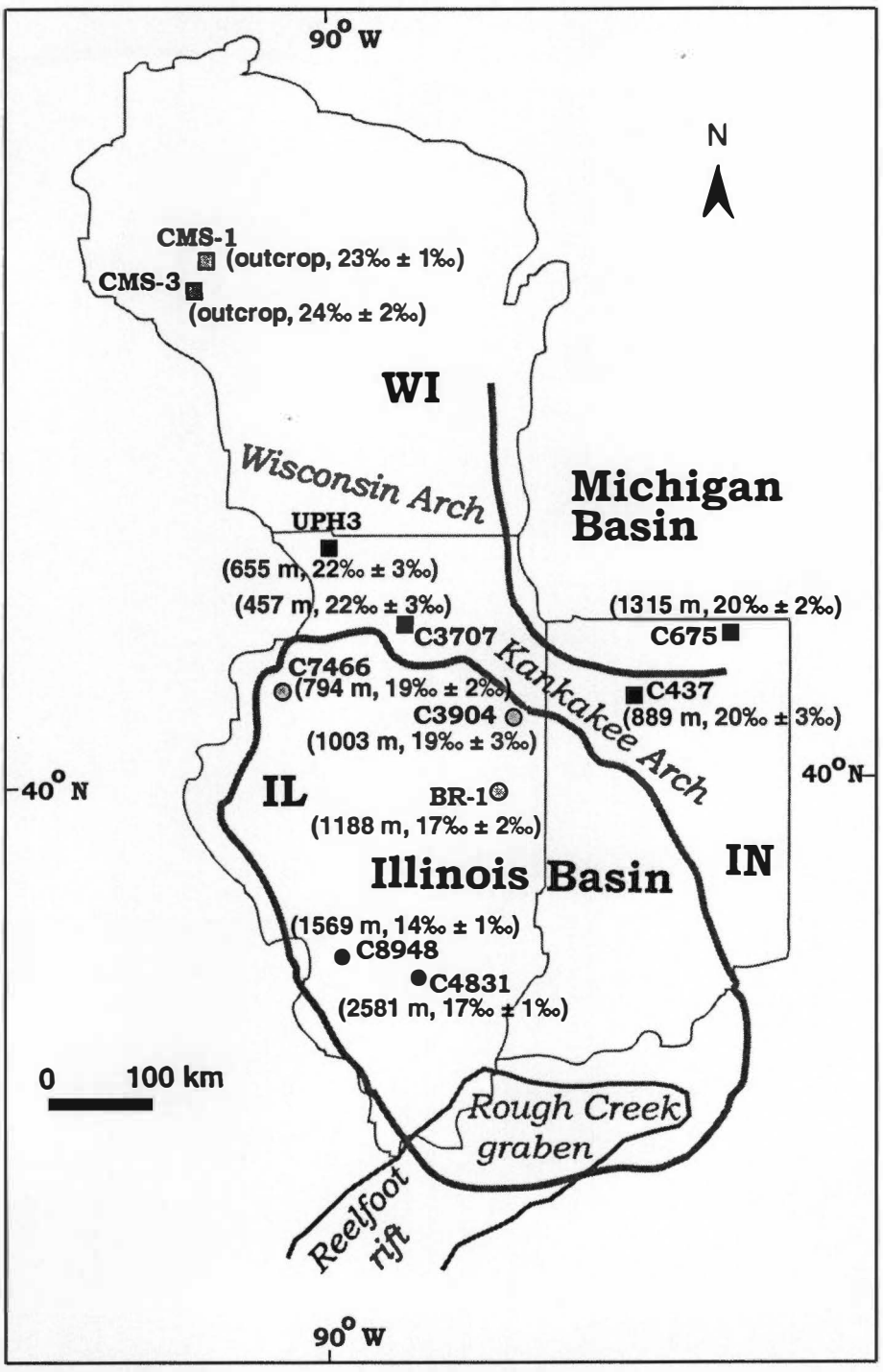

Figure 3-1. Map showing outline of Illinois basin and surrounding area, the locations of cores analyzed and core ID numbers. Sample recovery depth and average oxygen isotopic composition (V-SMOW) with 1σ error on the population of individual ion microprobe analyses measured on authigenic K-feldspar for each sample are shown in parentheses.

indicate temperatures of 100-130 °C (N=18) throughout the basin (Fishman, 1997), significantly higher than indicated by the modeling. Fluid inclusions of this type are generally unaffected by burial (Bodnar and Bethke, 1984; Goldstein and Reynolds, 1994); they may be more reliable to define the conditions of cement precipitation than temperature data derived from modeling burial curves.

Methods and Analytical Results

Authigenic K-feldspar overgrowths compose up to 5 vol% of sandstone samples in cores (Fishman, 1997) and up to 12 vol% in outcrop samples. Authigenic quartz varies from 0 to 23 vol% (Fishman, 1997). Nonluminescent, euhedral to subhedral K-feldspar overgrowths, ranging in width from 10 to 50 μm (Fig. 3-2), can be distinguished from detrital K-feldspar grains, which have bright, dull-blue to brownish-yellow luminescence.

The isotopic composition of authigenic K-feldspar from 11 localities and of quartz from 3 localities (Fig. 3-1) was measured with a modified Cameca 4f ion microprobe using a 20-μm-diameter Cs^+ primary ion beam and extreme energy filtering of negatively charged secondary ions (Riciputi et al., 1998). Precision for the $\delta^{18}O$ value of each individual analysis averaged ± 1‰ (1σ), based on the square root of the sum of the square of the two standard errors on the individual ratios comprising an individual analysis and the 1σ reproducibility of repeated analysis of quartz standard (N=4 to 12) during an analytical session. Owing to the small size of overgrowths, most target grains were analyzed only once.

The $\delta^{18}O$ values of individual authigenic K-feldspar overgrowths range from +13 to +26‰ relative to V-SMOW (Vienna Standard Mean Ocean Water), whereas the

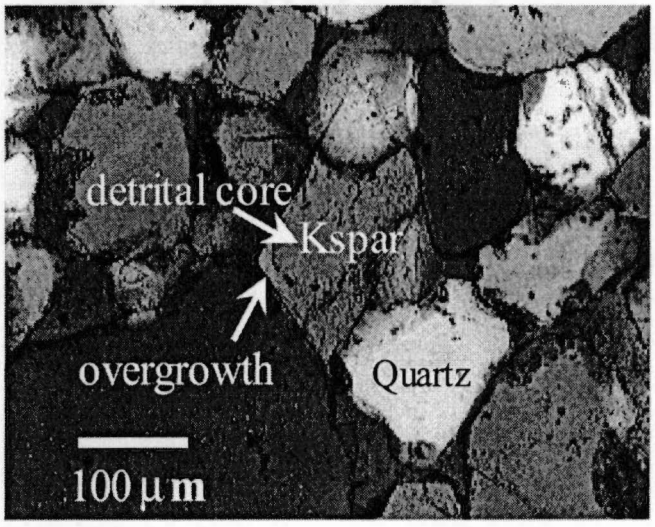

Figure 3-2. Photomicrograph of authigenic K-feldspar in Mount Simon Sandstone (core C3707, 457 m depth); notice euhedral shape of overgrowths and abundant pore space. See Figure 1 for location.

detrital cores of these feldspars have $\delta^{18}O$ values of +7 to +11‰ (summarized in Fig. 3-3; see complete data in Table 4-3). Authigenic and detrital quartz have $\delta^{18}O$ values of +20 to +30‰ and +6 to +14‰, respectively. Within-sample isotopic variations for the same authigenic mineral are 3-8‰, which is similar to or slightly greater than the expected result based on analytical precision (up to 4‰ difference between two analyses at 2σ). Variability beyond that expected from analytical precision probably reflects minor isotopic heterogeneity in the K-feldspar cements and/or possible contamination by beam overlap onto or sputtering into detrital K-feldspar cores during analysis of the small overgrowths.

The authigenic K-feldspar can be subdivided into four groups on the basis of geographic location and isotopic composition (Fig. 3-1). Group 1 K-feldspars are from the deeper, southern part of the basin and have average $\delta^{18}O$ values of +14‰ and +17‰. Group 2 is from the more shallowly buried rocks of the northern Illinois basin and has average $\delta^{18}O$ values of +17 to +19‰. Group 3 K-feldspars come from the northern periphery of the basin, along the Kankakee arch and the Michigan basin, and have average $\delta^{18}O$ values of +20 to +22‰. Group 4 comprises outcrop samples from Wisconsin and has $\delta^{18}O$ values of +23 to +24‰. A general northward-increasing trend of $\delta^{18}O$ values of authigenic K-feldspar is readily recognized. A similar regional trend is also observed for average $\delta^{18}O$ values of authigenic quartz overgrowths (Fig. 3-3), which increase from +22 to +28‰ (Group 1 to 3). There is no apparent trend in $\delta^{18}O$ values for either cement in an east-west direction.

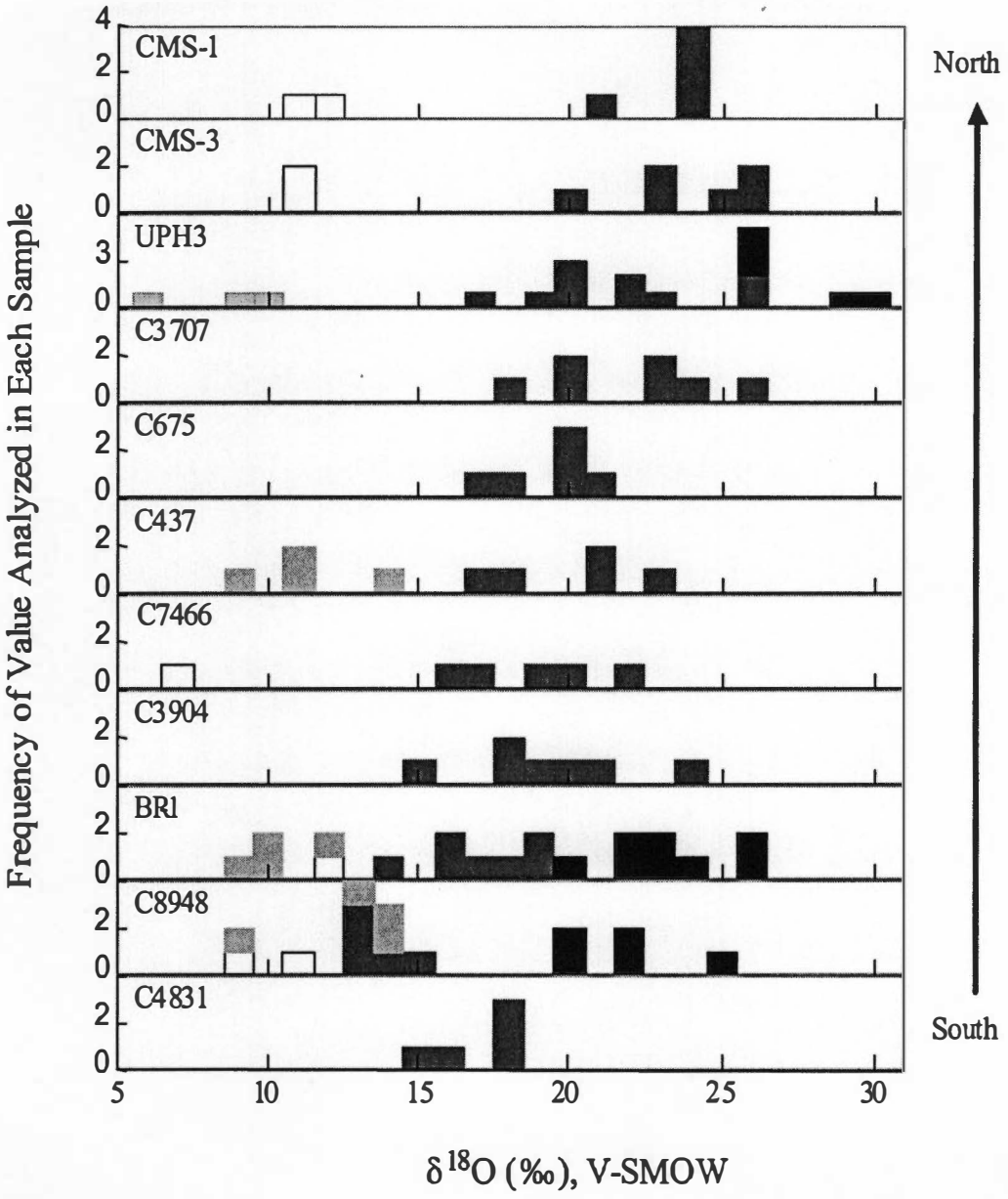

Figure 3-3 Histogram of individual ion-microprobe K-feldspar and quartz analyses in samples from Mount Simon Sandstone. Data are compared along a south-to-north traverse, from bottom to top. Open boxes - detrital K-feldspar; light-gray boxes - detrital quartz; medium-gray boxes - authigenic K-feldspar; black boxes - authigenic quartz.

Origin of Regional Isotopic Variations

Processes responsible for formation of widespread K-feldspar and quartz cements in the Mount Simon Sandstone must also be responsible for the formation of the regional trends in isotopic compositions. These processes can be evaluated on the basis of two end-member scenarios: (1) constant fluid composition and variable temperature (i.e., the cements were precipitated from local pore waters, with isotopic variation due to temperature differences linked to burial depths), or (2) variable fluid composition and constant temperature (i.e., cements are formed by regional migration of a heated basinal brine with isotopic variation due to differences in fluid composition). To extract pore-fluid $\delta^{18}O$ values from K-feldspar and quartz compositions, we used fractionation factors extrapolated from Matsuhisa et al. (1979), with K-feldspar – water fractionations (Δ) ranging from +12.2‰ at 130 °C to +20.4‰ at 50 °C and Δ(quartz-water) from +17.2‰ at 130 °C to +28.7‰ at 50 °C. Calculated fluid $\delta^{18}O$ values are ~3‰ lower if the fractionation factors of O'Neil and Taylor (1967) are used.

In the case of constant fluid compositions and by using temperature determined from burial curves, the $\delta^{18}O$ values of authigenic K-feldspar and quartz from a southern basin locality (sample C8948, $T \approx 90$ °C; Fishman, 1997) indicate pore-fluid $\delta^{18}O$ values of -1.6‰ and -0.4‰, respectively. If the northward enrichment in authigenic K-feldspar $\delta^{18}O$ values (Fig. 3-1) was due solely to temperature variation of the pore fluid, then isotopic compositions in the northern basin require the diagenetic fluid temperatures to have been very low (10-30 °C) (Fig. 3-1, Fig. 3-4A). Although authigenic quartz has been reported to precipitate from seawater at 20 °C (Si solubility of ~4.4 ppm, Mackenzie and Gees, 1971), the limited availability of Si, K, and Al in pore fluids at the very low

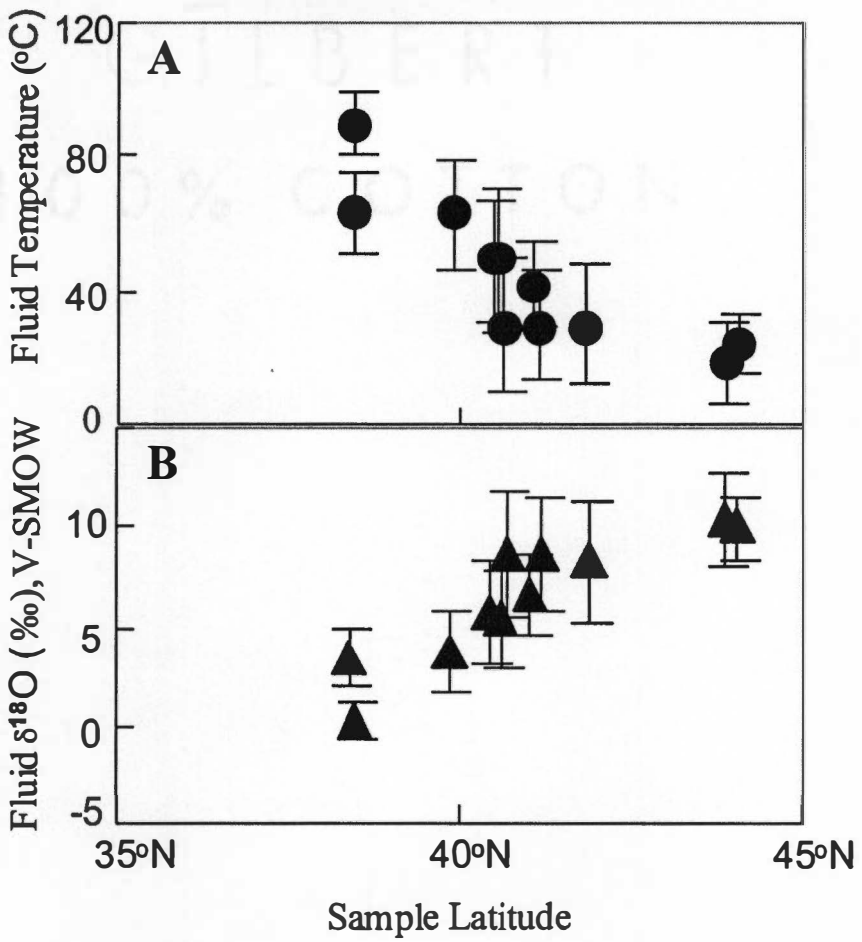

Figure 3-4. Possible models for development of regional $\delta^{18}O$ gradient in K-feldspar cements. Isotopic composition of fluid, or temperature (T), calculated from the K-feldspar - water fractionation factor of Matsuhisa et al. (1979). Individual points and error bars represent the medium and the overall deviation from each sample. A: Gradient caused by T variation across basin, assuming constant fluid composition of -1.6‰. B: Gradient caused by variation in fluid $\delta^{18}O$ values, at constant T of 115 °C.

temperatures required for northern samples in this scenario would likely preclude the formation of *abundant* euhedral K-feldspar and quartz cements. To form the 5-25 vol% of K-feldspar and quartz cement observed in the Mount Simon Sandstone at 10-30 °C would require integrated water/rock volume ratios of 20,000-100,000 (unreasonably high) just to account for the necessary Si, with even higher fluid requirements for Al.

Very low temperatures in the northern part of the basin are also inconsistent with fluid temperatures determined by oxygen isotope fractionation between authigenic K-feldspar and quartz (Δ=7 ± 1‰ and T = 70-125 °C if the quartz-albite fractionation factors of Clayton et al., 1989 are used) and from fluid inclusions (T_h = 60-145 °C) in quartz overgrowths. High and consistent salinities (>18 wt% NaCl equivalent) recorded in the fluid inclusions are further evidence that the cements formed from a highly evolved basinal fluid, rather than from relatively unmodified pore waters with a north-to-south thermal gradient. Given the agreement between fluid inclusion T*h* and quartz – K-feldspar isotope temperatures and the requirement of very high fluid volumes to precipitate the large volume of cements observed, a scenario whereby the isotopic variations were caused solely by changing temperatures resulting from progressive burial is highly unlikely.

In the case of constant temperature (115 °C, based on fluid-inclusion T_h from Fishman, 1997) and variable fluid compositions, oxygen isotope compositions of authigenic K-feldspar and quartz suggest that fluid $\delta^{18}O$ values increased from 0 ± 1‰ in southern, deeply buried samples to +10 ± 2‰ in samples from the northern part of the basin (Fig. 3-4B), by using the Matsuhisa et al. (1979) fractionation factors. The calculated fluid compositions for the deepest samples are evolved relative to Cambrian

seawater (~ -5‰, Lohmann and Walker, 1989). Typical diagenetic processes result in a progressive increase in pore-fluid $\delta^{18}O$ values (Kharaka and Thordsen, 1992). Thus, the regional trend in $\delta^{18}O$ values of authigenic K-feldspar and quartz (Fig. 3-3) is consistent with progressive diagenetic modification of pore fluids toward the north (Fig. 3-4), consistent with formation of cements as a result of regional-scale flow of heated fluids from south to north.

Note: Cathodoluminescence (CL) and fluid inclusion homogenization temperatures in quartz (60-145 °C) determined after publication of this chapter indicate that there were two generations of diagenetic fluids (Chapter 2, this thesis). Based on paragenetic relationships with quartz cements, authigenic K-feldspar in the Mount Simon Sandstone is interpreted to be closely related to diagenetic fluid flow at ~ 400 Ma and 60-95 °C. If an average temperature of 80 °C is used to calculate fluid compositions, rather than 115 °C as shown in Fig. 3-4B, fluid $\delta^{18}O$ values would increase from -2 ± 1‰ in the southern portion of the basin to +7 ± 2‰ in northern part of the basin. Fluid compositions are systematically lower by ~ 2 – 3‰ compared to compositions calculated at 115 °C. Similarly, calculated fluid compositions from quartz isotopic compositions at 80 °C vary from -2 ± 1‰ in the south to +3 ± 2‰ in the north of Illinois. In either case, fluid compositions are evolved relative to Cambrian seawater (~ -5‰), and the overall conclusions remain unchanged.

Regional Fluid Flow in the Illinois Basin

A number of different driving mechanisms for regional basinal fluid flow have been proposed, including (1) topography-driven flow, (2) flow driven by fluid-density gradients, (3) compaction-driven flow due to horizontal or vertical stress resulting from high sedimentation rate and/or tectonic compression, or (4) seismic pumping along active faults (e.g., Bethke, 1985; Sverjensky and Garven, 1992). Northward fluid flow through the Illinois basin in response to the Appalachian-Ouachita uplift is consistent with illite/smectite formation in the Mount Simon Sandstone at ca. 260 Ma (Duffin et al., 1989) and ore-formation in the Upper Mississippi Valley lead-zinc district (ca. 270 Ma, Brannon et al., 1992). By contrast, a direct link between tectonism and ca. 400 Ma K-feldspar precipitation in the Mount Simon Sandstone cannot be established. Duffin et al. (1989) suggested that flexural relaxation following the Taconic orogeny led to uplift along the eastern edge of the Michigan basin, driving westward fluid migration and associated quartz and K-feldspar cementation in the Illinois basin at ca. 400 Ma. Our results indicate northward, rather than westward, regional fluid flow. The failed Reelfoot rift and Rough Creek graben complex to the south of the basin, which was active until the Middle Cambrian, is implicated in the tilt to the south of the broad, cratonic, proto-Illinois basin. Thick accumulation (up to 5500 m) of Cambrian and older rocks in the Reelfoot rift (Drahovzal, 1997) provides a feasible source for relatively warm, basinal brines. The highly saline (>20 wt% NaCl equivalent) composition of the fluids from which quartz overgrowths precipitated is consistent with the idea that K-feldspar – precipitating solutions were derived from deeper parts of the basin (Fishman, 1997). Northward migration of fluids could have been caused by compaction-driven flow related

to a high sedimentation rate in the Reelfoot rift, although as far as is currently known, subsidence was not particularly significant in the rift at ca. 400 Ma. Seismic pumping is an alternative possibility, because the Reelfoot rift was seismically active (Clendenin et al., 1994). Although the mechanism for driving fluid flow remains enigmatic, microscale oxygen isotope analyses of authigenic minerals reveal regional trends in $\delta^{18}O$ values that can be used to identify potential regional fluid-flow directions and sources of diagenetic fluids.

Conclusions

Systematic increases of authigenic K-feldspar and quartz $\delta^{18}O$ values from the southernmost and deepest samples in Illinois to the northernmost outcrop sample in Wisconsin were revealed by ion microprobe analysis. The inconsistency between burial curves and fluid inclusion homogenization temperatures suggests the passage of anomalously hot fluid during the precipitation of authigenic minerals. Fluid temperatures determined by oxygen isotope fractionation between authigenic K-feldspar and quartz are also significantly higher than temperatures expected from burial curves. The geographic trend in oxygen isotope compositions is a result of diagenetic modification of a south-to-north migrating basinal fluid, evolving from ~ -2‰ V-SMOW in the south to +7‰ in the north.

Chapter 4

Multiple Generations of Diagenetic Fluids in the Mount Simon Sandstone: Evidence from *in situ* $^{18}O/^{16}O$ Ratios in Authigenic Quartz

Abstract

The ion microprobe was used to measure *in situ* oxygen isotope compositions from authigenic quartz overgrowths in the Mount Simon Sandstone which could be closely correlated to cathodoluminescence (CL) gray-scale images and measured fluid inclusion temperatures. $\delta^{18}O$ values vary significantly in quartz overgrowth zones having different CL intensities. Constraints on fluid compositions using point-matched fluid inclusion temperatures and the $\delta^{18}O$ values of quartz overgrowths containing the fluid inclusions were used to calculate the isotopic compositions of diagenetic fluids. The combination of CL, fluid inclusion, and oxygen isotopes reveal that quartz overgrowths were formed by two distinct fluids, in each case evolved basinal brines which migrated from south to north.

Introduction

Based on studies of cathodoluminescence (CL) and fluid inclusions in authigenic quartz (see Chapter 2) two major generations of basinal fluid migration were recognized in the Mount Simon Sandstone. Homogenization temperatures (T*h*) of fluid inclusions in quartz cements show a bi-modal distribution pattern with temperature ranges of 60– 95 °C and 100 – 145 °C, suggesting that authigenic quartz was probably precipitated from two distinct diagenetic fluids having significantly different temperatures.

CL studies indicate that the early-generation quartz cements (Qog-1) have relatively dark CL, and a later-generation cement has brighter CL (Qog-2). The second generation quartz may occur as overgrowths on Qog-1 or it may occur alone in secondary porosity. Variations of CL intensity in distinct overgrowth zones may reflect differences in the chemical composition of diagenetic fluids (Miller, 1988; Ramseyer et al., 1988, 1989; Houseknecht, 1991; Watt et al., 1997; Holten et al., 2000; Hoskin, 2000); variations in oxygen isotope compositions are thus also anticipated, particularly in light of temperature difference at which these overgrowths precipitated. Multiple generations of quartz cements in the sandstone may help to explain the wide range of quartz $\delta^{18}O$ values within individual samples reported in Chapter 3.

In this study, ion microprobe oxygen isotope analyses of authigenic quartz and K-feldspar cements from Mount Simon Sandstone, widely distributed in the Illinois basin and its periphery (Fig. 4-1), are presented. Systematic variations of isotopic compositions of both authigenic mineral phases in the basin are discussed. Two sets of characteristic $\delta^{18}O$ values from authigenic quartz overgrowths are reported. One set of analyses focuses on quartz overgrowths that show distinct CL zonation to evaluate the hypothesis that significant differences in $\delta^{18}O$ values within different CL zones may have contributed to large within-sample variations of oxygen isotope compositions. Another set of isotopic analyses is from quartz overgrowths containing fluid inclusions that were measured for homogenization temperatures. These temperatures, in combination with the $\delta^{18}O$ values of these quartz overgrowths, may be used to constrain fluid isotopic compositions. Isotopic studies on these different generations of quartz overgrowths may be useful to characterize changes in the physiochemical properties of diagenetic fluids.

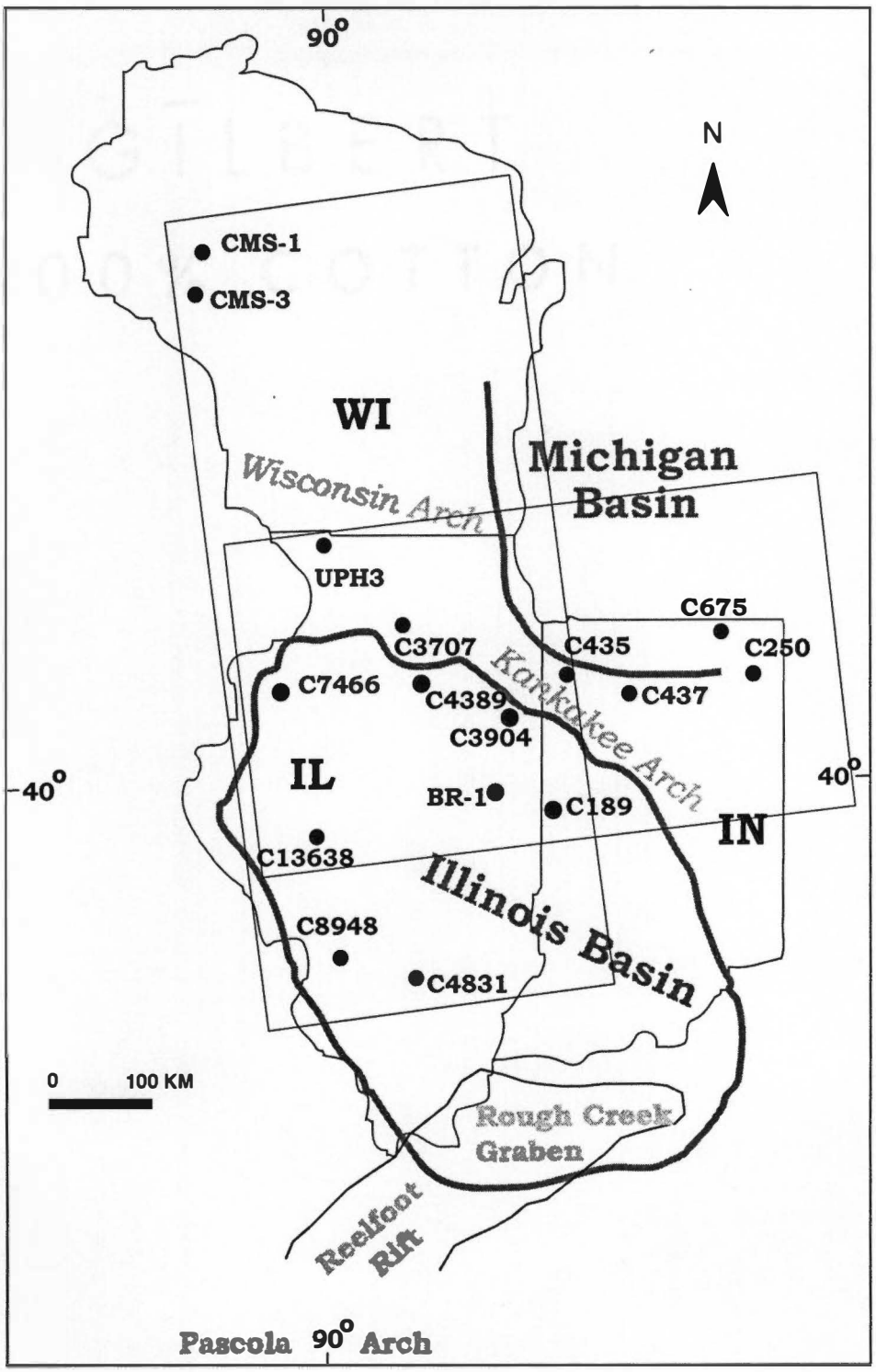

Figure 4-1 Map showing an outline of the Illinois Basin and surrounding area, and sample localities. Rectangular boxes define sampling transects used to evaluate regional fluid migration (south to north and west to east).

Sample Preparation and Experimental Techniques

Transmitted- and reflected- light digital images were taken to help locate desired quartz and K-feldspar overgrowths. Standard thin sections were prepared for ion microprobe analysis of oxygen isotopic composition in authigenic quartz and K-feldspar. Chips containing fluid inclusions in host quartz overgrowths, cored from fluid inclusion sections, were used for electron microprobe CL analysis after measurement for fluid inclusion temperature. These chips were mounted with epoxy, using 1"-diameter phenol rings as a sample holder. The carbon coat was removed from the chips after finishing the EMP CL analysis. The same samples were then analyzed by SIMS for oxygen isotope compositions of the desired quartz overgrowths. Four additional thin sections containing large quartz overgrowths were also selected for CL examination. Overgrowths with zoned CL were then analyzed by ion microprobe for their oxygen isotope compositions.

Samples with gold coat were sputtered by a primary beam of $^{133}Cs^{+}$ ions, with beam intensity of 2 – 5 nA and being accelerated at 10 keV, and negative secondary ions were extracted for analysis. The Cameca normal-incident electron gun was used to compensate for sample charging. The secondary-ion accelerating voltage was 4150 eV, and the secondary mass spectrometer accepted secondary ions with energy of 4500 ± 20 eV (an offset of 350 ± 20 eV for extreme energy filtering). Secondary ion intensities were measured using an electron multiplier, with dead time of ~15 nanoseconds. With ^{18}O counts for 5 seconds and ^{16}O for 1 second, 120 to 200 cycles of $^{18}O/^{16}O$ ratios were collected for each analysis in order to have an accumulation of ~ 10^{6} counts or more of ^{18}O for each analysis, yielding a theoretical internal precision of 0.6 to 1‰ (1σ) based on counting statistics. Estimated uncertainty is typically 0.4 to 0.8‰ based on the standard

deviation of the repeated-measured (N=4-12) standard minerals during an analytical session. Analytical precision (1σ) was calculated based on square root of the sum of the square of these two standard errors. Readers are referred to Riciputi and Paterson (1994) and Riciputi et al. (1998) for further analytical details.

Analytical Results and Discussion

Systematic Variations of Isotopic Compositions Throughout the Basin

Ion microprobe analyses of mineral $\delta^{18}O$ values collected in this study are listed in Table 4-1. A northward-increase in average $\delta^{18}O$ values of all authigenic quartz (i.e., overgrowth generations were undifferentiated), similar to the one previously presented for authigenic K-feldspar in Chapter 3, is shown in Figure 4-2. Samples localities have been plotted along a south-to-north traverse, as defined in Fig. 4-1 and Table 4-1. Data from the three eastern-most samples, located in the present day Michigan basin, are shown as open symbols. As discussed in a later section, the Michigan basin samples may have experienced a different history of fluid-rock interactions.

The $\delta^{18}O$ values for authigenic K-feldspar and quartz throughout the basin span a range of ~ 15‰ (Table 4-1). The maximum temperature difference of fluid inclusion homogenization temperatures reported in Chapter 2 is 85°C (range 60 –145 °C). Assuming fluid composition remains unchanged, a temperature change from 60 °C to 145°C would result in change in $\delta^{18}O$ of authigenic minerals of 6 – 7‰. Thus, temperature variation alone cannot fully account for the wide range of $\delta^{18}O$ values measured in authigenic minerals. Instead, the regional, northward increasing trend in $\delta^{18}O$ values is interpreted as the result of south-to-north migration and modification of

Table 4-1 Oxygen isotopic compositions (‰, V-SMOW) of quartz and K-feldspar in the Mount Simon Sandstone

Sample ID	Sample Latitude	Distance from the south (km)*	$\delta^{18}O$ Authigenic Quartz	$\delta^{18}O$ Authigenic K-feldspar	$\delta^{18}O$ Detrital Quartz	$\delta^{18}O$ Detrital K-feldspar
				24.1		12.2
				23.8		10.7
CMS1	44	580		24.4		
				20.5		
				23.5		
				27.9		
				20.1		11.1
				23.1		10.7
CMS3	43.8	563		22.7		
				26.4		
				24.6		
				25.6		
			26.2	26.2	5.7	
			26.2	20.2	8.7	
			29.3	26.2	10.1	
			29.7	18.5		
			26.2	22.2		
			25.7	20.1		
			21.5	19.5		
			29.1	17.2		
UPH3	41.9	362	23.5	22.2		
			23.4	23.3		
			26.8	18.6		
			26.4			
			26.6			
			24.3			
			27.8			
			27.5			
			23.8			
			23.0			
			26.4			
				20.0		
				20.1		
C675	41.6	312		23.3		
				17.3		
				18.3		
				20.4		

Table 4-1 Continued

				22.5		
				19.9		
				23.2		
C3707	41.3	284		26.5		
				23.6		
				20.4		
				18.2		
			17.2	16.8	10.4	
			16.4	21.0		
			20.9	21.6		
			22.4	17.4		
			18.1			
			24.9			
			23.9			
			23.1			
			22.2			
C250	41.1	269	24.0			
			24.3			
			17.8			
			20.9			
			21.7			
			17.4			
			23.0			
			23.3			
			23.0			
			25.2			
C435	41	260	25.6			
			23.4			
			27.2	26.5	8.6	12.0
			26.5	21.2	13.9	
C437	40.9	247	26.8	22.9	11.1	
			27.7	22.0	11.2	
			22.0	17.4		
			21.4			
			23.9	15.3		
			26.4	21.0		
			24.0	23.5		
C4389	40.8	245	21.7			
			24.7			
			23.9			
			23.1			
			23.7			

Table 4-1 Continued

			23.3	19.5		7.1
				22.4		
C7466	40.7	235		18.8		
				16.8		
				16.0		
			22.0	23.5		
				20.5		
				19.7		
C3904	40.5	217		17.5		
				15.2		
				18.2		
				18.9		
			18.9	19.2	10.0	12.0
			22.7	17.2	12.2	
			24.1	18.0	8.8	
			23.0	16.1	10.1	
BR-1	39.9	158	26.2	13.6		
			20.4	18.9		
			22.0	16.0		
			25.5			
			22.2			
C189	39.7	143	20.0	17.6		
			16.0			
C13638	39.4	116	25.8			
			21.5	12.7	13.5	9.2
			20.0	13.8	14.2	10.9
C8948	38.6	39	25.2	14.9	12.7	
			21.6	13.5	8.7	
			19.7	13.1		
			18.8	17.7		
			15.9	18.0		
			22.2	16.3		
			19.7	14.6		
			15.1	17.7		
C4831	38.4	20	24.9			
			24.6			
			20.4			
			20.2			
			17.6			

* Relative to a point ~ 20 km to the south of sample C4831, see Fig. 4-1 for localities.

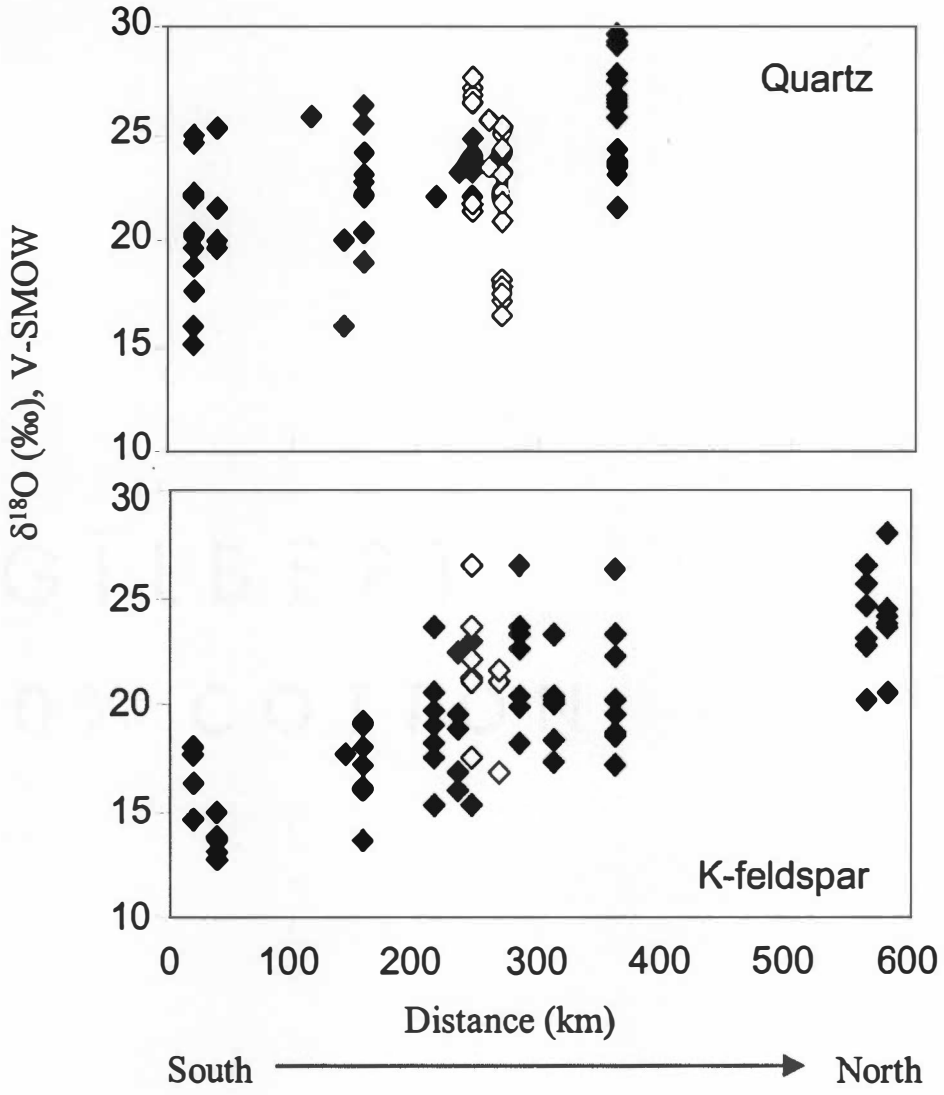

Figure 4-2 Oxygen isotopic compositions of authigenic quartz and K-feldspar from south to north. See Table 4-1 for explanation of how transect distance is defined. Solid symbols – samples from the Illinois basin, Kankakee arch and Wisconsin arch; Open symbols – samples from the Michigan basin.

evolving brines (Chapter 3). Diagenetic processes typically result in a progressive increase in pore fluid $\delta^{18}O$ values (Whitney and Northrop, 1987; Kharaka and Thordsen, 1992; Worden et al., 1999), and an increase in fluid $\delta^{18}O$ values is expected with migration of evolved basinal fluids. The calculated pore fluid compositions for the deepest (southernmost) samples average -2 to -4‰ (Fig. 4-3), slightly enriched relative to Cambrian seawater (~ -5‰, Lohmann and Walker, 1989), although uncertainty in low temperature mineral-fluid fractionation factors precludes conclusive determination of fluid compositions.

Based on the results presented in Chapter 2 and published data on diagenesis in the Mount Simon Sandstone, there is only one major diagenetic event associated with authigenic K-feldspar (~ 400 Ma); a second potassic diagenesis precipitated I/S. Fluid inclusion T*h* for generation 1 quartz (contemporaneous with the authigenic K-feldspar) fall in a narrow range from 60 to 95 °C. Assuming constant average fluid temperature of 80 °C for all samples, calculated fluid compositions based on oxygen isotope compositions of authigenic K-feldspar ($\Delta^{18}O_{feldspar\text{-}fluid}$ ~16.7‰, Matsuhisa et al., 1979) indicate that fluid $\delta^{18}O$ values increased from -2.6 ± 1‰ (1 standard deviation at population of individual analyses) in southern, deeply buried samples to ~ +5 ± 3‰ in the northern basin, and +7.4 ± 2‰ in outcrop samples from Wisconsin (Fig. 4-3A). Using the same temperature (~80 °C), average $\delta^{18}O$ values of fluids associated with bulk undifferentiated authigenic quartz increase from -3.5 ± 3‰ in the southern basin to +2.5 ± 2‰ in the northern basin (Fig. 4-3B); quartz overgrowths were too small to measure in the Wisconsin outcrop samples. For both minerals, fluid compositions increased ~ 6 –

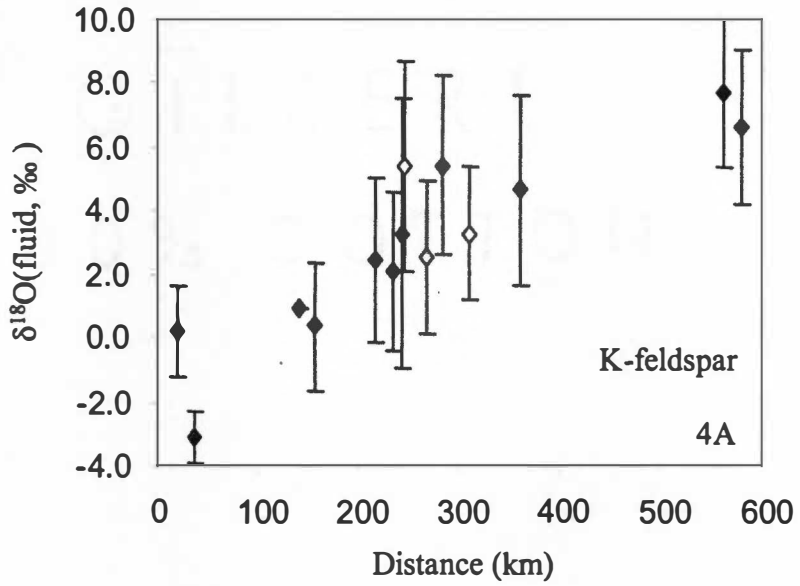

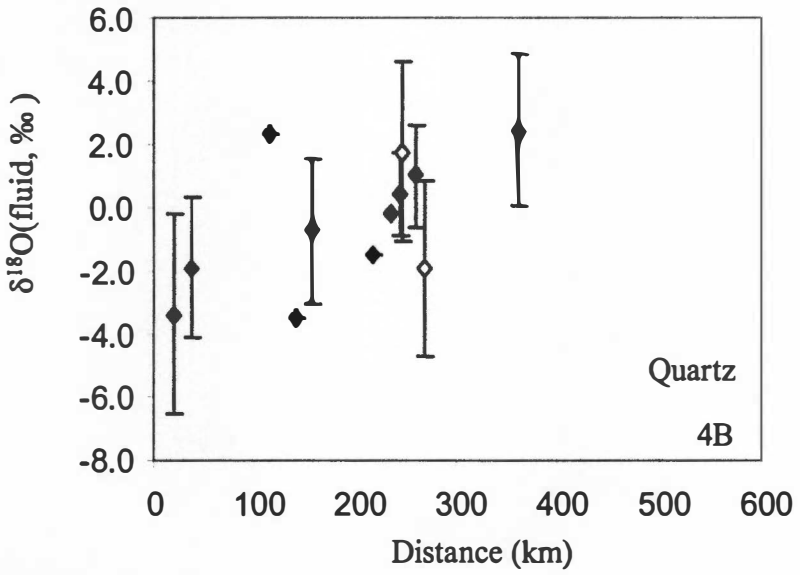

Figure 4-3 Model for development of regional $\delta^{18}O$ gradient in K-feldspar and quartz cements, assuming evolved fluid compositions and constant temperature (80 °C). Mineral-fluid fractionation factors from Matsuhisa et al. (1979). Medium calculated value (point) and the overall deviation (bar) from each sample are shown. Single quartz data from three samples also presented. Open symbols represent data from the Michigan basin.

10‰ from south to north, although fluid compositions derived from undifferentiated quartz are somewhat lower as compared to K-feldspar, which may just reflect uncertainty in fractionation factors at low temperature.

Isotopic Variations in Zoned Quartz Cements

The wide range of $\delta^{18}O$ values of authigenic minerals from individual samples in the Mount Simon Sandstone, and the south-to-north increasing trend of $\delta^{18}O$ values (Chapter 3), suggest a complicated diagenetic history. Evidence of multiple-generation quartz overgrowths in the Mount Simon Sandstone from fluid inclusion and cathodoluminescence (CL) studies (Chapter 2) suggest that there were at least two fluids (a higher- and a lower- temperature one) associated with authigenic quartz formation. Based on fluid inclusion results, an earlier generation of quartz cements with darker CL is likely related to the lower-temperature diagenetic fluid, whereas a later generation quartz cement having relatively bright CL is associated with a higher-temperature fluid. It is impossible, however, to identify different generations of quartz overgrowths without the assistance of CL images. Thus, the large range of $\delta^{18}O$ values from quartz overgrowths (Table 4-1), particularly those analyzed early in this project before EMP CL was used, may represent a mixture of various proportions of generation 1 and 2 quartz compositions.

Zoned quartz overgrowths having an early, inner, and darker-luminescent generation 1 (i.e., Qog-1 as defined in Chapter 2) cement and a later, outer, and brighter-luminescent, generation 2 cement (Qog-2) were analyzed to characterize $\delta^{18}O$ values of the different generations of quartz cement (Table 4-2, Fig. 4-4). In all of the pairs

Table 4-2 Oxygen isotopic compositions of zoned quartz overgrowths

Pair No.	Sample Number	Sample Description	$\delta^{18}O$ (‰, V-SMOW)*	Δ (inner-outer)**
1	250d3a2	Outer zone, relatively bright CL	18.1 ± 0.9	6.8
1	250d3a3	Inner zone, relatively dark CL	24.9 ± 0.9	
2	250d3b1	Outer zone, relatively bright CL	23.1 ± 0.9	0.8
2	250d3b1	Inner zone, relatively dark CL	23.9 ± 0.9	
3	250d2a2	Outer zone, relatively bright CL	17.8 ± 0.9	6.5
3	250d2a1	Inner zone, relatively dark CL	24.3 ± 0.9	
4	250d1a2	Outer zone, relatively bright CL	17.4 ± 0.7	4.3
4	250d1a1	Inner zone, relatively dark CL	21.7 ± 1.0	
5	250d1c1	Outer zone, relatively bright CL	23.0 ± 1.0	2.2
5	250d1c2	Inner zone, relatively dark CL	25.2 ± 1.0	
6	4389d5	Outer zone, relatively bright CL	21.7 ± 1.0	3.0
6	4389d5	Inner zone, relatively dark CL	24.7 ± 1.0	
7	4389d4	Outer zone, relatively bright CL	23.9 ± 1.0	-0.8
7	4389d4	Inner zone, relatively dark CL	23.1 ± 1.0	
8	4831d3a	Outer zone, relatively bright CL	24.9 ± 1.1	-0.3
8	4831d3a	Inner zone, relatively dark CL	24.6 ± 1.0	
9	4831d5aa	Outer zone, relatively bright CL	20.2 ± 1.1	0.2
9	4831d5aa	Inner zone, relatively dark CL	20.4 ± 1.0	

* Errors are 1σ of each individual analysis (see text).

** Difference of oxygen isotope compositions between the inner- and outer- zone overgrowths.

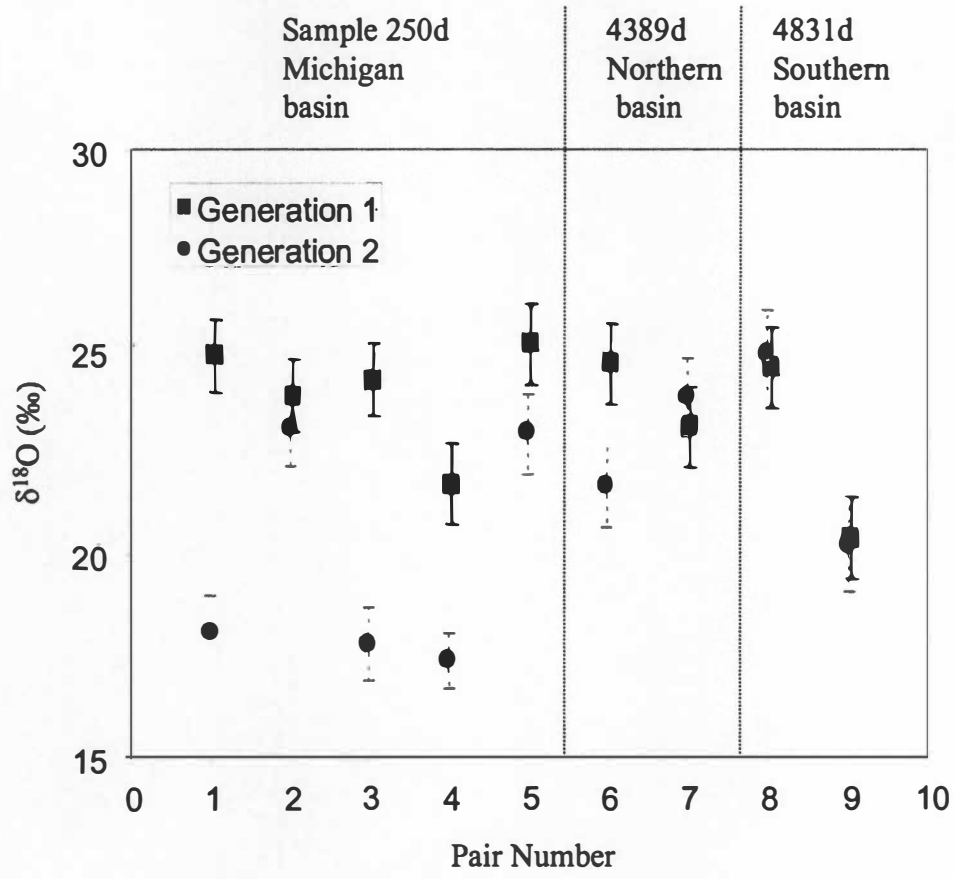

Figure 4-4 Differences in the oxygen isotope compositions between inner-zone (generation 1) and outer-zone (generation 2) quartz overgrowths covering individual detrital grains. Errors are 1σ of individual analysis.

analyzed, $\delta^{18}O$ values of Qog-1 are equal to, or greater than $\delta^{18}O$ values of Qog-2 [within analytical error (± 1‰ at 1σ)].

The $\delta^{18}O$ values of authigenic quartz are mostly > 20‰, except for three quartz overgrowths measured from the Michigan basin (sample 250d), which range from 17 to 18‰ (Fig. 4-4). The $\Delta^{18}O$ (inner-outer) values between these Qog-1 and Qog-2 pairs range from 4.3 to 6.8‰, and are much larger than other pairs (Table 4-2).

Constraints of Diagenetic Fluids Based on T*h* - $\delta^{18}O$ *Point-matched Analyses*

Working with electron microprobe CL gray-scale images, the oxygen isotope compositions of quartz overgrowths from chips used for fluid inclusion studies were analyzed (Table 4-3). Fluid inclusions entrapped in these same overgrowths were measured for homogenization temperatures prior to any other analysis. Unfortunately, many overgrowths with entrapped fluid inclusions are not large enough for ion microprobe analysis, and many more large overgrowths that are suitable for ion microprobe analysis do not contain workable fluid inclusions. These limitations demonstrate the difficulty of obtaining data such as shown in Table 4-3!

Using $\delta^{18}O$ values of individual quartz overgrowths and the T*h* of associated fluid inclusions entrapped within these specific overgrowths, the isotope compositions of the diagenetic fluids can possibly be better constrained as much of the temperature uncertainty is eliminated. There appears to be no systematic relationship between T*h* in fluid inclusions and $\delta^{18}O$ values of the undifferentiated authigenic quartz (Fig. 4-5), supporting our previous observations (this chapter) that fluid temperature variation is not the dominant control on the observed regional variation of mineral $\delta^{18}O$ values.

Table 4-3 Position-matched oxygen isotopic compositions of authigenic quartz and homogenization temperature of fluid inclusions

Sample	Sample Locality (Latitude, ° N	T*h* (°C)	$\delta^{18}O$ (‰, V-SMOW)
UPH3	41.9	70	25.7
	41.9	75	21.5
	41.9	115	29.1
	41.9	80	23.5
	41.9	85	23.4
	41.9	100	26.8
	41.9	100	26.4
	41.9	100	26.6
C250	41.1	90	17.2
	41.1	100	16.4
	41.1	140	20.9
C435	41.0	90	25.6
	41.0	110	23.4
C4389	40.8	75	23.9
	40.8	75	26.4
	40.8	125	24.0
C7466	40.7	145	23.3
C3904	40.5	95	22.0
BR-1	39.9	80	18.9
C189	39.7	85	20.0
	39.7	145	16.0
C13638	39.4	95	25.8
C4831	38.4	80	18.8
	38.4	85	15.9
	38.4	100	22.2

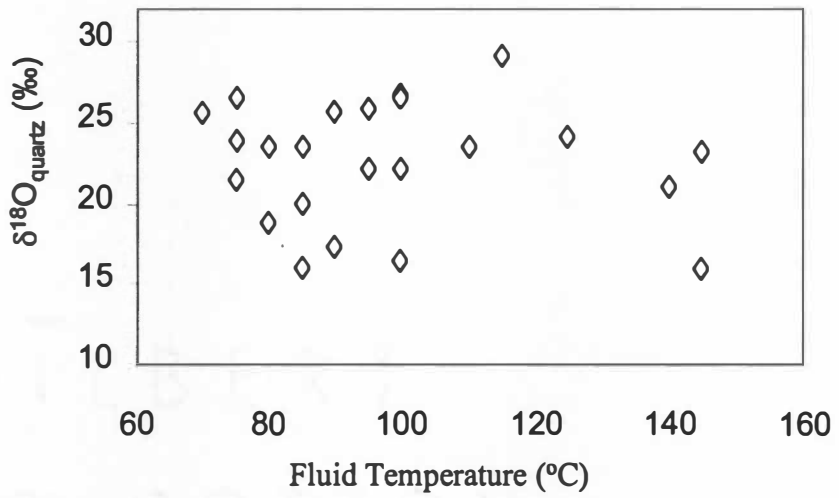

Figure 4-5 Diagram showing no relation between fluid temperature and $\delta^{18}O$ values of authigenic quartz.

Calculating fluid $\delta^{18}O$ values using the matched fluid inclusion temperatures and $\delta^{18}O$ values of host quartz cements (Fig. 4-6) indicates that temperature does play a role in determining isotopic compositions. Two distinct $\delta^{18}O_{fluid}$ trends can be seen, which correspond to Qog-1 ($T < 95$ °C) and Qog-2 ($T > 95$ °C) diagenetic fluids. The calculations suggest that Apparently the < 95°C and > 95°C fluids had distinct $\delta^{18}O$ values, but similar trends in the evolution of their compositions, consistent with the observation of two major CL types in the quartz overgrowths. The northward increasing trends of $\delta^{18}O$ values of diagenetic fluids shown in Fig. 4-6 confirm that diagenetic fluids evolved as they migrated from south to north.

On the basis of the $\delta^{18}O$ values of quartz, the $\delta^{18}O_{fluid}$ in equilibrium with generation 1 quartz in the southern basin is ~ -5‰ (using Matsuhisa's 1979 fractionation curve), similar to the Late Cambrian seawater (~ -5‰, Lohmann and Walker, 1989), and it evolved to 0 ~ + 2‰ in the northern basin. Calculated fluid compositions are 3‰ higher, if the fractionation curve of Kawabe (1978) is used. Even more evolved isotopic values are expected for samples in Wisconsin. Given the consistency between $\delta^{18}O_{seawater}$ and the slightly evolved $\delta^{18}O_{fluid}$ in the south part of the basin (Fig. 4-6), between fluid inclusion temperatures (60 – 90 °C) and maximum burial temperatures (<95 °C) in the south at ~ 400 Ma, and the petrographic observation of contemporaneous quartz (Qog-1) and K-feldspar cements (Fishman, 1997), a northward migration of basinal fluid is implied in association with the formation of Qog-1. This scenario does not require a superheated fluid for the formation of Qog-1 and contemporaneous authigenic K-feldspar.

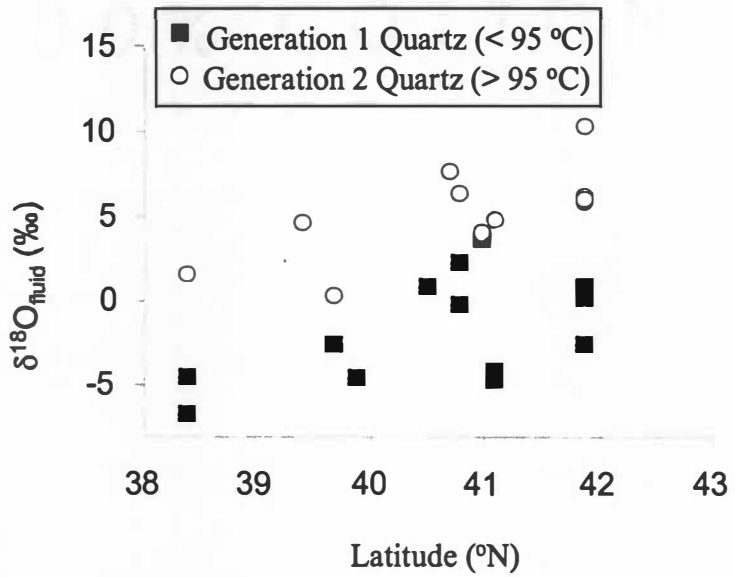

Figure 4-6 Calculated $\delta^{18}O$ (fluid) values based on isotopic compositions of Qog-1 and Qog-2 cements at temperatures determined from fluid inclusion microthermometry in same quartz overgrowths. The data define two separate, northward increasing trends in $\delta^{18}O$ values of migrating basinal fluids.

The $\delta^{18}O_{fluid}$ values calculated from generation 2 quartz (excluding the three Michigan Basin analyses) are systematically 6‰ higher than generation 1 fluid. The higher $\delta^{18}O_{fluid}$ values of Qog-2 cements (from ~ 1‰ in the south to ~ +7‰ in the north, Fig. 4-6) are interpreted to indicate precipitation from more-evolved basinal brines, perhaps emanating from further south and deeper areas. A diagenetic fluid with temperatures much higher than generation 1 fluid is expected.

Relatively lower $\delta^{18}O$ values of Qog-2 cements may result from lower fluid isotopic compositions and/or higher fluid temperatures. Graham et al. (1996) reported ion microprobe $\delta^{18}O$ values of authigenic and detrital quartz from the St. Peter Sandstone in the Michigan basin and Wisconsin arch. They found that $\delta^{18}O$ values of authigenic quartz from the Wisconsin arch (16 – 32‰) are systematically higher than those from Michigan basin (13 – 22‰). They suggested that authigenic quartz in the Michigan basin was precipitated from formation water or basinal brines at high temperature (T_h = 80-150 °C), with little or no meteoric component. Most homogenization temperatures of fluid inclusions in sample C250 cluster between either 90-100 °C or 135-140 °C (Chapter 2, Table 2-1). As indicated in Chapter 2 previously, Qog-2 overgrowths were precipitated at higher temperatures than Qog-1. If the low $\delta^{18}O$ values of the three Qog-2 quartz (17 – 18‰) formed at higher fluid temperatures (135 - 140 °C), they suggest $\delta^{18}O_{fluid}$ values of + 1‰ (using the fractionation curve of Matsuhisa et al., 1979). Using the average T_h of 110 °C determined for all data from sample C250 yields $\delta^{18}O_{fluid}$ values of -2‰. These fluids are ~5‰ lighter than those calculated from Qog-2 cements in the northern part of the basin. These results suggest that at least some Qog-2 cements from sample C250d were precipitated from upwelling basinal brines of higher temperatures and different

compositions than samples in the Illinois basin. Because the Kankakee arch developed concurrently with these two basins, and owing to the subsidence of the two basins (Root and Onasch, 1999), there may have some difference between the Illinois basin and the Michigan basin with respect to diagenetic history and basinal fluid temperature. Duffin et al. (1989) suggested a westward Michigan basin brine migration in response to the uplift of Findlay and Algonquin arch on the east side of Michigan basin.

Conclusions

Bulk $\delta^{18}O$ values of authigenic K-feldspar and quartz in the Mount Simon Sandstone show similar northward-increasing trends. The $\delta^{18}O$ values for authigenic K-feldspar and quartz throughout the basin span a range of ~15‰. Variation of measured fluid temperature across the basin can only account for part of the variations of $\delta^{18}O$ in authigenic minerals. Regional, northward-increasing trend in $\delta^{18}O$ values is interpreted as the result of south-to-north migration and modification of evolving brines.

Ion microprobe oxygen isotope analyses of CL-zoned authigenic quartz overgrowths in the Mount Simon Sandstone reveal differences in the $\delta^{18}O$ values of the different quartz phases. $\delta^{18}O$ values of generation 1 quartz overgrowths (Qog-1) are higher, or equal to, those of generation 2 quartz (Qog-2). These differences may account for large within-sample $\delta^{18}O$ variations in undifferentiated quartz population. These results confirm the conclusion from CL and fluid inclusion studies that at least two generations of diagenetic fluids were responsible for the formation of quartz overgrowths in the Mount Simon Sandstone.

Fluid $\delta^{18}O$ compositions calculated from $\delta^{18}O$ values of some quartz overgrowths matched with homogenization temperatures measured in their entrapped fluid inclusions show two distinct trends of fluid composition (Fig. 4-6). Each trend shows a south-to-north increase in fluid $\delta^{18}O$ compositions. Qog-1 was precipitated from a northward migrating basinal brine having relatively lower fluid temperature (< 95 °C); this temperature is concordant with the maximum burial temperature in the south part of the basin. It appears that no superheated fluid is required for the formation of Qog-1 and contemporaneous authigenic K-feldspar. Generation 2 quartz overgrowths were associated with a fluid with higher temperatures that could have originated from deeper burial of the Mt. Simon Sandstone during the Permian. The evolution of fluid isotopic compositions for both episodes of northward fluid migrations in the Illinois basin are interpreted as the result of fluid-sediment interaction as the fluids passed through the Mount Simon Sandstone.

Chapter 5

Ion Microprobe Trace Element Study of Authigenic K-feldspar and Quartz in the Mount Simon Sandstone

Abstract

The trace element contents of authigenic K-feldspar and quartz in the Mount Simon Sandstone were determined by ion microprobe. Authigenic K-feldspar contained relatively abundant (>1 ppm) Rb, Sr, Ba, Pb, Fe, Mg, B, Ti, and Cl. K, Al, Fe, B, Ti, Mg, and Cl were significant (>1 ppm) in quartz cements. Positive covariation was observed among Sr-Ba-Pb-Rb and Mg-Ca-Cl in authigenic K-feldspar, and among Na-Mg-Ca-Cl and K-Al in authigenic quartz. Covariation of trace elements may be attributed to several factors, including their similar geochemical behavior, continuous chemical changes in the fluid as a result of geological processes, variations in temperature, and the requirements of solid solution charge compensation. Concentrations of Ba, Sr, Rb,Pb, Fe, Ca, and Ce in diagenetic fluids were estimated based on trace element contents of authigenic K-feldspar cements and distribution coefficients between sanidine and hydrothermal fluids. Calculated fluid compositions show weak, northward-increasing trends in Fe, Ce, and Sr content, which may be related to the northward migration of diagenetic fluids. Two generations of diagenetic fluids are suggested by systematically different total concentrations of alkaline and alkaline earth elements in different quartz CL zones.

Introduction

South-to-north trends of increasing $\delta^{18}O$ values of authigenic K-feldspar and quartz in the Mount Simon Sandstone were interpreted to be associated with northward migrations of basinal fluids (Chapter 3 and 4). Evidence from homogenization temperatures (T*h*) of fluid inclusions and cathodoluminescence (CL) zonation in authigenic quartz cements indicate that there are at least two generations of fluids (Chapter 2). Calculated $\delta^{18}O$ values of diagenetic fluids using paired isotopic compositions and fluid inclusion T*h* suggest that the two fluids have distinct isotopic compositions and evolved during separate events of south-to-north fluid migration (Chapter 4). Temporal and spatial variations in the trace element content of authigenic minerals may provide additional evidence of fluid composition, mass transfer, and basinal fluid migration through the Mount Simon Sandstone.

Conventional trace element analysis of whole rock powders or bulk mineral separates may mix authigenic and detrital components, or several generations of authigenic material. Mechanical separation of authigenic and detrital minerals, or several generations of authigenic phase is tedious and thorough separation is difficult. Thus, evidence of diagenetic mass transfer can be significantly obscured (Milliken et al., 1994). In this study, results of an investigation of trace elements in authigenic K-feldspar and quartz in the Mount Simon Sandstone, using secondary ion mass spectrometry (SIMS), are presented. The objectives were to utilize the *in situ*, high-resolution (15 - 30 μm), analytical capabilities of SIMS to characterize trace element abundances in authigenic minerals, and to evaluate their usefulness for defining fluid migration and mass transfer in the Illinois basin. The data presented in this study may further constrain the

composition and flow direction of these diagenetic fluids and provide additional insight into the microscale processes controlling fluid or rock chemistry.

Methodology

Authigenic K-feldspar from seven localities and authigenic quartz from nine localities (Fig. 5-1) were selected for trace element analysis. This study used the same polished thin sections and fluid inclusion chips discussed in Chapter 3 and 4. The samples selected were previously analyzed for fluid inclusion T*h* and SIMS $\delta^{18}O$ of authigenic minerals (Chapter 3 and 4). Both transmitted light and electron microprobe CL images were used to help navigate and find the overgrowths (>25 μm) selected for ion microprobe analysis.

Ion microprobe analyses were performed on the Cameca 4f ion microprobe at Oak Ridge National Laboratory. Thin sections or sample chips mounted in phenol rings were coated with gold to ensure surface conductivity. An O^- primary beam accelerated at 12.5 kV and with 2.5 nA current was used to sputter the sample with an area ~ 20 μm in diameter. Positive charged secondary ions were extracted for analysis using an energy offset of 80 eV. Secondary ions were counted using an electron multiplier, with a system deadtime of ~ 15 nanoseconds. Counting times for each element varied according to its abundance, but did not exceed 8 seconds in each magnetic cycle through the selected masses. From 6 to 15 magnetic cycles were used for each analysis. Elemental intensities were ratioed to that of ^{30}Si, and trace element contents were calibrated using a synthetic glass (NIST-610) as standard (containing ~ 500 ppm of individual trace contents). Readers are referred to Riciputi et al. (1994) for further analytical details.

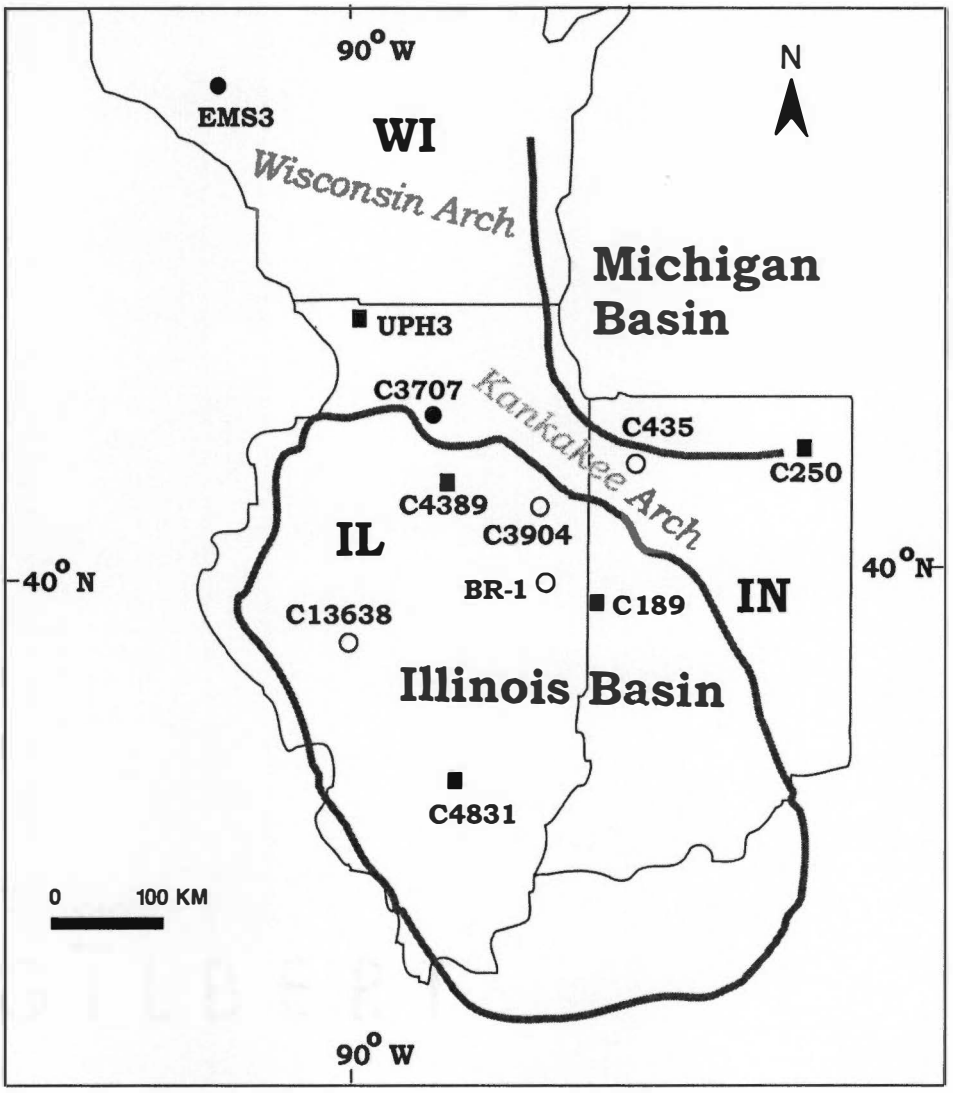

Figure 5-1 Map showing an outline of the Illinois Basin and surrounding area, and locations of cores analyzed. ■ - K-feldspar and quartz analyzed; ● - K-feldspar analyzed; ○ - Quartz analyzed.

A total of 28 single-spot analyses of authigenic K-feldspar in seven Mount Simon Sandstone samples and 45 single-spot analyses of authigenic quartz in nine samples were performed (localities indicated in Fig. 5-1). K-feldspar cements were analyzed for 13 trace elements (Li, Rb, Mg, Ca, Sr, Ba, Pb, B, Fe, Ti, Ce, Y, and Cl). Eleven elements (Li, Na, K, Be, Mg, Ca, B, Al, Fe, Ti, and Cl) were analyzed in quartz overgrowths. Sodium is present to some degree in almost all alkali feldspar, however, it was not measured in K-feldspar overgrowths as its ion signal was too intense for the electron multiplier to count the signal properly. Detection limits of most elements generally are << 1 ppm. Precision is based on the two standard errors for multiple element/Si ratios measured for each analysis, and is generally similar to the 1σ (standard deviation) error estimated from the number of ion counts based on counting statistics. It is generally better than 10% for most analyses; but can be much worse for elements with very low abundances (see Table 5-1 and 5-2). Absolute accuracy is poor (probably 30-200% depending on the element) due to differences in the matrix effects between the synthetic standard and authigenic cements in sandstone. However, relative variations between different analyses are accurate at the level of counting statistics. For purposes of comparing local and regional trace element trends, these data are useful and provide information about trace element behaviors in the diagenetic system.

Analytical Results

Trace Elements in Authigenic K-feldspar Overgrowths

Trace element concentrations in K-feldspar overgrowths are shown in Table 5-1. The contents of individual trace elements in authigenic K-feldspars may differ by three

Table 5-1 Trace element concentrations (ppm) in authigenic K-feldspar *

Analytical #	3-2tr18		3-2tr19		3-2tr20		3-2tr21		3-2tr12		3-2tr13	
Sample #	4831ak3		4831ak4		4831ak6		4831ak2		189fb3		189fb3	
Grain description	Ksp tip		Ksp tip		Ksp Og-tip		Ksp Og-tip		Ksp Og		Ksp Og-tip	
Ti	5771 ±	92	2.7 ±	0.3	4.9 ±	0.2	9.5 ±	0.3	1.9 ±	0.3	2.5 ±	0.5
Rb	83 ±	3	41 ±	2	38 ±	1	422 ±	16	85 ±	3	60 ±	2
Y	0.8 ±	0.1	0.03 ±	0.01	0.06 ±	0.01	0.14 ±	0.04	0.1 ±	0.1	0.04 ±	0.02
Ba	134 ±	6	40 ±	1	46 ±	2	1059 ±	4	12.9 ±	0.7	69 ±	1
Ce	60 ±	1	0.09 ±	0.03	0.16 ±	0.03	0.3 ±	0.1	1.1 ±	0.4	3.5 ±	0.6
Pb	23 ±	4	8 ±	1	6 ±	2	54 ±	6	6 ±	3	5 ±	2
Li	0.85 ±	0.04	1.3 ±	0.1	1.3 ±	0.1	0.5 ±	0.1	5.4 ±	0.6	7.0 ±	0.9
Mg	39 ±	2	11.3 ±	0.9	6.9 ±	0.5	21 ±	2	8.0 ±	0.3	23 ±	3
Cl	37 ±	3	42 ±	2	13.7 ±	0.6	37 ±	1	38 ±	3	85 ±	6
Ca	1.15 ±	0.01	0.76 ±	0.01	0.37 ±	0.02	0.54 ±	0.02	0.17 ±	0.01	0.362 ±	0.002
Fe	328 ±	8	287 ±	4	295 ±	2	486 ±	6	299 ±	4	332 ±	4
Sr	75 ±	2	7.2 ±	0.2	7.5 ±	0.2	10.7 ±	0.4	0.40 ±	0.01	2.0 ±	0.1
B	3.7 ±	0.1	3.6 ±	0.2	3.1 ±	0.1	4.7 ±	0.2	2.2 ±	0.1	4.91 ±	0.04
Analytical #	3-2tr14		3-2tr9		3-2tr10		3-2tr11		3-2tr4		3-2tr5	
Sample #	189fb2		4389fb1		4389fa1		4389fa1		250fa1		250fa2	
Grain description	Ksp tip		Ksp tip		Ksp tip1		Ksp tip2		Ksp tip1		Ksp tip2	
Ti	12.0 ±	0.8	1.3 ±	0.2	2.7 ±	0.1	10.3 ±	1.6	22 ±	8	18.3 ±	0.9
Rb	196 ±	4	44 ±	1	55 ±	2	39 ±	3	68 ±	2	106 ±	2
Y	0.05 ±	0.02	0.04 ±	0.02	0.01 ±	0.07	0.06 ±	0.02	0.16 ±	0.05	0.7 ±	0.2
Ba	3579 ±	35	29 ±	3	13 ±	1	13 ±	1	35 ±	4	1375 ±	14
Ce	0.05 ±	0.03	138 ±	21	0.27 ±	0.09	0.6 ±	0.1	2.9 ±	0.3	0.13 ±	0.03
Pb	50 ±	9	4 ±	4	7 ±	3	7 ±	4	7 ±	5	34 ±	7
Li	2.7 ±	0.3	0.42 ±	0.05	1.3 ±	0.2	1.4 ±	0.2	1.21 ±	0.09	0.9 ±	0.1
Mg	16 ±	2	4.1 ±	0.5	1.9 ±	0.2	29 ±	2	48 ±	2	25.9 ±	0.8
Cl	37 ±	1	56 ±	2	37 ±	3	40 ±	1	1806 ±	34	35 ±	3
Ca	0.493 ±	0.009	0.318 ±	0.002	0.167 ±	0.006	0.172 ±	0.005	0.52 ±	0.02	1.157 ±	0.004
Fe	346 ±	4	301 ±	4	277 ±	4	328 ±	6	297 ±	6	429 ±	6
Sr	74.2 ±	0.8	3.2 ±	0.2	0.98 ±	0.09	1.15 ±	0.05	0.80 ±	0.04	175.78 ±	0.01
B	19.8 ±	0.6	4.8 ±	0.1	9.7 ±	0.4	22 ±	1	18.2 ±	0.6	7.8 ±	0.1

Table 5-1 Continued

Analytical #	3-2tr15		3-2tr16		3-2tr28		3-2tr29		3-2tr30		3-2tr31	
Sample #	250fb1		250fb1		3707ak1		3707ak1		3707ak2		3707ak4	
Grain description	Ksp OG1		Ksp tip		RhombTip		Ksp Og		Ksp Og		Ksp tip1	
Ti	38.2 ±	0.9	7.1 ±	0.5	2.0 ±	0.2	1.7 ±	0.2	369 ±	78	25.4 ±	0.1
Rb	152 ±	2	193 ±	5	73 ±	2	37 ±	2	52 ±	3	765 ±	14
Y	0.62 ±	0.01	0.14 ±	0.02	0.05 ±	0.04	0.010 ±	0.003	0.19 ±	0.05	0.16 ±	0.02
Ba	684 ±	4	5456 ±	35	429 ±	11	7.7 ±	0.4	10.4 ±	0.6	42 ±	1
Ce	7.1 ±	0.3	0.2 ±	0.1	0.04 ±	0.02	0.05 ±	0.03	0.7 ±	0.5	4.6 ±	0.3
Pb	56 ±	2	89 ±	8	23 ±	3	13 ±	4	19 ±	7	49 ±	8
Li	0.80 ±	0.02	2.8 ±	0.3	0.7 ±	0.1	0.07 ±	0.01	0.15 ±	0.02	0.72 ±	0.04
Mg	142 ±	4	5.3 ±	0.4	4.5 ±	0.3	5.9 ±	0.3	35.7 ±	0.6	144 ±	15
Cl	109 ±	2	39 ±	3	16 ±	1	38 ±	1	13 ±	2	125 ±	3
Ca	1.55 ±	0.02	0.326 ±	0.002	0.24 ±	0.01	0.91 ±	0.05	0.338 ±	0.009	3.8 ±	0.1
Fe	728 ±	4	338 ±	4	358 ±	10	376 ±	12	815 ±	75	801 ±	16
Sr	83.7 ±	0.9	290 ±	2	57.3 ±	0.7	1.1 ±	0.1	2.02 ±	0.07	22.9 ±	0.3
B	14.2 ±	0.3	1.5 ±	0.1	6.7 ±	0.1	2.6 ±	0.7	10.8 ±	0.3	17.2 ±	0.3
Analytical #	3-2tr32		3-2tr33		3-2tr6		3-2tr8		3-2tr22		3-2tr23	
Sample #	3707ak4		3707ak4		UPH3fc1		UPH3fg1		CMS3c		CMS3c	
Grain description	Ksp Og		Ksp Tip2		Ksp tip		Ksp rhomb		Ksp Og1		Ksp Og2	
Ti	60 ±	9	56 ±	5	104 ±	7	3.4 ±	0.3	28 ±	2	32 ±	3
Rb	23.2 ±	0.7	199 ±	10	87 ±	3	40.8 ±	0.8	166 ±	1	168 ±	5
Y	0.15 ±	0.05	0.29 ±	0.03	1.6 ±	0.5	0.03 ±	0.01	0.7 ±	0.1	0.04 ±	0.01
Ba	30.6 ±	0.6	2087 ±	11	31 ±	1	8.8 ±	0.5	1049 ±	46	432 ±	18
Ce	0.6 ±	0.2	2.7 ±	0.4	9 ±	3	0.7 ±	0.2	23 ±	2	0.20 ±	0.04
Pb	16 ±	2	41 ±	7	8 ±	4	12 ±	5	42 ±	5	20 ±	3
Li	0.28 ±	0.03	0.50 ±	0.01	3.3 ±	0.1	3.6 ±	0.6	1.59 ±	0.04	2.33 ±	0.03
Mg	59 ±	4	17.4 ±	0.9	1025 ±	38	5.4 ±	0.3	35 ±	1	49 ±	3
Cl	102 ±	3	34 ±	3	1019 ±	24	88 ±	12	16 ±	1	13.5 ±	0.5
Ca	0.81 ±	0.02	0.74 ±	0.02	4 ±	1	0.16 ±	0.01	0.69 ±	0.02	0.49 ±	0.01
Fe	285 ±	6	486 ±	6	479 ±	8	273 ±	4	1347 ±	10	874 ±	14
Sr	6.9 ±	0.3	154 ±	1	5.9 ±	0.2	1.2 ±	0.1	130 ±	1	18.8 ±	0.3
B	26.9 ±	0.3	7.2 ±	0.4	14.8 ±	0.3	4.8 ±	0.1	7.3 ±	0.2	7.5 ±	0.2

Table 5-1 Continued

Analytical #	3-2tr24		3-2tr25		3-2tr26		3-2tr27	
Sample #	CMS3d		CMS3e		CMS3e		CMS3e	
Grain description	Ksp Og		Ksp Og1		RhomTip1		RhombTip2	
Ti	13.3 ±	0.9	16 ±	3	22 ±	4	3.2 ±	0.4
Rb	38 ±	1	53 ±	1	77 ±	2	66.2 ±	0.9
Y	0.08 ±	0.01	0.11 ±	0.02	0.15 ±	0.03	0.08 ±	0.02
Ba	32 ±	2	27.0 ±	0.7	875 ±	7	69 ±	6
Ce	0.3 ±	0.1	0.5 ±	0.2	0.43 ±	0.09	0.16 ±	0.05
Pb	17 ±	3	6 ±	2	42 ±	7	18 ±	2
Li	0.19 ±	0.02	0.24 ±	0.02	0.51 ±	0.05	0.29 ±	0.01
Mg	41 ±	3	16 ±	1	78 ±	8	22 ±	1
Cl	49 ±	1	19 ±	2	44 ±	2	66 ±	2
Ca	0.88 ±	0.03	0.48 ±	0.01	1.09 ±	0.02	1.04 ±	0.03
Fe	421 ±	4	581 ±	20	730 ±	22	447 ±	6
Sr	2.5 ±	0.1	3.9 ±	0.1	116 ±	1	10.0 ±	0.3
B	5.8 ±	0.1	5.83 ±	0.07	10.5 ±	0.3	10.5 ±	0.3

* Ksp -K-feldspar; Og -overgrowth; tip - rhombic shape overgrowth; 1and 2 -different individual overgrowths
Analytical errors are the two standard error of multiple (N=6 to 15) ratios measured for each analysis (see text).

Table 5-2 Trace element concentrations (ppm) in authigenic quartz*

Analytical #	2-28tr5		2-28tr6		2-28tr7		3-1tr7		3-1tr26		3-1tr27		3-1tr28	
Sample #	4831Ic		4831Ic		4831Ic		4831Ie		4831d5a		4831d5a		4831d6	
Grain description	Qog (FI)		Qog		Qog		Qog(FI)		inner darker		outer bright		outer bright	
Ti	5.4 ±	0.3	3.6 ±	0.4	3.40 ±	0.08	5.9 ±	0.6	5.1 ±	0.7	1.7 ±	0.3	6.7 ±	0.7
Li	0.63 ±	0.05	2.5 ±	0.3	4.7 ±	0.3	3.9 ±	0.5	1.26 ±	0.06	0.45 ±	0.03	0.12 ±	0.01
Be	0.012 ±	0.001	0.003 ±	0.001	0.005 ±	0.001	0.007 ±	0.002	0.008 ±	0.002	0.003 ±	0.001	0.003 ±	0.001
Mg	17.7 ±	0.6	3.42 ±	0.04	3.6 ±	0.3	6.1 ±	0.4	12 ±	1	63 ±	7	1.22 ±	0.08
Cl	12.6 ±	0.6	9 ±	1	20 ±	1	17 ±	2	78 ±	4	21 ±	3	13 ±	1
K	116 ±	1	50 ±	2	67 ±	2	55 ±	3	145 ±	8	142 ±	7	127 ±	4
Ca	0.144 ±	0.010	0.0159 ±	0.0004	0.034 ±	0.003	0.034 ±	0.002	0.596 ±	0.004	0.41 ±	0.03	0.025 ±	0.002
Fe	76 ±	4	12.4 ±	0.5	99 ±	3	11 ±	1	68 ±	3	8.0 ±	0.8	9.3 ±	0.9
B	4.1 ±	0.2	1.7 ±	0.1	2.93 ±	0.07	20 ±	1	5.8 ±	0.3	7.7 ±	0.4	8.1 ±	0.5
Na	0.095 ±	0.003	0.016 ±	0.001	0.025 ±	0.001	0.024 ±	0.001	0.368 ±	0.008	0.31 ±	0.02	0.098 ±	0.003
Al	13.02 ±	0.09	5.43 ±	0.09	8.9 ±	0.4	7.19 ±	0.06	27.1 ±	0.4	5.0 ±	0.2	7.3 ±	0.2

Analytical #	3-1tr29		3-1tr30		3-1tr31		2-28tr13		2-28tr14		2-28tr15		3-1tr13	
Sample #	4831d6		4831d1r1		4831d3a		13638IId		13638IIb		13638IIb		189IIc1a	
Grain description	inner darker		darker cl		outer bright		Qog (FI)		Qog		Qog		Qog(FI)	
Ti	2.2 ±	0.2	2.1 ±	0.4	1.6 ±	0.2	149 ±	31	9.0 ±	0.5	3.1 ±	0.4	5.2 ±	0.8
Li	0.4 ±	0.1	1.4 ±	0.2	0.34 ±	0.04	1.4 ±	0.2	2.1 ±	0.0	3.6 ±	0.2	0.6 ±	0.1
Be	0.003 ±	0.001	0.007 ±	0.002	0.004 ±	0.001	0.07 ±	0.01	0.016 ±	0.002	0.029 ±	0.004	0.0068 ±	0.0007
Mg	2.7 ±	0.1	1.5 ±	0.1	3.4 ±	0.2	181 ±	35	44 ±	1	37 ±	3	5.2 ±	0.8
Cl	13 ±	1	22 ±	4	26 ±	3	58 ±	4	71 ±	3	29 ±	3	18 ±	1
K	27 ±	1	89 ±	5	194 ±	13	967 ±	21	89 ±	1	458 ±	13	78 ±	6
Ca	0.0065 ±	0.0007	0.0180 ±	0.0008	0.035 ±	0.002	0.512 ±	0.002	0.5839 ±	0.0008	1.188 ±	0.008	0.27 ±	0.01
Fe	10 ±	1	18.8 ±	0.9	18 ±	2	130 ±	4	344 ±	5	202 ±	7	12 ±	1
B	1.6 ±	0.1	5.7 ±	0.2	13 ±	2	21 ±	1	9.0 ±	0.2	6.9 ±	0.1	18 ±	1
Na	0.021 ±	0.002	0.062 ±	0.003	0.26 ±	0.02	0.33 ±	0.01	0.044 ±	0.002	0.59 ±	0.03	0.053 ±	0.004
Al	11.4 ±	0.2	10.4 ±	0.3	8.9 ±	0.4	85.4 ±	0.6	32.1 ±	0.3	61 ±	2	9.1 ±	0.1

Table 5-2 Continued

Analytical #	3-1tr14		3-1tr15		3-1tr9		3-1tr10		3-1tr11		3-1tr4		3-1tr5	
Sample #	189IIc1a		189IIa		BR-1c		BR-1c		BR-1c		3904IIb		3904IIb	
Grain description	Qog		Qog		Qog (FI)		Qog		Qog		Qog		Qog (FI)	
Ti	3.0 ±	0.4	3.9 ±	0.4	5.1 ±	0.5	4.7 ±	0.3	5.6 ±	0.5	52 ±	11	8.0 ±	0.9
Li	0.1 ±	0.0	2.1 ±	0.1	23.7 ±	3.0	0.8 ±	0.0	2.2 ±	0.1	1.5 ±	0.5	0.091 ±	0.009
Be	0.005 ±	0.003	0.012 ±	0.003	0.04 ±	0.03	0.04 ±	0.03	0.008 ±	0.003	0.05 ±	0.01	0.021 ±	0.006
Mg	1.2 ±	0.2	11 ±	1	10.7 ±	0.4	0.7 ±	0.1	22 ±	5	47 ±	17	27 ±	2
Cl	12.6 ±	0.8	35 ±	3	25 ±	4	7.8 ±	0.7	22 ±	2	15 ±	2	15 ±	2
K	19 ±	1	130 ±	7	323 ±	13	31 ±	2	238 ±	12	227 ±	21	151 ±	12
Ca	0.0220 ±	0.0007	0.165 ±	0.006	0.185 ±	0.005	0.0052 ±	0.0006	0.18 ±	0.02	0.338 ±	0.007	0.074 ±	0.003
Fe	235 ±	13	27 ±	3	18 ±	1	7.4 ±	0.5	20 ±	1	92 ±	1	19.3 ±	0.9
B	3.2 ±	0.2	19 ±	1	40 ±	2	6.0 ±	0.4	25 ±	2	4.6 ±	0.6	4.8 ±	0.3
Na	0.014 ±	0.001	0.085 ±	0.003	0.156 ±	0.004	0.014 ±	0.001	0.101 ±	0.003	0.12 ±	0.01	0.101 ±	0.007
Al	5.24 ±	0.09	7.5 ±	0.2	21.4 ±	0.2	10.52 ±	0.09	14.8 ±	0.2	4.32 ±	0.09	5.92 ±	0.06

Analytical #	3-1tr6		3-1tr12		2-28tr8		2-28tr9		2-28tr10		2-28tr2		2-28tr3	
Sample #	3904IIb		4389Ia		4389IIC		4389IIC		4389IIC		435IIa		435IIa	
Grain description	Qog		Qog (FI)		Qog (FI)		Qog		Qog		Qog		Qog (FI)	
Ti	20 ±	3	48 ±	7	3.3 ±	0.2	4.4 ±	0.3	22 ±	2	8.4 ±	0.2	54.1 ±	0.8
Li	0.51 ±	0.06	4 ±	1	2.2 ±	0.3	1.2 ±	0.1	2.4 ±	0.3	0.18 ±	0.01	0.115 ±	0.007
Be	0.007 ±	0.003	0.024 ±	0.008	0.011 ±	0.002	0.013 ±	0.003	0.0074 ±	0.0008	0.004 ±	0.001	0.005 ±	0.001
Mg	45 ±	2	55 ±	17	36 ±	3	40.9 ±	0.7	54 ±	2	17.0 ±	0.6	49.4 ±	0.2
Cl	14.1 ±	0.8	24 ±	3	28 ±	2	19 ±	2	51 ±	2	32 ±	3	35 ±	1
K	302 ±	4	279 ±	23	265 ±	2	394 ±	4	151 ±	2	108 ±	6	110 ±	2
Ca	0.328 ±	0.004	0.25 ±	0.02	2.0 ±	0.2	0.31 ±	0.04	0.224 ±	0.009	0.33 ±	0.01	0.397 ±	0.004
Fe	38 ±	2	23 ±	3	121 ±	14	58 ±	2	128 ±	4	31 ±	2	30 ±	2
B	33 ±	1	124 ±	14	6.3 ±	0.3	7.3 ±	0.3	5.0 ±	0.1	1.7 ±	0.1	3.1 ±	0.2
Na	0.327 ±	0.003	0.29 ±	0.02	0.267 ±	0.006	0.045 ±	0.004	0.078 ±	0.001	0.051 ±	0.004	0.068 ±	0.002
Al	6.69 ±	0.09	4.7 ±	0.2	28 ±	1	41.0 ±	0.3	20.11 ±	0.06	4.81 ±	0.03	6.85 ±	0.06

Table 5-2 Continued

Analytical #	2-28tr4		2-28tr16		3-1tr8		3-1tr23		3-1tr24		3-1tr25		3-1tr18	
Sample #	435IIa		250IIc		250IIa		250d2r1		250d1r1		250d1r2		250d3r1	
Grain description	Q-og		Qog (FI)		Qog(FI)		outer bright		inner darker		outer bright		inner darke	
Ti	20.6 ±	0.6	56 ±	15	39 ±	1	29 ±	4	25.5 ±	0.6	7.2 ±	0.8	3.8 ±	0.5
Li	0.92 ±	0.09	1.6 ±	0.4	1.3 ±	0.1	0.580 ±	0.110	1.42 ±	0.04	0.53 ±	0.08	0.61 ±	0.07
Be	0.009 ±	0.002	0.05 ±	0.01	0.080 ±	0.009	0.010 ±	0.002	0.005 ±	0.002	0.003 ±	0.001	0.005 ±	0.001
Mg	17.0 ±	0.3	66 ±	4	230 ±	49	30 ±	8	8.8 ±	0.8	3.5 ±	0.3	4.0 ±	0.5
Cl	20 ±	2	17 ±	1	32 ±	3	20 ±	2	12 ±	1	12.4 ±	0.9	14 ±	1
K	115 ±	2	288 ±	8	950 ±	6	208 ±	15	83 ±	4	98 ±	6	93 ±	5
Ca	0.266 ±	0.005	0.20 ±	0.01	0.41 ±	0.01	0.26 ±	0.02	0.063 ±	0.002	0.041 ±	0.002	0.027 ±	0.002
Fe	82 ±	4	978 ±	15	184 ±	6	244 ±	11	18 ±	1	5.4 ±	0.7	5.4 ±	0.9
B	2.8 ±	0.1	79 ±	7	65 ±	4	34 ±	3	14.9 ±	0.5	18 ±	1	15 ±	1
Na	0.131 ±	0.007	0.076 ±	0.005	0.184 ±	0.004	0.178 ±	0.012	0.083 ±	0.004	0.099 ±	0.046	0.104 ±	0.007
Al	11.8 ±	0.1	15.4 ±	0.2	50.6 ±	0.3	9.9 ±	0.6	6.94 ±	0.06	5.9 ±	0.1	5.1 ±	0.1

Analytical #	3-1tr19		3-1tr20		3-1tr21		3-1tr22		2-28tr17		2-28tr18		2-28tr19	
Sample #	250d3r1		250d3r2		250d3r2		250d2r1		UPH3IIa		UPH3IIa		UPH3IIb	
Grain description	outer bright		darker, qog		qog		inner darke		Qog dark		Qog, outer bright		Qog (FI)	
Ti	72 ±	1	2.6 ±	0.4	2.7 ±	0.3	343 ±	140	2.5 ±	0.3	49 ±	3	576 ±	142
Li	0.6 ±	0.1	0.85 ±	0.05	1.7 ±	0.5	3.0 ±	0.7	2.3 ±	0.5	0.7 ±	0.1	0.2 ±	0.3
Be	0.014 ±	0.003	0.004 ±	0.003	0.002 ±	0.001	0.007 ±	0.001	0.025 ±	0.004	0.011 ±	0.001	0.011 ±	0.002
Mg	18 ±	2	5 ±	1	9 ±	1	26 ±	6	26 ±	2	5.5 ±	0.9	12 ±	2
Cl	15 ±	1	15 ±	2	19 ±	2	23 ±	2	13.1 ±	0.9	17 ±	1	13 ±	2
K	128 ±	11	78 ±	4	136 ±	12	227 ±	17	57 ±	4	72 ±	6	51 ±	4
Ca	0.18 ±	0.01	0.037 ±	0.002	0.032 ±	0.003	0.19 ±	0.02	0.026 ±	0.003	0.0077 ±	0.0006	0.082 ±	0.008
Fe	14 ±	1	5.4 ±	0.6	6.2 ±	0.8	8.2 ±	0.4	17 ±	1	14 ±	1	14 ±	1
B	27 ±	2	15 ±	1	26 ±	1	36 ±	3	21 ±	2	14 ±	1	26 ±	1
Na	0.090 ±	0.007	0.100 ±	0.007	0.197 ±	0.014	0.255 ±	0.020	0.020 ±	0.002	0.044 ±	0.004	0.105 ±	0.008
Al	5.8 ±	0.6	7.5 ±	0.1	4.84 ±	0.09	9.4 ±	0.3	3.2 ±	0.1	2.2 ±	0.2	3.3 ±	0.2

Table 5-2 Continued

Analytical #	2-28tr20		2-28tr11		2-28tr12	
Sample #	UPH3IIg		UPH3IIc		UPH3IIc	
Grain description	Qog (FI)		outerQog(FI)		innerQog(FI)	
Ti	29 ±	21	14.1 ±	0.8	5.2 ±	0.9
Li	0.61 ±	0.09	3.19 ±	0.04	1.8 ±	0.4
Be	0.007 ±	0.002	0.011 ±	0.002	0.028 ±	0.007
Mg	9 ±	2	203 ±	27	393 ±	103
Cl	17 ±	1	107 ±	6	495 ±	23
K	71 ±	4	263 ±	8	99 ±	9
Ca	0.073 ±	0.004	1.005 ±	0.008	3.5 ±	0.1
Fe	16 ±	1	54 ±	3	28 ±	3
B	7.7 ±	0.8	11 ±	1	42 ±	4
Na	0.097 ±	0.007	0.76 ±	0.07	4.4 ±	0.1
Al	4.04 ±	0.06	15.45 ±	0.09	5.2 ±	0.1

* Analytical errors are the two standard error of multiple (N=6 to 15) ratios measured for each analysis (see text).
Qog- Quartz overgrowth; outer brigh - outer zone, brighter CL; inner dark - inner zone, darker CL; cl= Cathodoluminescence; FI=Fluid inclusion chip

orders of magnitude. However, very large variation can typically be accounted for by one or two extreme analyses. For example, Cl concentration ranges from 13 to 125 ppm, with two exceptions (in a total of 28 spot analyses) having > 1000 ppm. Mg concentration ranges from 2 to 144 ppm, with one high value of 1025 ppm, and Ti ranges from 1 to 369 ppm with one sample having 5771 ppm. These exceptionally high concentrations probably originate in minute mineral inclusions (*e.g.*, oxides, clays) in the analyzed K-feldspar. Abundance of other trace elements in authigenic K-feldspars are: Li (< 1–7ppm), B (2–27 ppm), Ca (< 1–4 ppm), Fe (273–1347 ppm), Rb (23–422 ppm), Sr (< 1–289 ppm), Ba (8–5456 ppm), Pb (4–89 ppm), and Ce (< 1–138 ppm). Y is <1ppm in all analyses.

Trace Elements in Authigenic Quartz Overgrowths

Trace element compositions in quartz overgrowths are shown in Table 5-2. Trace element concentrations are expected to be lower in quartz overgrowths than in the K-feldspar overgrowths, due to the mineral structure and charge constraints of cation substitution in quartz. Notable amounts of some trace elements were still detected (Table 5-2). The contents of trace elements in quartz overgrowths are: Cl (9–495 ppm), Li (< 1–24 ppm), B (2–124 ppm), Mg (1–393 ppm), Al (2–85 ppm), K (27–967 ppm), Fe (5–978 ppm), and Ti (2–576 ppm). Fewer samples had anomalous trace element contents compared to K-feldspar.

Discussion

Trace element contents in authigenic minerals may be useful in evaluating geochemical changes of diagenetic fluids, if the factors controlling mineral-fluid distribution coefficients ($D = C_{solid}/C_{liquid}$) are well constrained. Trace elements are likely distributed according to equilibrium D values in high-temperature igneous systems (*e.g.*, Allegre and Minister, 1978), and it is relatively straight forward to conduct exchange experiments at high temperature. However, experiments are difficult in low temperature systems, and the basic assumption of equilibrium exchange and solid solution may not be correct. Studies of carbonate-fluid distribution coefficients indicate a host of other potential results, including conditions of carbonate precipitation, processes of carbonate growth, and crystal surface conditions (Veizer, 1983). In many cases, to interpret trace element behavior in lower temperature systems, geologists rely on an understanding of mineral soild solution and crystal chemical models and on empirical data.

Trace elements may be incorporated into minerals by means of impurities (fluid or mineral inclusions), sorption, substitution, and occlusion (McIntire, 1964; Farquhar et al., 1999). Important processes likely to occur in low-temperature diagenetic environments are mineral dissolution/re-precipitation, sorption, and cation exchange. These processes may cause redistribution and transfer of trace elements between phases. The process of dissolution of framework grains may affect pore fluid compositions in a manner somewhat similar to wall-rock assimilation in a magmatic system. Precipitation of authigenic minerals from low-temperature fluids affects the compositions of remaining fluid in a manner similar to fractional crystallization of magma. Mixing of low-temperature fluids may be grossly comparable to the process of magma mixing in altering

trace element contents of both original fluids. In addition to the common factors that may affect distribution coefficients, such as rock/mineral composition, temperature, pressure, oxygen fugacity, trace concentration, cation charge and radius (e.g., Murata et al., 1957; Haskin and Gehl, 1963; Schmitt et al., 1964; Gast, 1968; Fleischer and Altschuler, 1969; Allegre et al., 1981; Milliken et al., 1994; Icenhower and London, 1996; Ottonello, 1997), trace element behavior in diagenetic systems is also controlled by local differences in fluid flow rate, precipitation rate of authigenic minerals, pH, oxidation potential, ion complexes, salinities, and microbial activities and other environmental factors (Milliken et al., 1994; Riciputi et al., 1994; Watson, 1996; Fayek and Kyser, 1997; Huerta-Diaz et al., 1998; Farquhar et al., 1999; Lev et al., 1999; Hadizadeh and Foit, 2000; Sternbeck et al., 2000). Clearly, trace element behaviors in diagenetic systems can be quite complicated and interpretation of trace element compositions must consider many (and many non-unique) scenarios.

Correlations of Trace Elements in Authigenic K-feldspar

Trace element incorporation by solid solution in K-feldspar is most readily accommodated if the ionic size and charge is similar to one of the major elements (K, Al, Si) in K-feldspar. Trace elements having similar size and charge may exhibit similar behavior during fluid-rock interaction or other geological processes. To identify elements that possibly exhibit similar behavior, Table 5-3 presents correlation coefficients (R values) between analyzed trace elements measured in authigenic K-feldspar. The R values are mostly positive; some negative values also present, but they are generally minor. Significant correlations are found among several groups of elements, including Sr-

Table 5-3 Correlation coefficients of trace elements in authigenic K-feldspar *

	Ti	Rb	Y	Ba	Ce	Pb	Li	Mg	Cl	Ca	Fe	Sr
Rb	-0.0552											
Y	0.2431	0.0456										
Ba	-0.0984	0.2175	0.0265									
Ce	-0.0736	-0.0722	0.0037	-0.0996								
Pb	-0.0244	0.5687	0.1198	0.8110	-0.1619							
Li	-0.1726	-0.0828	0.0719	0.1017	-0.1100	-0.1210						
Mg	0.2238	0.0546	0.8451	-0.1206	-0.0055	-0.0827	0.1648					
Cl	0.0599	-0.0604	0.3741	-0.1471	-0.0169	-0.2072	0.0773	0.4706				
Ca	0.1222	0.4960	0.6945	-0.1242	-0.0447	0.1373	-0.0526	0.8008	0.3219			
Fe	0.3369	0.3625	0.3236	0.0039	-0.0190	0.3424	-0.1943	0.0907	-0.1394	0.2574		
Sr	-0.0812	0.1669	0.2203	0.8425	-0.0798	0.7930	-0.0221	-0.0983	-0.1698	-0.0241	0.2193	
B	0.1937	0.1345	0.1906	-0.0836	-0.1245	0.0094	-0.1938	0.2545	0.3483	0.3175	0.0357	-0.1595

* R = 0.367 at 95% Significance and 0.470 at 99% significance

Ba-Pb-Rb, Mg-Ca-Cl, B-Ti, and Ce-Y (Fig. 5-2). Li, B, Fe, Ti, and Ce, Y appear to have no correlation with these other trace elements measured. Y and Ce correlate fairly well except for one extreme analytical point.

Possible Causes for Variations in Trace Elements

The positive correlations among element groups of Sr-Ba-Pb-Rb, Ca-Mg, Y-Ce, and Ti-B (Fig. 5-2) suggest that they have similar behaviors in K-feldspar in diagenetic environments. Several possibilities may have caused the covariance of their concentrations in authigenic K-feldspar. Charge and size of cations may play an important role in their behavior. Sr, Ba, Pb, and Rb may be partitioned into K-feldspars as the result of having ionic radii similar to K^+ (Goldschmidt, 1954) and their exclusion from common coexisting phases, such as quartz and plagioclase. In fact, Ba is well-known to substitute almost exclusively into K-feldspar (Smith, 1975).

Temperature often hss a critical control on the distribution coefficients (D) of trace elements. There appears to be some correlations between geographic locations along a south-to-north transect and trace element abundances in authigenic K-feldspar (Fig. 5-2), with most concentrations increasing northwards. On the basis of diagenetic fluid temperature studies (Chapter 2), fluid temperatures associated with the precipitation of authigenic K-feldspar in the Mount Simon Sandstone are fairly constant (60-95 °C). Assuming relatively constant D, this variation would suggest that trace element concentrations in the fluid were slightly enriched northward.

Trace element concentrations in diagenetic fluid are controlled by the dissolution and precipitation of minerals along the fluid flow path. Evolution of trace element

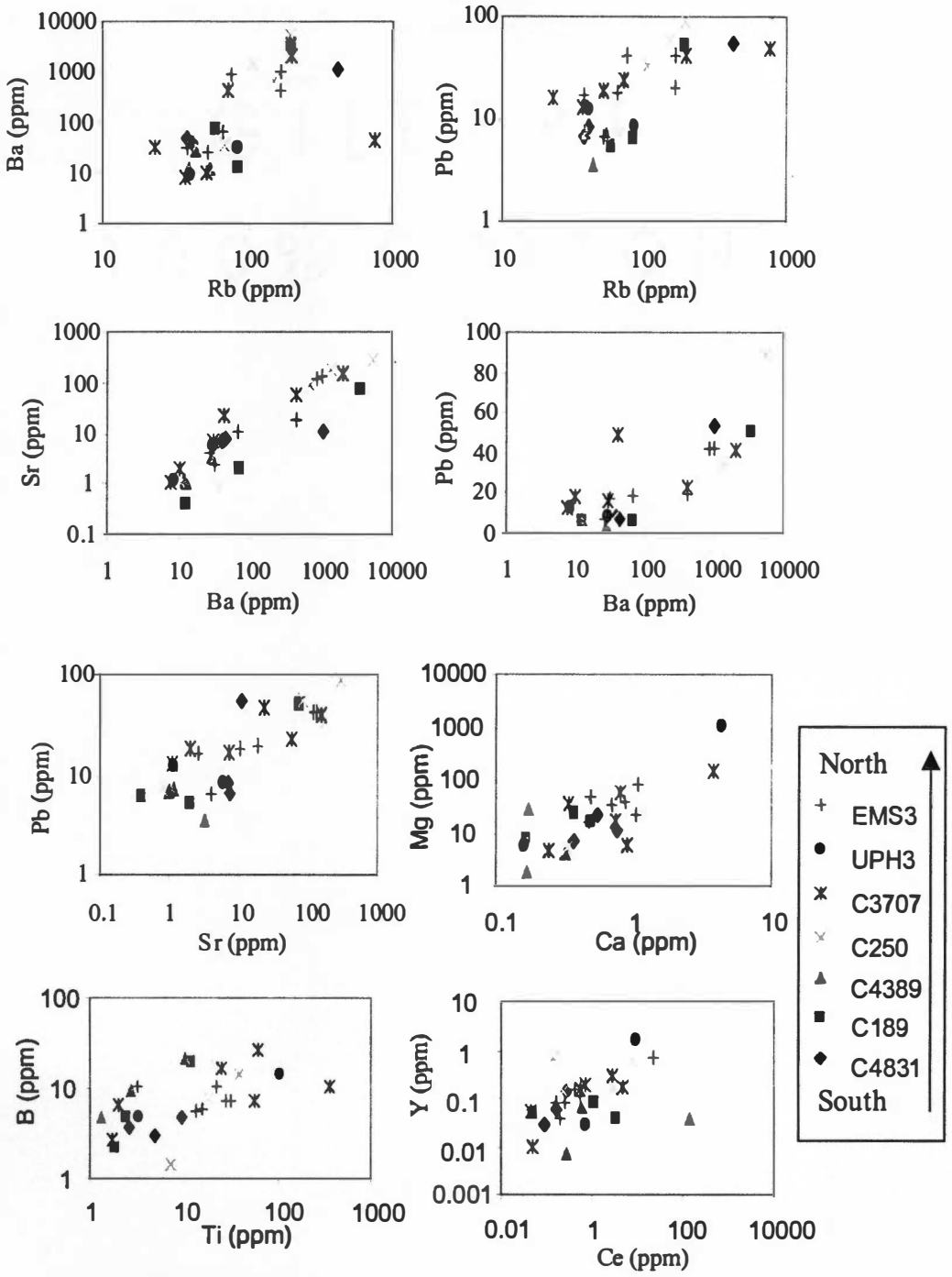

Figure 5-2 Correlation of trace element concentrations in authigenic K-feldspars. Notice that samples from the south of the basin (square, triangle, and rhomb symbols) mostly appear to have lower Trace element contents than those from the north.

concentrations in basinal fluid may be the result of fluid-rock interaction, especially if fluid chemistry and the bulk sandstone are significantly out of equilibrium. K-feldspar precipitation and dissolution may control Ba, Pb, and Rb concentrations in diagenetic fluids; and carbonates may be a major control on Sr. In each case, the increase of trace elements in diagenetic fluids may result in the apparent increase of trace element concentrations in authigenic K-feldspar.

Temperature variation at the local and basinal scale during the precipitation of authigenic K-feldspar may have changed the distribution coefficients to some extent. Changes in D values may affect directly the incorporations of different amounts of trace elements into authigenic K-feldspar. However, we do not know how D is changed with temperature variations at low-temperature conditions.

Linear correlations in trace element plots may also be caused by mixing of two end members with significantly different trace element concentrations (e.g., DePaolo, 1981). The fractions of different fluids in the mixture directly control trace element concentrations in the mixing fluid. Musgrove and Banner (1993) reported three groups of groundwaters in the U.S. Midcontinent, on the basis of isotopic compositions and ion concentrations: a Paleozoic seawater brine in north-central Oklahoma; a dilute meteoric water recharged in southern Missouri; and a long-traveled, meteoric-water-origin, saline fluid. Migrating basinal brines from the deep Illinois basin may mix with pore waters initially residing in the sediments, but the volume of residual pore water is negligible compared to the volume of migrating fluids. The consistent salinities in fluid inclusions throughout the entire sandstone unit noted in Chapter 2 suggest that fluid mixing, such as seawater mixing with meteoric water, was unlikely.

The results we present in this study suggest that the correlations between Sr, Ba, Pb, and Rb trace elements may be controlled by, in addition to their similar chemical behavior, co-fluctuations of these trace element concentrations in diagenetic fluids. If we assume temperature and other conditions were relatively constant during the precipitation of authigenic K-feldspar cements, then the broad variations of trace element contents in K-feldspar cements suggests that changes in fluid chemistry may have had an important impact on the behaviors of trace elements. As the properties of most mineral remains virtually unchanged, a realistic interpretation for the positive covariance among trace element might be that the fluid chemistry changed (Kontak and Smith, 1993).

Distribution Coefficients and Constraining Diagenetic Fluid Compositions Associated with Authigenic K-feldspar

To characterize the trace element composition of diagenetic fluid, which cannot be sampled and analyzed directly, distribution coefficients (D) between trace elements in authigenic mineral phases and the diagenetic fluid, assuming equilibrium, need to be known. D is defined as a ratio that compares the quantity of an element in the solid phase to the quantity in the fluid ($D = C_{solid}/C_{liquid}$). Previous studies of low temperature trace element mineral-fluid distribution coefficients mostly focus on the interface of surface water and sediments, where sorption and desorption prevail (*e.g.*, Patterson and Spoel, 1981; Robin et al., 1991; Freedman et al., 1994; Gao et al., 1995; Ohkouchi et al., 1995; Guy et al., 1999) and on carbonate-fluid systematics. Even in the relatively well-studied carbonate systems, distribution coefficients vary significantly with solution chemistry, temperature, and growth rate, up to two orders of magnitude for some elements (e.g.,

Lorens, 1981; Mucci and Morse, 1983; Tesoriero and Pankow, 1996; Rimstidt et al., 1998; Temmam et al., 2000; Huang and Fairchild, 2001). Trace element behavior in carbonate systems is further discussed in numerous studies, including Brand and Veizer (1980), Morse and Bender (1990), Srinivasan et al. (1994), Sholkovitz and Shen (1995), Allison (1996), and Spangenberg et al. (1999).

D values are not well constrained for K-feldspar in diagenetic systems, probably owing to the difficulty in establishing experimental equilibrium conditions between fluid and mineral phases at low temperature. At high temperature (i.e., magmatic conditions), trace element partitioning coefficients between alkali-feldspar and silicate liquid (*i.e.*, glass) have been determined. Work thus far has shown that high temperature D values exhibit large variations, which may be the result of changing mineral and liquid compositions, temperature, pressure, oxygen fugacity, volatiles, and minute mineral inclusions (Stix and Gorton, 1990). Table 5-4 lists some of the reported trace element distribution coefficients between alkali feldspar and silicate glass or hydrothermal fluids. D values for Ba and Sr vary an order of magnitude, and Ba and Sr appear sensitive to the K content of alkali feldspar, with D (Ba) values increasing and D (Sr) decreasing with increasing K content in alkali feldspar. Values of D (Rb) and D (Ce) are relatively constant with different K content (Long, 1978; Stix and Gorton, 1990).

Lagache (1984) reported experimentally determined trace element distribution coefficients between sanidine and hydrothermal solution at temperatures ranging from 400 to 850 °C. D values decrease significantly with decreasing hydrothermal fluid temperatures. For example, D (Rb) at 800 °C = 0.42-0.48, at 400 °C = 0.26; D (Ba) at 850 °C =250, at 600 °C =25. The available D values for the lowest hydrothermal temperatures

Table 5-4 Some trace element distribution coefficients between alkali feldspar and silicate glass or hydrothermal fluids

Trace Element	D values (1)	D values (2)	D values (3)	D values (4)	D values (5)	D values (6)*	D values (6)*	D values (6)*
Temperature	melting	melting	melting	melting	melting	400 °C	600 °C	800-850 °C
Ba	6.4-14	0.3-14	13-27	1-19	1.48-8.71		25	250
Sr	1.2-5.0		28	8-23			8.3	86
Rb	0.77-1.1	0.28-0.32	0.33-0.43	<1		0.26	0.42	0.42-0.48
Pb			1					
Fe			0.11-0.2					
Ca		0.06-0.92					0.12	6.1
Ce		0.017-0.037	0.054-0.074					

(1) Long, 1978; (2) Stix and Gorton, 1990; (3) Leeman and Phelps, 1981; (4) Icenhower and London, 1996; (5) Gao and Green, 1989; (6) Lagache, 1984

* Distribution coefficients between Sanidine and hydrothermal fluids

are: at 600 °C, D (Ba) = 25, D (Sr)=8.3, D (Ca) =0.12; while at 400 °C, D (Rb)=0.26, D (Na)=0.025. These data fall in the range of high temperature D values from feldspar/glass. As there are no reported distribution coefficients for low temperature authigenic K-feldspar, D values from hydrothermal and high-temperature systems must be used to roughly evaluate the concentrations of Sr, Ba, Pb, and Rb in diagenetic fluids.

Trace element compositions of diagenetic fluids were calculated using the lowest hydrothermal distribution coefficients of Lagache (1984). Results are shown in Table 5-5. Digenetic fluid associated with the formation of K-feldspar cements contained about ~ 1-83 ppm Ba, ~1-22 ppm Sr, ~143-765 ppm Rb, and ~ 6-62 ppm Ca. Concentrations of several other trace elements (Pb, Fe, and Ce) are also calculated using D values from high-temperature systems. Pb (D=1) in the fluid ranges from 4 to 90 ppm. Fe (D=0.1) is estimated to be very high, 0.3 –0.8%, and Ce (D ~ 0.03) ranges from ~1 – 300 ppm, mostly < 30 ppm. The concentration of Ca in the fluid (Table 5-5) appears to be lower than expected, based on fluid inclusion analysis (Chapter 2), most likely due to the D value we used in the calculation. Regional variation of trace element concentrations in the calculated diagenetic fluids is likely to be more significant than the actual trace element concentrations determined in authigenic minerals, because most trace elements were left in the fluid (D <1) during fluid migration and mineral precipitation.

Fig. 5-3 shows the relationships between trace element concentrations in a fluid and the geographic localities of these samples. The distance is relative to a point ~ 20 km to the south of borehole C4831. There is no obvious correlation between trace element concentrations and sample localities. Variations within individual samples appear to be

Table 5-5 Estimated concentrations (ppm) of some trace elements in diagenetic fluids associated with authigenic K-feldspar

Sample	Distance (km)*	Description	Rb	Ba	Ce	Pb	Ca	Fe	Sr
4831ak4	20	Ksp tip	159.06	1.59	3.04	8.12	30.56	2872.68	0.90
4831ak6	20	Ksp Og-tip	147.76	1.83	5.25	6.49	14.83	2953.60	0.94
4831ak2	20	Ksp Og-tip	1624.67	42.38	8.68	53.79	21.67	4855.23	1.34
189fb3	143	Ksp OG	326.37	0.52	36.85	6.07	6.72	2994.06	0.05
189fb3	143	Ksp Og-tip	231.33	2.78	116.83	5.24	14.48	3317.74	0.25
189fb2	143	Ksp tip	753.16	143.14	1.60	50.19	19.72	3459.35	9.28
4389fb1	245	Ksp tip	170.90	1.15		3.58	12.70	3014.29	0.39
4389fa1	245	Ksp tip1	211.60	0.52	8.93	6.96	6.69	2771.52	0.12
4389fa1	245	Ksp tip2	151.53	0.50	19.50	7.38	6.88	3277.28	0.14
250fa1	269	Ksp tip1	261.81	1.41	97.08	7.15	20.96	2973.83	0.10
250fa2	269	Ksp tip2	408.86	54.99	4.36	33.83	46.28	4288.78	21.97
250fb1	269	Ksp OG1	582.80	27.35	237.10	56.01	62.00	7282.84	10.46
250fb1	269	Ksp tip	740.61		7.88	89.01	13.06	3378.43	36.21
3707ak1	284	RhombTip	281.54	17.15	1.45	23.24	9.68	3580.73	7.16
3707ak1	284	189fb2	143.28	0.31	1.60	12.78	36.42	3762.80	0.14
3707ak2	284	189fb2	200.84	0.42	23.80	18.58	13.50	8152.73	0.25
3707ak4	284	Ksp tip1		1.67	154.63	48.80	152.78	8011.12	2.86
3707ak4	284	189fb2	89.30	1.22	18.47	16.03	32.60	2852.45	0.87
3707ak4	284	189fb2	765.71	83.48	91.06	41.04	29.58	4855.23	19.26
UPH3fc1	362	Ksp tip	333.54	1.24	310.98	8.12	176.76	4794.54	0.74
UPH3fg1	362	Ksp rhomb	156.91	0.35	23.54	12.48	6.51	2731.06	0.15
CMS3c	563	189fb2	640.18	41.95	759.42	41.87	27.71	13473.25	16.28
CMS3c	563	Ksp Og2	645.56	17.29	6.53	19.58	19.45	8739.41	2.35
CMS3d	563	189fb2	146.69	1.29	8.48	16.55	35.17	4207.86	0.31
CMS3e	563	189fb2	204.43	1.08	17.53	6.43	19.19	5806.04	0.49
CMS3e	563	RhomTip1	297.68	35.01	14.26	41.59	43.52	7303.07	14.51
CMS3e	563	RhombTip2	254.64	2.76	5.26	17.77	41.66	4470.85	1.25

* Distance is estimated relative to a point ~ 20 km to the south of sample C4831. See Fig. 5-1 for sample localities.

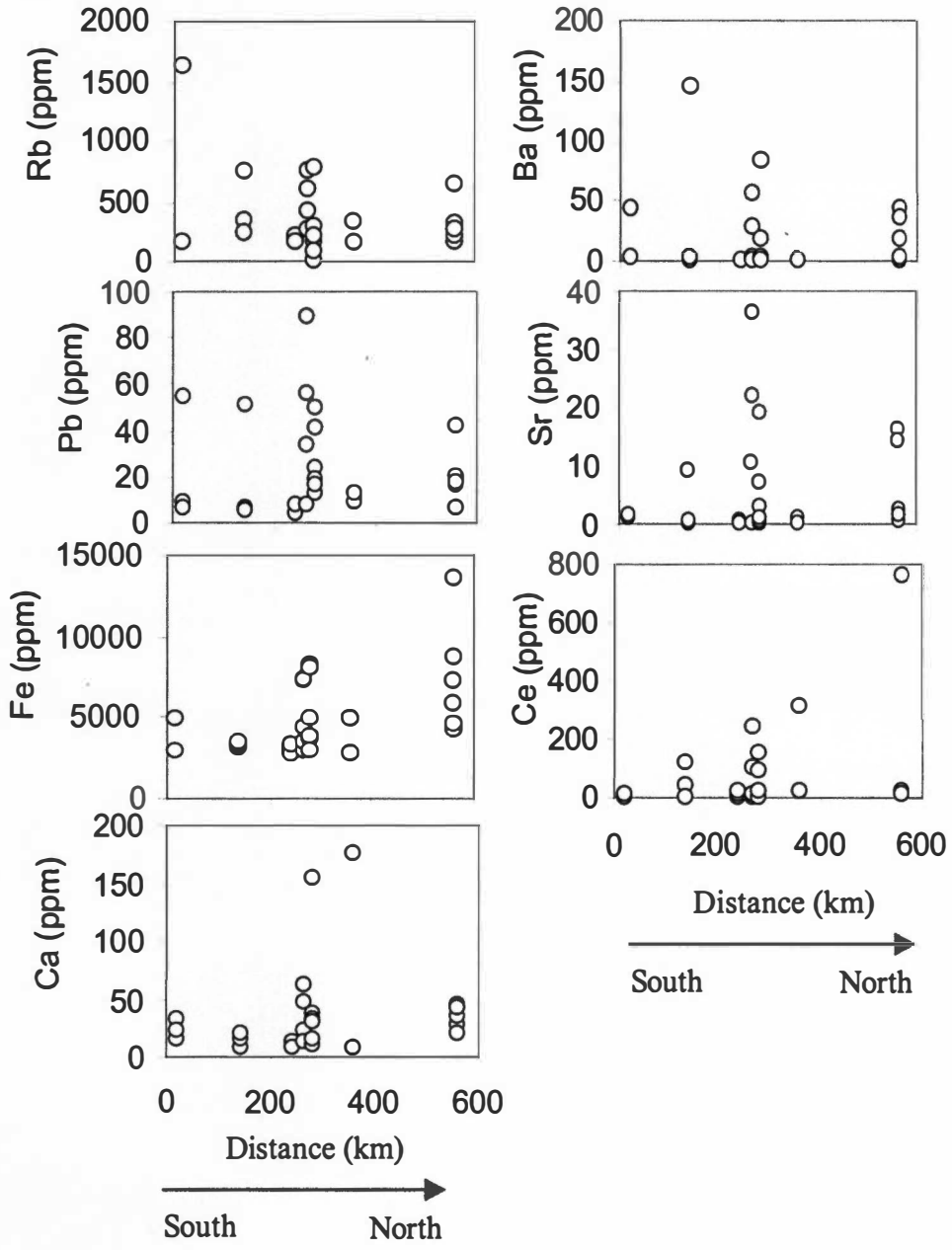

Figure 5-3 Estimated trace element concentrations in diagenetic fluid associated with authigenic K-feldspar

greater than variations across whole basin. Fe, Ce, perhaps Sr concentrations appear to increase slightly from the southern part of the Illinois basin to the north (Fig. 5-3).

Internal Relationships of Trace Elements in Authigenic Quartz

Table 5-6 shows correlation coefficients between trace elements in authigenic quartz overgrowths, and indicates strong positive correlation ($R > 0.5$) between Na-Ca-Mg-Cl and K-Al. In general, large ions such as K, Na, Ca, Mg, and Cl are not favored in the quartz lattice. The strong positive correlation between Al and K suggest that K^+ may be incorporated into quartz overgrowths, in part, to compensate for the charge deficit created by substitution of Al into the quartz tetrahedral site.

Distribution coefficients are not available for quartz-fluid trace element partitioning at low temperature, thus, estimation of trace element concentrations in diagenetic fluids associated with authigenic quartz is not possible. Seyedolali et al. (1992) suggested that trace element composition in quartz is mainly a function of the availability of the trace element in the system rather than a function of trace element ionic size and charge. Thus, strong Na-Ca-Mg-Cl correlation suggests that variation in the concentration of these elements reflect the enrichment/depletion of trace elements in the fluid during quartz precipitation.

The high K/Na ratios (mostly 500 - 2800) in quartz cements suggests relatively high K/Na ratios in the diagenetic fluids from which quartz precipitated, although this is strongly dependent on the actual differences between D (K) and D (Na). High K/Na ratios in basinal brines are consistent with high K/Na ratios reported for MVT precipitating brines (Sverjensky, 1984). High K/Na ratios may have resulted from

Table 5-6 Correlation coefficients (R) of trace elements in authigenic quartz*

	Ti	Li	Be	Mg	Cl	K	Ca	Fe	B	Na
Li	(0.062)									
Be	0.074	0.249								
Mg	0.013	(0.009)	0.515							
Cl	(0.061)	0.019	0.133	0.810						
K	0.084	0.146	0.758	0.494	0.014					
Ca	(0.079)	0.030	0.180	0.747	0.847	0.169				
Fe	(0.020)	(0.027)	0.413	0.129	(0.017)	0.229	0.066			
B	0.176	0.221	0.447	0.318	0.133	0.359	0.089	0.328		
Na	(0.039)	0.018	0.135	0.797	0.975	0.037	0.861	(0.048)	0.183	
Al	0.012	0.128	0.591	0.345	0.034	0.831	0.234	0.258	0.027	0.012

* Significance at 95% R = 0.288; at 99% R=0.372; R values in brackets indicates negative number.

albitization in the deeper basin (Diehl and Goldhaber, 1995). The Lamotte Sandstone in the Reelfoot rift, equivalent to the Mount Simon Sandstone, shows increased alteration to albite with depth (Diehl and Goldhaber, 1995).

Trace Elements in Different Generations of Quartz Overgrowths

Two generations of diagenetic quartz in the Mount Simon Sandstone have been recognized based on cathodoluminescence (CL) studies (Chapter 2). Quartz overgrowths covering the same detrital grains show an earlier generation inner-zone overgrowth with lower CL intensity and a later generation outer-zone overgrowth with higher CL intensity (see Fig. 2-2). Different generations of quartz overgrowths in sandstone may have different trace element contents (Bruhn et al., 1996), reflecting compositional differences in diagenetic fluids, and/or fluctuations in temperature, pH, flow rate, and cement growth rate (Holten et al., 2000).

Trace element concentrations in different zonations of quartz overgrowths are summarized in Table 5-7. Total concentrations of alkaline and alkaline earth elements in the inner-zone quartz overgrowths appear to be lower than the outer zones as shown in Fig. 5-4. These observations suggest that the incorporation of mono- and divalent cations into quartz overgrowths correlates with increased CL. Ionic radii of these trace elements are significantly larger than Si^{4+} and Al^{3+}; most likely these monovalent and divalent cations are incorporated into interstitial positions in response to Al substitution for Si. Based on this study, lattice defects associated with the incorporation of large cations should be the major contributor to CL emission in authigenic quartz in the Mount Simon Sandstone.

Table 5-7 Trace element concentrations (ppm) in zoned quartz overgrowths in the Mount Simon Sandstone

Label	Sample	Description	Ti	Li	Be	Mg	Cl	K	Ca	Fe	B	Na	Al
3-1tr26	4831d5a	inner-zone OG	5.12	1.26	0.01	12.31	78.35	145.36	0.60	68.23	5.80	0.37	27.11
3-1tr27	4831d5a	outer-zone OG	1.69	0.45	0.00	63.43	21.20	141.71	0.41	8.03	7.72	0.31	4.97
3-1tr29	4831d6	inner-zone OG	2.16	0.39	0.00	2.75	13.41	26.73	0.01	9.56	1.58	0.02	11.38
3-1tr28	4831d6	outer-zone OG	6.68	0.12	0.00	1.22	12.74	127.29	0.03	9.34	8.06	0.10	7.28
3-1tr24	250d1r	inner-zone OG	25.45	1.42	0.01	8.76	11.70	83.45	0.06	18.02	14.92	0.08	6.94
3-1tr25	250d1r	outer-zone OG	7.18	0.53	0.00	3.48	12.36	98.25	0.04	5.44	17.87	0.10	5.86
3-1tr18	250d3r1	inner-zone OG	3.79	0.61	0.00	3.96	13.98	92.68	0.03	5.36	15.34	0.10	5.12
3-1tr19	250d3r1	outer-zone OG	72.39	0.65	0.01	17.59	14.83	127.86	0.18	14.01	27.47	0.09	5.80

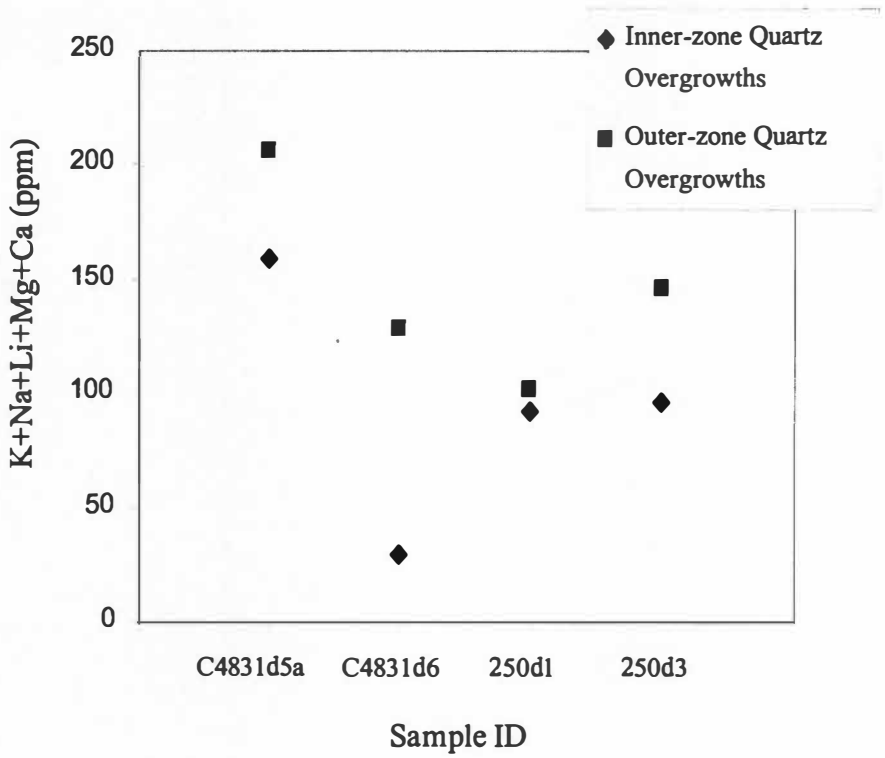

Figure 5-4 Trace element concentrations of the total uni- and divalent cations in zoned quartz overgrowths. The outer overgrowth zones with higher cathodoluminescence intensities are associated with higher K+Na +Li+Mg+Ca cation contents than the inner zones.

Previous CL studies suggested that uptake of single-charged cations associated with the substitution of Al for silica is the dominant cause of CL emission in quartz (Ramseyer et al., 1988; Ramseyer and Mullis, 1990). Perny et al. (1992) concluded that, in addition to Al substitution for Si and the corresponding charge-compensating alkali ions and H, incorporation of trace elements in quartz also depends on fluid chemistry, temperature, and growth speed. As was demonstrated earlier in Chapter 2, fluid temperatures associated with the two generations of quartz overgrowths in the Mount Simon Sandstone may have varied by > 40 °C; this temperature difference may have caused variations in chemical solubility, distribution coefficient, and growth rate between different zonations of quartz overgrowths.

Table 5-7 shows that concentration differences of individual trace elements between the paired overgrowths are usually less than an order of magnitude. In addition to possible difference in fluid compositions between the two generations of fluids, temperature and growth rate may contribute to trace element distribution in different zonations. Variations in trace element contents of more than an order of magnitude in quartz zones, however, are not an effect of temperature and growth rate; change of fluid composition is a predominant control (Perny et al., 1992). Thus, the consistent difference of total alkali and alkaline earth element contents in the two overgrowth zones in Mount Simon Sandstone quartz overgrowths is interpreted to be related to two generations of diagenetic fluids with different properties, including fluid temperatures and compositions.

Inner zone quartz overgrowths also have relatively low B contents compared to outer zone quartz overgrowths. A R=–0.5 correlation value is obtained between B and Al

trace element based on data presented in Table 5-7. It appears that B may have competed with Al for incorporation into quartz tetrahedral site.

Correlations of Trace Element Behaviors in Diagenetic Quartz and K-feldspar

Trace element studies of authigenic quartz and K-feldspar in the Mount Simon Sandstone reveal some interesting results. Dominant anions are Cl^- in diagenetic fluids associated with authigenic K-feldspar and quartz. The concentrations of Li, Mg, Ca, B, and Ti in both authigenic mineral phases are very similar, suggesting that they probably are not competitive with other trace elements. Although these trace elements in quartz overgrowths predominantly occupy interstitial positions, they may occupy lattice defects in K-feldspar. Similar Mg-Ca-Cl correlations were observed in both authigenic mineral phases, suggesting that they have taken similar positions in crystal lattice. The covariance of Mg-Ca-Cl is probably not caused by minute fluid inclusions in overgrowths, because the measured Ca concentration in overgrowths is much lower than the detected Mg and Cl concentrations.

There is the suggestion of regional differences in trace element concentrations. Estimated Fe and Ce concentrations in diagenetic fluids associated with authigenic K-feldspar appear to increase from south to north. Their low D values imply that these trace elements would be enriched in an evolving diagentic fluid. Thus, a northward increase in the concentration of these elements in the calculated fluid supports the theory of northward fluid migrations, consistent with conclusions from Chapter 2 –4. Giving the variability of trace element concentrations within single samples, it is likely that we have too few data to reliably examine regional trends.

Conclusions

Positive correlations were observed among Sr-Ba-Pb-Rb, Na-Mg-Ca-Cl, and K-Al in authigenic cements. They were interpreted as the results of similar geochemical behaviors (Sr-Ba-Pb-Rb in K-feldspar), charge compensation requirement (K-Al in quartz), and continuous enrichment/depletion of trace element concentrations in the diagenetic fluid with respect to fluid-rock interaction and fluid evolution. Minute mineral inclusions may contribute to some high trace element contents in some spot analyses of authigenic mineral phases.

In the absence of distribution coefficients for low-temperature authigenic minerals, distribution coefficients reported for trace elements between sanidine and silicate glass, alkali feldspar and glass, and sanidine and hydrothermal fluids were used to evaluate fluid compositions. The possible northward-increasing trend of Fe and Ce concentrations in diagenetic fluids was interpreted as the results of northward migrations of diagenetic fluids, consistent with conclusions from previous chapters.

Trace element concentrations in different zonations of quartz overgrowths show that total concentrations of alkaline and alkaline earth elements in inner overgrowths are consistently lower than the outer zones. Variations in trace element concentrations in the fluids, the amounts of charge compensation in authigenic minerals, and fluid temperatures may contribute to the differences of trace elements in different zonations, dominated by the variations of fluid chemistry. The amounts of lattice defects in quartz cements are closely associated with the emission of CL. Two generations of diagenetic fluids are implied.

Chapter 6

Preliminary Evaluation of Laser-Probe, *in situ* $^{40}Ar/^{39}Ar$ Dating of Authigenic K-feldspar

Abstract

A preliminary investigation of laser-probe, *in situ* $^{40}Ar/^{39}Ar$ dating techniques was conducted in the Noble Gas Laboratory, Massachusetts Institute of Technology on four samples of the Upper Cambrian Mount Simon Sandstone. Samples analyzed using a single-shot, high-resolution UV-laser technique did not yield detectable radiogenic Ar gas. Multiple shots on overgrowths by the UV laser yielded only small amounts of radiogenic gases. Ages ranging from 888 ± 423 Ma to 1334 ± 242 Ma were obtained in several cases, similar to the ages of potential Precambrian source rocks (1100 – 1890 Ma) in the Midcontinent (Bickford et al., 1986). The UV-laser ablation technique appeared to shatter the K-feldspar, rather than to melt it. Step heating tests of sandstone samples using an Ar-laser at different power levels (0.15 to 1.50 watts) yielded largely meaningless ages. It is hypothesized that the release of relatively large amounts of atmospheric Ar gas compared to radiogenic Ar severely affected Ar corrections and resulted in unsuccessful age calculation. The ceramic mounting material may have been the source of most atmospheric Ar released.

Introduction

Establishing the ages of diagenetic events in the Illinois basin using either conventional K-Ar or $^{40}Ar/^{39}Ar$ age dating of authigenic K-feldspar and illite may help

identify the tectonic events responsible for regional fluid flow during diagenesis and elucidate basinal fluid flow patterns and mass transport. Low-temperature K-feldspars are highly retentive in radiogenic Ar and can be used for age dating (Hay et al., 1988). Just as changes in the chemical compositions of diagenetic minerals and fluids are expected in response to regional fluid migration, the ages of authigenic minerals might vary along the flow path, although these age differences may not always be detectable due to analytical error.

Previous work suggests that the Mount Simon Sandstone has undergone a complicated diagenetic history marked by precipitation of abundant authigenic quartz and K-feldspar cements (Hoholick et al., 1984; Duffin et al., 1989; Fishman, 1997). Duffin et al. (1989) reported a K-Ar ages of 395 Ma for authigenic K-feldspar separates from the Mount Simon Sandstone, using the 2 – 74 μm fraction obtained from a sandstone sample with no detrital feldspar. The Hay et al. (1992) summary of K-Ar dates of authigenic K-feldspar in the Mississippi Valley area indicates that they range from 375 to 448 Ma; $^{40}Ar/^{39}Ar$ incremental heating analysis on 42 – 48 mesh grains of authigenic K-feldspar from the Precambrian – Cambrian unconformity at west Wisconsin yielded ages of 400 – 464 Ma (Hay et al., 1992). The wide range of K-feldspar ages may indicate a lengthy, regional potassic alteration in the Midcontinent. On the other hand, the wide range of age data may be the result of admixture of detrital with authigenic material.

$^{40}Ar/^{39}Ar$ age-dating techniques have been applied to geological materials for more than three decades (Merrihue and Turner, 1966; McDougall and Harrison, 1988). Most $^{40}Ar/^{39}Ar$ ages are obtained from aggregate grains of a separated mineral using step-heating and melting techniques (York et al., 1981; Harrison and McDougall, 1982; Hearn

and Sutter, 1985; Lo Bello et al., 1987; Deino and Potts, 1990; Girard and Onstott, 1991). Age determinations of authigenic K-feldspar have been most successful in carbonate rocks (Hearn and Sutter, 1985; Spötl et al., 1996) from which separates are readily obtained. Authigenic age plateaus are not apparent, but age spectra can be calculated (Hearn and Sutter, 1985) or interpreted (Warnock et al., 1996) to set reasonable constraints on the age of authigenic minerals. Mixing of Ar released from detrital cores into the gas fraction released from the authigenic mineral during heating gives rise to an older, mixed ages.

Development of laser probe $^{40}Ar/^{39}Ar$ dating techniques has been slow (York et al., 1981; Layer et al., 1987; Girard and Onstott, 1991). Girard and Onstott (1991) concluded that the laser would melt an area significantly larger than the beam size, even at low power settings, as a result of laser beam scattering by mineral defects. Beam penetration into underlying detrital feldspar may yield mixed ages, with Ar contributed from both the overgrowth and the core grain (Walgenwitz et al., 1990). Therefore, powerful lasers, e.g., the CO_2 and Ar-ion lasers previously used in laser probe analysis may not permit the spatial resolution necessary for *in situ* $^{40}Ar/^{39}Ar$ analysis of small, authigenic overgrowths.

The low-power ultraviolet laser generated by a Nd-YAG (yttrium-aluminum-garnet) instrument potentially provides the higher spatial resolution and gas yield necessary to obtain meaningful dates of fine-grained, diagenetic minerals (Onstott et al., 1996). Unfortunately, normal epoxies used for thin section preparation cannot fully withstand neutron bombardments necessary for $^{40}Ar/^{39}Ar$ dating (Cohen et al., 1993). These epoxies may cause trouble during analysis, introducing organic compounds that

can significantly affect the Ar systematics during $^{40}Ar/^{39}Ar$ analysis. Based on the results of Cohen et al. (1993), a Ca-free Ceramabond 552 ceramic may be effective as an adhesive to substitute for epoxies. Their results suggest that this ceramic survives processes in a nuclear reactor and their subsequent dating results were acceptable.

The goal of this preliminary study was to obtain $^{40}Ar/^{39}Ar$ ages of K-feldspar overgrowths < 100 μm in thickness using high-resolution, *in situ* UV-laser-microprobe analysis. The advantages of this *in situ* technique include: (1) it avoids the need to mechanically separate authigenic minerals from their detrital grains, (2) the detailed textures of authigenic minerals can be further elucidated, and (3) the technique offer high spatial resolution.

Sample Preparation

Small (~ 3 x 6 cm) sandstone samples from seven localities were cut into billets, with one side of the billet polished using 1000-size grit. Billets were dried before being impregnated overnight with Ca-free Ceramabond 552 ceramic adhesive (Aremco) under vacuum. This Ca-free ceramic adhesive does not interfere with the Ar systematics of the sample, but does contribute a large amount of atmospheric Ar (Cohen et al., 1993). The penetrating capability of this ceramic adhesive is not as good as epoxy, and consequently, impregnation was not always thorough. In most cases, the ceramic adhesive appears to only partially fill the pore spaces near the surface of sample billets. These billets were carefully polished to expose the near-surface area with pore spaces being filled with ceremic. The same ceramic adhesive was used to mount the billets on frosted glass slides. Ceramic and billets were cured, step by step, at 50 °C, 100 °C, 150 °C, and 200 °C for a

total of 12 – 15 hours (each step ~ 3 hours), so that the thin sections could survive irradiation without separating from the glass slide and falling apart. No further curing was made to prevent possible Ar diffusion or Ar loss, although the ceramic reaches its highest strength after being cured at ~ 500 °C. Billets were cooled overnight before polishing into thin sections of 100 to 150 μm thick.

Sections were examined using CL microscopy to select relatively large (several tens of μm in cross-section) K-feldspar overgrowths for $^{40}Ar/^{39}Ar$ dating. Transmitted-light petrographic observation was not possible due to the opacity of the ceramic adhesive. Four of the seven sections were found to contain useful K-feldspar overgrowths (> 20 μm). Reflected light and CL photomicrographs were used to map the K-feldspar overgrowths, and to help locate laser probe targets. Twenty smaller chips (5 mm in diameter) from these sections were cored using a drill press and sent to the Noble Gas Laboratory, Massachusetts Institute of Technology (MIT), for irradiation.

Laser Probe $^{40}Ar/^{39}Ar$ Methodology

$^{40}Ar/^{39}Ar$ analyses of authigenic K-feldspar overgrowths in the Mount Simon Sandstone were carried out in Noble Gas Laboratory at MIT, under the supervision of Drs. Kip Hodges and Bill Olszewski. Chips were irradiated in the McMaster research reactor, Ontario, Canada, for a total 60 hours from October 2 to October 6, 2000. Samples of reagent-grade CaF_2, K_2SO_4, and KCl were included in the irradiation package to routinely monitor reactions of Ca, K, and Cl that produce interfering Ar isotopes. The fast neutron flux and J-values were monitored using natural standards of MMhb-1 hornblende (520.4 Ma) and Fish Canyon sanidine (27.95 Ma).

Four to six sample chips (5 mm diam.) were loaded and the sample chamber was pumped down overnight to reach high vacuum (~ 1.3 x 10^{-8} torr). Blank analyses were conducted before laser extraction of Ar gas from the samples. The operational M/e=40 blanks of the extraction system were consistent through the day and range from 7 x 10^{-16} moles to 1 x 10^{-15} moles, depending on the number of samples in the chamber.

A frequency-quadrupled Nd-YAG instrument was used to produce an ultraviolet (266 nm) beam focusable to a spot size of ~ 5 μm, enabling high spatial resolution age studies of individual crystals in thin section. K-feldspar overgrowths were targeted for UV laser beam ablation, and released Ar gases measured using a MAP 215-50 noble gas mass spectrometer. Incremental step-heating analyses of K-feldspar using an Ar-ion laser beam with different powers and beam sizes (~ 50 μm) were also conducted, as further described below. $^{40}Ar/^{39}Ar$ ages were calculated after corrections with the blank, excess air and a series of interferences (K, Ca, and Cl) on Ar systematics (Turner, 1971a,b; Podosek and Huneke, 1973; McDougall and Harrison, 1988)

Analytical Results and Discussion

UV laser ablation and $^{40}Ar/^{39}Ar$ analyses were performed on two chips from sample C675 (-1305 m) containing relatively large (up to 80 μm) K-feldspar overgrowths. Single shots of the UV laser shattered the overgrowths, releasing large amounts of gas which contained no radiogenic Ar. This result suggests that the gas released by the laser shots was atmospheric air, most likely confined in the porous texture of the ceramic adhesive during thin section preparation.

By increasing the numbers of shots while decreasing power, and by combining gases released from multiple K-feldspar overgrowths, we attempted to obtain enough radiogenic Ar for age calculation purposes. Unfortunately, multiple shots on individual overgrowths enlarged the damaged area on sample surface, increasing the chance of additional detrital K-feldspar being probed. Experiments on samples 675-chip-5 and 675-chip-E yielded $10^{-14} - 10^{-15}$ moles Ar gas, with ~ 4 x 10^{-16} moles $^{40}Ar^{*}$ gas, a gas amount equal to or lower than the Ar blank level. The Ca/K ratios from these samples were extremely high (up to 68), inconsistent with the Ca-poor and K-rich properties of our sandstone samples, and suggesting that normal procedures for correction of ^{37}Ar are not suitable for this set of samples. The correction of Ca (i.e., ^{37}Ar) significantly affects the correction of ^{36}Ar and ^{40}Ar, and ultimately the ages. The calculated ages are 888 ± 423 Ma and 1334 ± 242 Ma, respectively (Table 6-1).

To evaluate the cause of the ^{37}Ar problem, whether instrument- or sample-induced, we analyzed a large grain of detrital quartz. No radiogenic Ar was detected, ruling out instrumental problems. This indicated that our problem was due to poor coupling of the UV laser with the feldspar, resulting in mineral heating and release of Ar gas. An alternative laser source (Ar-ion laser) was employed to melt (Test 1) and heat without melting (Test 2) a large area (~ 2 mm^2) on chip 189-C. A large amount of Ar gas (10^{-12} moles) was detected.

The calculated ages range from 794 ± 144 Ma to 951 ± 376 Ma (Table 6-2), a reasonable age assuming a mixture of detrital (1100 to 1890 Ma of Precambrian basement rocks) and authigenic minerals (~ 400 Ma and younger, based on previous studies). The errors, however, are huge (Table 6-2). These errors probably originate

Table 6-1 $^{40}Ar/^{39}Ar$ analytical results from in situ laser ablation analysis using a ultraviolet laser beam

Sample	J value	36/40Ar	37/40Ar	38/40Ar	39/40Ar	% 39Ar	40Ar*	Age (Ma)
675ch5	1.5440E-2 ± 2.1400E-4	0.000E0 ± 1.869E-3	8.839E-1 ± 8.973E-1	2.852E-3 ± 9.531E-3	2.427E-2 ± 5.858E-3	100	3.566E-01	888 ± 423
675chE	1.5512E-2 ± 6.6950E-4	0.000E0 ± 6.695E-4	2.106E-1 ± 4.260E-1	2.506E-4 ± 3.972E-3	1.417E-2 ± 2.299E-3	100	9.067E-01	1334 ± 242

Table 6-2 $^{40}Ar/^{39}Ar$ analytical results of Mount Simon Sandstone whole rock (Test 1 and 2) using an Ar-ion laser beam *

Sample	J value	36/40Ar	37/40Ar	38/40Ar	39/40Ar	% 39Ar	40Ar*	Age (Ma)
189chC	1.5512E-2 ± 6.695E-4	1.958E-3 ± 3.071E-4	8.153E-2 ± 6.971E-2	4.823E-5 ± 5.225E-4	1.183E-2 ± 7.231E-4	100	2.2040E+00	794 ± 144
189chC	1.5512E-2 ± 6.695E-4	2.891E-3 ± 2.384E-4	4.204E-2 ± 4.540E-2	9.582E-5 ± 2.859E-4	3.253E-3 ± 5.081E-4	26	9.5590E-01	951 ± 376

* Test 1 - Sample melting experiment using an Ar laser; Test 2 - Sample heating experiment using an Ar laser.

from large atmospheric air corrections and the presence of relatively small amounts of radiogenic Ar.

The Ar-ion laser tests suggest that radiogenic Ar gas is present in our samples and may be used for age dating. However, the contamination of large amount of atmospheric air from the porous ceramic adhesive significantly affects the various corrections for Ar-isotope systematics. These tests also suggest that the UV-laser was probably not effective in releasing Ar gas from K-feldspar grains and overgrowths. The high Ca/K ratios collected from the samples suggest that somehow the minor ^{37}Ar (Ca) was detected while the major ^{39}Ar (K) was missed when using the UV-laser beam on our samples. It seems that this problem was caused by the overwhelming amount of air entrapped in the porous ceramic being released during laser probe analysis. Large amount of atmospheric air released from the porous ceramic during the analysis could have resulted in significant errors in the correction program.

Realizing that there was no way to accomplish the original goal of *in situ* UV-laser $^{40}Ar/^{39}Ar$ dating of authigenic K-feldspar overgrowths, we decided to examine spectra released by incremental step-heating of our samples, using the Ar-ion laser. Ar-ion lasers operate at different wavelengths than the UV laser, which may prove more effective in melting the mineral grains and releasing radiogenic Ar. Ar gases obtained from step heating should represent mixtures of Ar released from detrital K-feldspar, K-feldspar overgrowths, and atmospheric Ar entrapped in the mounting ceramic. Age data, after air Ar correction, should represent a mixture of ages from detrital and authigenic K-feldspars, and we hoped that the detrital and overgrowth K-feldspar would have different Ar release behavior, allowing us to distinguish the two.

Table 6-3 summarizes results from the incremental step-heating analysis. In about half the steps measured, there was no radiogenic ^{40}Ar detected. Most of the calculated ages are meaningless, with analytical errors greater than the apparent ages themselves. Step-heating of sample 3707chL yielded promising age data (Table 6-3). From step 1 to step 7, ~ 97% of ^{39}Ar was released. Laser-heating experiments give rise to ages ranging from 878 Ma to 1445 Ma, with analytical errors of about one-half the ages. The last step yielded less than 3% ^{39}Ar and thus meaningless data.

On the basis of the apparent $^{40}Ar/^{39}Ar$ age spectrum of sample 3707chL (Fig. 6-1), it appears that ^{39}Ar was gradually released as the laser beam source power was increased from 1.10 watts to 1.40 watts. Gases released at 1.10 watts yield an apparent $^{40}Ar/^{39}Ar$ age of 1415 ± 773 Ma, a Middle Proterozoic age that is much older than the Upper Cambrian depositional age or previous reported diagenetic age of K-feldspar (~ 400 Ma). The large analytical error (± 773 Ma) again indicates gas contamination by atmospheric Ar. Although a very large amount of gas was detected from this initial heating step, only 4% of ^{39}Ar was released at this step. Most likely, the gas released in this step was dominated by air coming out from the porous ceramic adhesive, introducing a large analytical error in the gas corrections.

The next heating (1.15 watts) released a net 10.9% of total ^{39}Ar, with an associated apparent $^{40}Ar/^{39}Ar$ age of 878 ± 435 Ma, the youngest age derived from the entire heating series. The net ^{39}Ar% released in the next heating step dropped to 7.75% (Fig 6-1, Table 6-3). This drop suggests that radiogenic Ar released from low-temperature authigenic K-feldspar cements peaked at ~1.15 watts (step 2). The Precambrian age likely represents a mixture of detrital K-feldspar and authigenic K-

Table 6-3 $^{40}Ar/^{39}Ar$ incremental step-heating analysis of K-feldspar

Sample	Increment	Cumulative % 39Ar	Net % 39Ar	40Ar*%	Age (Ma)
13638chF	1	92.32	92.32	Error	Error
	2	100.00	7.68	Error	4031 ± Error
189chA	1	0.48	0.48	Error	Error
	2	2.20	1.72	9.24	Error
	3	49.88	47.68	19.14	2747 ± Error
	4	50.36	0.48	26.88	964 ± Error
	5	50.83	0.47	Error	Error
	6	51.16	0.33	Error	Error
	7	66.22	15.06	Error	Error
	8	73.64	7.42	Error	Error
	9	91.14	17.50	Error	Error
	10	91.45	0.31	Error	1600 ± Error
	11	99.78	8.33	Error	Error
	12	100.00	0.22	Error	1738 ± Error
189ch8	1	Error	Error	100.00	Error
	2	16.22	16.22	100.00	1950 ± 2472
	3	66.11	49.89	100.00	455 ± 2101
	4	100.00	33.89	100.00	383 ± 2399
3737chK	1	0.45	0.45	Error	Error
	2	1.22	0.77	Error	Error
	3	2.02	0.80	Error	Error
	4	Error	Error	Error	Error
	5	Error	Error	Error	Error
	6	4.01	1.99	Error	Error
	7	12.03	8.02	5.27	Error
	8	10.13	Error	Error	Error
	9	13.74	3.61	7.59	Error
	10	55.75	42.01	0.37	147 ± Error
	11	57.94	2.19	8.18	1082 ± Error
	12	64.09	6.15	Error	Error
	13	100.00	35.91	11.95	2499 ± 2504
3707chL	1	4.27	4.27	8.04	1415 ± 773
	2	15.17	10.90	8.61	878 ± 435
	3	22.92	7.75	14.59	1091 ± 533
	4	32.11	9.19	14.02	991 ± 498
	5	45.58	13.47	23.59	1229 ± 306
	6	57.92	12.34	18.67	929 ± 371
	7	96.57	38.65	70.43	1445 ± 93
	8	97.82	1.25	63.01	170 ± Error
	9	98.94	1.12	71.83	150 ± Error
	10	99.82	0.88	83.47	596 ± Error
	11	100.00	0.18	73.28	1333 ± Error

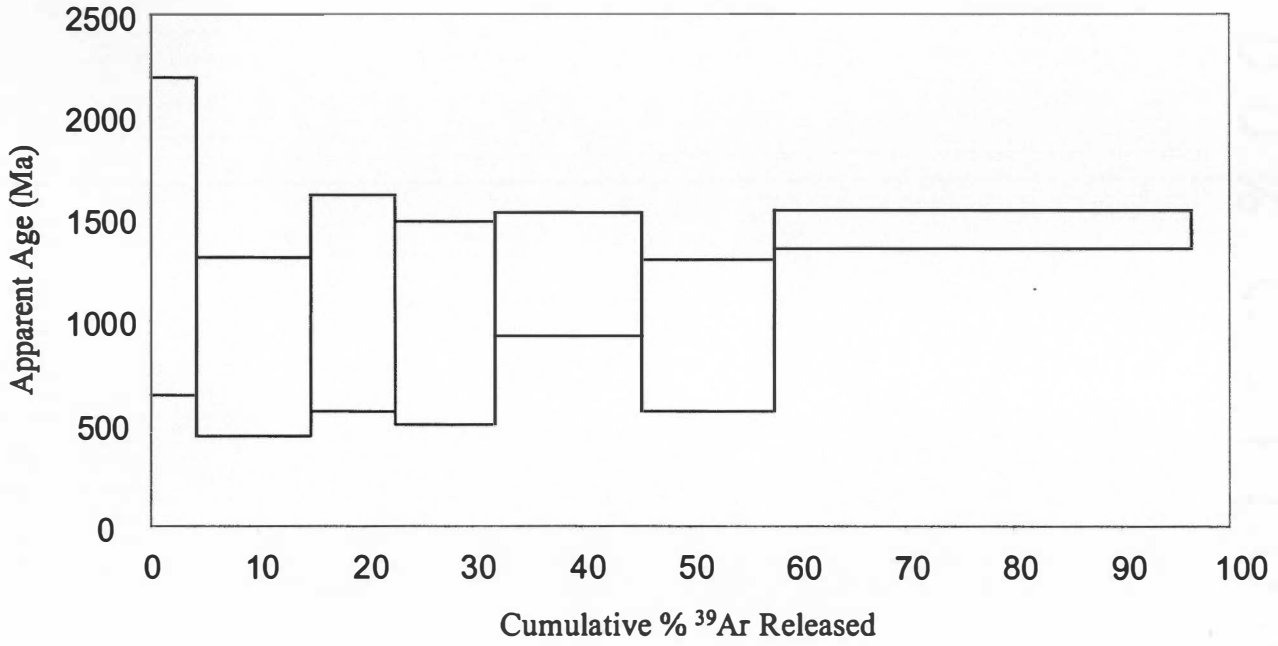

Figure 6-1 Age spectrum for C3707chL K-feldspar from the Mount Simon Sandstone, Illinois basin.

feldspars, although most radiogenic Ar from the detrital K-feldspar was likely not yet released; the formation temperature and Ar retentive temperature of the parental rocks of detrital grains are expected to be much higher than that of cements in the Mount Simon Sandstone.

A steady increase in the release of ^{39}Ar from 1.20 watts to 1.40 watts (step 3 to step 7) indicates release of radiogenic Ar from detrital K-feldspar, increasing with heating temperature. Approximately 97% of the total radiogenic Ar was released in the first 7 steps of heating. Further heating mostly caused the release of entrapped air from the ceramic adhesive, resulting in apparently meaningless ages.

Gases released from step 7 (1.40 watts) comprise a majority of 39% of the total ^{39}Ar, with an apparent age of 1445 ± 93 Ma. The relatively low analytical error of this analysis suggests a relatively large amount of radiogenic Ar released, and a much smaller correction error. The apparent age suggests that detrital K-feldspar grains in the Mount Simon Sandstone probably originated in Middle Proterozoic rocks. This age is consistent with the reported ages of Precambrian basement rocks (1100 – 1890 Ma) in the Midcontinent (Bickford et al., 1986).

Conclusions

Step-heating $^{40}Ar/^{39}Ar$ age dating of detrital K-feldspar from the Mount Simon Sandstone suggests that the grains originated in Middle Proterozoic rocks ~ 1445 ± 93 Ma in age. Ages of authigenic K-feldspar overgrowths were not obtained from this step-heating technique, due to the relatively large area heated by the laser relative to the size of K-feldspar overgrowths. Atmospheric air released from the ceramic contaminated the

Ar released from K-feldspar, and correction of this air compound resulted in large analytical errors.

Preliminary experiments using an UV laser beam for *in situ* $^{40}Ar/^{39}Ar$ analysis of authigenic K-feldspar overgrowths on sandstone thin sections mounted in ceramic adhesive proved to be unsuccessful. Atmospheric air entrapped in the porous-texture ceramic adhesive is not retained within the adhesive, although only the mineral surface was bombarded by the laser beam. The amount of atmospheric air released from the adhesive during laser probing was overwhelming in most cases, due to heat transfer to the whole sample, rather than overgrowths alone. Further investigations should evaluate the use of an excimer laser, as it may couple better with K-feldspar and allow controlled heating of fine overgrowths.

Chapter 7

Future Research

Experimental Determination of Oxygen Isotope Fractionation Between Quartz and Water at Low-Temperature, Low-Pressure Conditions

Oxygen isotope fractionation factors between quartz and waters at medium- and high- temperature conditions have been experimentally and theoretically determined (Clayton et al., 1972; Bottinga and Javoy, 1973; Matsuhisa et al., 1979; Matthews and Beckinsale, 1979; Zhang et al., 1989). The quartz-water fractionation factors determined in different studies are similar at high temperature but diverge with decreasing temperature. At temperatures < 200 °C (*e.g.*, temperatures at diagenetic conditions), low-temperature quartz-fluid fractionation factors are generally extrapolated from these curves. Unfortunately, the differences among these fractionation curves at low-temperature may be very significant, making the evaluation of fluid compositions problematic. Only one theoretical fractionation curve is available for low-temperature quartz-water fractionation (Kawabe, 1978), which has lower fractionation between quartz and water than other curves.

Experimental determination of quartz-water isotope fractionation at low temperature is fundamental to improving geochemical constraints on isotopic compositions of low-temperature fluids in diagenetic processes and fluid-rock interactions. Mackenzie and Gees (1971) synthesized authigenic quartz at room temperature, with precipitated authigenic quartz crystals as large as ~10 μm. Experimental determination of low-temperature quartz-water and K-feldspar-water

fractionation factors may possibly be achieved by synthesizing the minerals at a series of fluid temperatures using different starting materials. Fractionation factors for concentrated brines, as well as water, should be evaluated.

Investigation of Mass Transfer in the Illinois Basin

In this dissertation, I conducted preliminary research on trace elements in the Mount Simon Sandstone. Internal relationships of trace elements in authigenic cements were observed. Unlike oxygen isotope compositions, which indicate northward-increasing $\delta^{18}O$ values and south-to-north fluid migration in the Illinois basin, trace element concentrations in authigenic quartz and K-feldspar show only ambiguous relationships with sample geographic distribution.

Basinal fluid migrations are expected to leave behind an interpretable record of trace element compositions in authigenic minerals. Although a variety of controls may affect trace element incorporation into authigenic minerals, systematic variation of trace element contents in authigenic cements may reveal mass transfer in association with fluid migration in the basin. Future research should try to identify, with confidence, different generations of quartz and K-feldspar before attempting any geochemical analysis. This work requires preparations of a large number of thin sections, detailed petrographic work, and a series of CL analyses in order to obtain the best overgrowths of different generations for trace element and isotope analysis. Only data obtained from the same generation should be compared with each other relative to their geographic localities. A set of these 'clean' data will give us a better look at mass transfer and trace element behaviors in the basin.

^{40}Ar-^{39}Ar age studies of authigenic minerals in the Illinois basin

A preliminary study of ^{40}Ar-^{39}Ar ages on authigenic K-feldspar from the Mount Simon Sandstone was carried out as part of this dissertation research. Lack of success with UV laser *in situ* ^{40}Ar-^{39}Ar dating techniques on authigenic K-feldspar overgrowths of Mount Simon Sandstone may not be solely related to the ceremic mounting technique, because the same sample chips appeared to work well using an alternative Ar-laser beam. Poor-coupling of the UV-laser with K-feldspar resulted in sample heating and release of trapped air. Future work should further test UV laser ablation using relatively larger K-feldspar grains in a thick, very well polished sample section, and also evaluate the potential use of excimer laser probing. The excimer laser may couple better with the feldspar and permit *in situ* analysis of overgrowths. On the other hand, ^{40}Ar-^{39}Ar dating of authigenic K-feldspar separates may give us useful information on diagenetic ages. A better separation technique needs to be established. Acid etching techniques (Girard and Onstott, 1991; Girard and Barnes, 1995) and cathodoluminescence may be used to help obtain purified authigenic phase minerals for diagenetic age dating. The advantage of ^{40}Ar-^{39}Ar dating on separated mineral aggregates is that this technique is well established. Step heating of mineral separates may also give us an idea of the thermal history of authigenic minerals. The disadvantage is obvious, in addition to the tedious separating work, age data obtained from these aggregates represent a mixture without any spatial resolution.

References

Aleinikoff, J.N., Walter, M.; Kunk, M.J., and Hearn, P.P., Jr., 1993, Do ages of authigenic K-feldspar date the formation of Mississippi Valley-type Pb-Zn deposits, central and southeastern United States?: Pb isotopic evidence. Geology, v. 21, p. 73-76.

Allegre, C.J., and Minister, J.F., 1978, Quantitative models of trace element behavior in magmatic processes. Earth and Planetary Science Letters, v. 38, p. 1-25.

Allegre, C.J., Provost, A., and Jaupart, C., 1981, Oscillatory zoning: A pathological case of crystal growth. Nature, v. 294, p. 223-228.

Allison, N., 1996, Comparative determinations of trace and minor elements in coral aragonite by ion microprobe analysis, with preliminary results from Phuket, southern Thailand. Geochimica et Cosmochimica Acta, v. 60, p. 3457-3470.

Appold, M.S. and Garven, G., 1999, The hydrology of ore formation in the southeast Missouri district: Numerical models of topography-driven fluids flow during the Ouachita orogeny. Economic Geology, v. 94, p. 913-936.

Bachu, S., 1995, Synthesis and model of formation-water flow, Alberta Basin, Canada. American Association of Petroleum Geologists Bulletin, v. 79, p. 1159-1178.

Bailey, S.W. and Cameron, E.N., 1951, Temperatures of mineral formation in bottom-run lead-zinc deposits of the Upper Mississippi Valley, as indicated by liquid inclusions. Economic Geology, v. 46, p. 626-651.

Bally, A.W., 1989, Phanerozoic basins of North America, in A.W. Bally and A.R. Palmer eds., The geology of North America - an overview. The Geology of North America, v. A, p. 397-446.

Bear, G.W., 1997, Integration of seismic reflection and potential field analyses—architecture of Precambrian sedimentary basins in Indiana, Illinois, and Kentucky. Unpublished Ph.D. Dissertation, Indiana University, Bloomington, 173 p.

Bethke, C.M., 1985, A numerical model of compaction-driven groundwater flow and heat transfer and its application to the paleohydrology of intracratonic sedimentary basins. Journal of Geophysical Research, v. 90, p. 6817-6828.

Bethke, C.M., 1986, Hydrologic constraints on the genesis of the Upper Mississippi Valley mineral district from Illinois Basin brines. Economic Geology, v. 81, p. 233-248.

Bethke, C.M., and Marshak, S., 1990, Brine migrations across North America – The plate tectonics of groundwater. Annual Review of Earth and Planetary Sciences, v. 18, p. 287-315.

Bethke, C.M., Oltz, D. F., and Reed, J.D., 1990, Long-Range Petroleum Migration in the Illinois Basin: *in* Leighton, M.W., Kolata,D.R., Oltz, D.F., and Eidel, J.J., eds., Interior Cratonic Basins. American Association of Petroleum Geologists Memoir 51, p. 455-472.

Bickford, M.E., van Schmus, W.R., and Zeitz, I., 1986, Proterozoic history of the midcontinent region of North America. Geology, v. 14, p. 492-496.

Bodnar, R.J. and Bethke, P.M., 1984, Systematics of stretching of fluid inclusions I: fluorite and spahalerite at 1 atmosphere confining pressure. Economic Geology, v. 79, p. 141-161.

Bodnar, R.J., 1990, Petroleum migration in the Miocene Monterey Formation, California,

USA: constraints from fluid-inclusion studies. Mineralogical Magazine, v. 54, p. 295-304.

Bottinga, Y., and Javoy, M., 1973, Comments on oxygen isotope geothermometer. Earth and Planetary Science Letters, v. 20, p. 250-265.

Braile, L.W., Hinze, W.J., Sexton, J.L., Keller, G.R., and Lidiak, E.G., 1984, Tectonic development of the New Madrid Seismic Zone: Symposium on New Madrid Seismic Zone. U.S. Geological Survey, Open File Report 84-770, p. 204-233.

Brand, U., and Veizer, J., 1980, Chemical diagenesis of a multicomponent carbonate system – 1: trace elements. Journal of Sedimentary Petrology, v. 50, p. 1219-1236.

Brannon, J.C., Podosek, F.A., and McLimans, R.K., 1992, Alleghenian age of the Upper Mississippi Valley zinc-lead deposit determined by Rb-Sr dating of sphalerite. Nature, v. 356, p. 509-511.

Brannon, J.C., Cole, S.C., Podosek, F.A., Ragan, V.M., Coveney, R.M., Jr., Wallace, M.W., and Bradley, A.J., 1996, Th-Pb and U-Pb dating of ore-stage calcite and Paleozoic fluid flow. Science, v. 271, p. 491-493.

Bruhn, F., Bruckschen, P., Meijer, J., Stephan, A., Richter, D.K., and Veizer, J., 1996, Cathodoluminescence investigations and trace-element analysis of quartz by micro-PIXE: implications for diagenetic and provenance studies in sandstone. Canadian Mineralogist, v. 34, p. 1223-1232.

Buschbach, T.C., and Kolata, D.R., 1990, Regional setting of Illinois Basin, *in* Leighton,M.W., Kolata,D.R., Oltz, D.F., and Eidel, J.J., eds., Interior Cratonic Basin. American Association of Petroleum Geologists Memoir 51, p. 29-55.

Buyce, M.R. and Friedman, G.M., 1975, Significance of authigenic K-feldspar in Cambrian-Ordovician carbonate rocks of the proto-Atlantic shelf in North America. Journal of Sedimentary Petrology, v. 45, p. 808-821.

Byrnes, A.P. and Wilson, M.D., 1992, Porosity, permeability, and capillary pressure trends in the St. Peter and Mt. Simon sandstones, Illinois Basin. American Association of Petroleum Geologists Bulletin, v. 76, v. 1272-1273.

Chen, Z., Riciputi, L.R., Mora, C.I., Bodnar, R.J., and Fishman, N.S., 2000, Diagenetic fluids of the Sandstone in the Illinois basin – fluid inclusion and cathodoluminescence from diagenetic quartz. Geological Society of America Abstracts With Programs, v. 32, No.7, p. 11.

Chen, Z., Riciputi, L.R. Mora, C. I., and Fishman, N.S., 2001, Regional fluid migration in the Illinois basin: Evidence from in situ oxygen isotope analysis of authigenic K-feldspar and quartz from the Mount Simon Sandstone. Geology (in press).

Chesley, J.T., Halliday, A.N., Kyser, T.K., and Spry, P.G., 1994, Direct dating of Mississippi Valley-type mineralization – use of Sm-Nd in fluorite. Economic Geology, v. 89, p. 1192-1199.

Clayton, R.N., O'Neil, J.R., and Mayeda, T.K., 1972, Oxygen isotope exchange between quartz and water. Journal of Geophysical Research, v. 77, p. 3057-3067.

Clayton, R.N., Goldsmith, J.R., and Mayeda, T.K., 1989, Oxygen isotope fractionation in quartz, albite, anorthite and calcite. Geochimica et Cosmochimica Acta, v. 53, p. 725-733.

Clendenin, C.W. and M.J. Duane, 1990, Focused fluid flow and Ozark Mississippi Valley-type deposits. Geology, v. 18, p. 116-119.

Clendenin, C.W., Niewendorp, C.A., Duane, M.J., and Lowell, G.R., 1994, The paleohydrology of Southeast Missouri Mississippi Valley-type deposits: Interplay of faults, fluids, and adjoining lithologies. Economic Geology, v. 89, p. 322-332.

Cohen, H.A., Cumbest, R.J., and Onstott, T.C., 1993, Alumina ceramic as a mounting medium for electron microprobe analysis and $^{40}Ar/^{39}Ar$ laser microprobe dating of mineral grains. Chemical Geology, v. 106, p. 443-452.

Cottingham, J.T., 1990, Cambrian/Early Ordovician sequence stratigraphy and Mt. Simon Sandstone petrology – Michigan Basin. American Association of Petroleum Geologists Bulletin, v. 74, p. 634.

Crawford, M.L., 1981, Phase equilibria in aqueous fluid inclusions, *in* Hollister, L.S. and Crawford, M.L., eds., Fluid inclusions: Application to Petrology. Mineralogical Association of Canada Short Course Handbook 6, p. 75-100.

Deino, A., and Potts, R., 1990, Single-crystal $^{40}Ar/^{39}Ar$ dating of the Olorgesailie Formation, southern Kenya Rift. Journal of Geophysical Research, v. 95, p. 8453-8470.

Demars, C., Pagel, M., Deloule, E., and Blanc, P., 1996, Cathodoluminescence of quartz from sandstones: Interpretation of the UV range by determination of trace element distributions and fluid-inclusion P-T-X properties in authigenic quartz. American Mineralogist, v. 81, p. 891-901.

Deming, D., 1994, Fluid flow and heat transport in the upper continental crust: *in* Parnell, J., ed., Geofluids: Origin, Migration and Evolution of fluids in Sedimentary Basins, Geological Society Special Publication No.78, p. 27-42.

DePaolo, D.J., 1981, Trace element and isotopic effects of combined wall rock

assimilation and fractional crystallization. Earth and Planetary Science Letters, v. 53, p. 189-202.

Diehl, S.F., and Goldhaber, M.B., 1995, Feldspar diagenesis in Cambrian clastic rocks of the southern Ozark Mountains and Reelfoot Rift, southeastern Missouri and northeastern Arkansas – implications for Mississippi Valley-type ore genesis. U.S. Geological Survey Bulletin, 1989-F, p. 1-17.

Doe, B.R., Stuckless, J.S., and Delevaux, M.H., 1983, The possible bearing of granite of the UPH deep holes, Northern Illinois, on the origin of Mississippi Valley ore-deposits. Journal of Geophysical Research, v. 88, p. 7335-7345.

Drahovzal, J.A., 1997, Proterozoic sequences and their implications for Precambrian and Cambrian geologic evolution of western Kentucky – Evidence from seismic reflection data. Seismological Research Letters, v. 68, p. 553-566.

Driese, S.G., Byers, C.W., and Dott, R.H., Jr., 1981, Tidal deposition in the basal Upper Cambrian Mt. Simon Formation in Wisconsin. Journal of Sedimentary Petrology, v. 51, p. 367-381.

Duffin, M.E., Lee, M., Klein, G., and Hay, R.L., 1989, Potassic diagenesis of Cambrian sandstones and Precambrian granitic basement in UPH-3 Deep Hole, Upper Mississippi valley, U.S.A. Journal of Sedimentary Petrology, v. 59, p. 848-861.

Elliott, W.C. and J.L. Aronson, 1987, Alleghenian episode of K-bentonite illitization in the southern Appalachian basin. Geology, v. 15, p. 735-739.

Erickson, A.J., Jr., 1965, Temperatures of calcite deposition in the Upper Mississippi Valley lead-zinc deposits. Economic Geology, v. 60, p. 506-528.

Farquhar, M.L., Wogelius, R.A., and Tang, C.C., 1999, In situ Synchrotron x-ray

reflectivity study of the oligoclase feldspar mineral-fluid interface. Geochimica et Cosmochimica Acta, v. 63, 1587-1594.

Fayek, M., and Kyser, T.K., 1997, Characterization of multiple fluid-flow events and rare-earth-element mobility associated with formation of unconformity-type uranium deposits in the Athabasca Basin, Saskatchewan. Canadian Mineralogist, v. 35, p. 627-658.

Fishman, N.S., 1997, Basin-wide fluid movement in a Cambrian paleoaquifer—evidence from the Mt. Simon Sandstone, Illinois and Indiana, in Montañez, I.P., Gregg, J.M., and Shelton, K.L., eds., Basin-wide diagenetic patterns: SEPM (Society for Sedimentary Geology) Special Publication No. 57, p. 221-234.

Fleischer, M., and Altschuler, Z.S., 1969, The relationship of the rare-earth composition of minerals to geological environment. Geochimica et Cosmochimica Acta, v. 33, p. 725-732.

Freedman, Y.E., Magaritz, M., Long, G.L., and Ronen, D., 1994, Interaction of metals with mineral surfaces in a natural groundwater environment. Chemical Geology, v. 116, p. 111-121.

Friedman, G.M., 1993, Do ages of authigenic K-feldspar date the formation of Mississippi Valley-type Pb-Zn deposits, central and southeastern United States?: Pb isotopic evidence: comment. Geology, v. 21, p. 861-862.

Gao, J., and Green, T.H., 1989, Barium partitioning between alkali feldspar and silicate liquid at high temperature and pressure. Contributions to Mineralogy and Petrology, v. 102, p. 328-335.

Gao, L., Santschi, P.H., Baskaran, M., and Zindler, A., 1995, Distribution of dissolved

and particulate (super 230) Th and (super 232) Th in seawater from the Gulf of Mexico and off Cape Hatteras as measured by SIMS. Earth and Planetary Science Letters, v. 133, p. 117-128.

Garven, G. and Freeze, R.A., 1984, Theoretical analysis of the role of groundwater flow in the genesis of stratabound ore deposits; 1, Mathematical and numerical model. American Journal of Science, v. 284, p. 1085-1124.

Garven, G. and Freeze, R. A., 1984, Theoretical analysis of the role of groundwater flow in the genesis of stratabound ore deposits; 2, Quantitative results. American Journal of Science, v. 284, p. 1125-1174.

Gast, P.W., 1968, Trace element fractionation and the origin of tholeiitic and alkaline magma types. Geochimica et Cosmochimica Acta, v. 32, p. 1057-1086.

Girard, J.P., and Barnes, D.A., 1995, Illitization and paleothermal regimes in the Middle Ordovician St. Peter Sandstone, Central Michigan Basin: K-Ar, oxygen isotope and fluid inclusion data. American Association of Petroleum Geologists Bulletin, v. 79, p.49-69.

Girard, J.P., and Deynoux, M., 1991, Oxygen isotope study of diagenetic quartz overgrowths from the Upper Proterozoic quartzites of western Mali, Taoudeni basin: implications for conditions of quartz cementation. Journal of Sedimentary Petrology, v. 61, p. 406-418.

Girard, J.P. and Onstott, T.C., 1991, Application of $^{40}Ar/^{39}Ar$ laser-probe and step-heating techniques to the dating of diagenetic K-feldspar overgrowth. Geochimica et Cosmochimica Acta, v. 55, p. 3777-3793.

Goldhaber, M.B., Mosier, E., and Church S.E., 1990, The Illinois Basin as a flow path for

ore fluid. American Association of Petroleum Geologists Bulletin, v. 74, p. 663.

Goldschmidt, V.M., 1954, Geochemistry. Oxford University Press, London, 730 p.

Goldstein, R. H., and Reynolds, T.J., 1994, Systematics of Fluid Inclusions in Diagenetic Minerals. Society for Sedimentary Geology (SEPM) Short Course 31.

Gotze, J., and Plotze, M., 1997, Investigation of trace-element distribution in detrital quartz by electron paramagnetic resonance (EPR). European Journal of Mineralogy, v, 9, p. 529-537.

Graham, C.M., Valley, J.W., and Winter, B.L., 1996, Ion microprobe analysis of 18O/16) in authigenic and detrital quartz in the St. Peter Sandstone, Michigan basin and Wisconsin arch, USA: Contrasting diagenetic histories. Geochemica et Cosmochimica Acta, v. 60, p. 5101-5116.

Gratz, J.F., and Misra, K.C., 1987, Fluid inclusion study of the Gordonsville zinc deposit, central Tennessee. Economic Geology, v. 82, p. 1790-1804.

Guy, C., Daux, V., and Schott, J., 1999, Behaviour of rare earth elements during seawater/ basalt interactions in the Mururoa Massif. Chemical Geology, v. 158, p. 21-35.

Haas, J.L., 1978, An empirical equation with the tables of smoothed solubilities of methane in water and aqueous sodium chloride solutions up to 25 weight percent, 360 °C and 138 MPa. U.S. Geological Survey Open-File Report 78-1004.

Hadizadeh, J., and Foit, F.F., 2000, Feasibility of estimating cementation rates in a brittle fault zone using Sr/Ca partition coefficients for sedimentary diagenesis. Journal of Structural Geology, v. 22, p. 401-409.

Hagni, R.D., 1983, Ore microscopy, paragenetic sequence, trace element content, and

fluid inclusion studies of the copper-lead-zinc deposits of the southeast Missouri lead district, *in* Kisvarsanyi, G., Grant, S.K., Pratt, W.P., and Koenig, J.W., eds., International Confereence on Mississippi Valley Type Lead-Zinc Deposits. Proceedings volume: Rolla, University of Missouri_Rolla Press, p. 243-256.

Hanor, J.S., 1980, Dissolved methane in sedimentary brines: Potential effect on the PVT properties of fluid inclusions. Economic Geology, v. 75, p. 603-617.

Harper, D.A., F.J. Longstaffe, M.A. Wadleigh, and R.H. McNutt, 1995, Secondary K-feldspar at the Precambrian-Paleozoic unconformity, southwestern Ontario. Canadian Journal of Earth Sciences, v. 32, p. 1432-1450.

Harrison, T.M., and McDougall, I., 1982, The thermal significance of potassium feldspar K-Ar ages inferred from $^{40}Ar/^{39}Ar$ age spectrum results. Geochimica et Cosmochimica Acta, v. 46, 1811-1820.

Haskin, L. and Gehl, M.A., 1963, The rare earth contents of standard rocks G-1 and W-1 and their comparison with other rare-earth distribution patterns. Journal of Geophysical Research, v. 68, p. 2037-2043.

Hay, R.L., M. Lee, D.R. Kolata, J.C. Matthews, and J.P. Morton, 1988, Episodic patassic diagenesis of Ordovician tuffs in the Mississippi Valley area. Geology, v. 16, p. 743-747.

Hay, R.L., Liu, J. Deino, A., and Kyser, T.K., 1992, Age of authigenic K-feldspar in low Paleozoic and uppermost Precambrian rocks of the Mississippi Valley area. Geological Society of America Abstracts With Programs, v. 24, No. 7, p. 198.

Hay, R.L., Heimann, A., and Deino, A., 1993, Dating of authigenic K-feldspar by different methods. Abstracts With Programs-Geological Society of America, v.

25, No. 6, p. 75.

Hearn, P.P. and Sutter, J. F., 1985, Authigenic potassium feldspar in Cambrian carbonates: Evidence of Alleghanian brine migration. Science, v. 228, p. 1529-1531.

Hervig, R.L., Williams, L.B., Kirkland, I.K., and Longstaffe, F.J., 1995, Oxygen isotope microanalyses of diagenetic quartz: Possible low temperature occlusion of pores. Geochimica et Cosmochimica Acta, v. 59, p. 2537-2543.

Heyl, A.V., 1983, Geological characteristics of three Mississippi Valley-type districts, *in* Kisvarsanyi, G., Grant, S.K., Pratt, W.P., and Koenig, J.W., eds., International Conference on Mississippi Valley Type Lead-Zinc Deposits. Proceedings volume: Rolla, University of Missouri-Rolla Press, p. 27-60.

Hoholick, J.D., Metarko, T., and Potter, P.E., 1984, Regional variations of porosity and cement: St. Peter and Mount Simon sandstones in Illinois Basin. American Association of Petroleum Geologists Bulletin, v. 68, p. 753-764.

Holten, T., Jamtveit, B., and Meakin, P., 2000, Noise and Oscillatory zoning of minerals. Geochimica et Cosmochimica Acta, v. 64, p. 1893-1904.

Hoskin, P.W.O., 2000, Patterns of chaos: Fractal statistics and the oscillatory chemistry of zircon. Geochimica et Cosmochimica Acta, v. 64, p. 1905-1923.

Houseknecht, D.W., 1991, Use of cathodoluminescence petrography for understanding compaction, quartz cementation, and porosity in sandstones, *in* Barker, C.E. and Kopp, O.C. eds., Luminescence Microscopy and Spectroscopy: Qualitative and Quantitative Applications. Society for Sedimentary Geology (SEPM) Short Course 25, p. 59-66.

Huang, Y., and Fairchild. I.J., 2001, Partition of Sr and Mg into calcite under karst-analogue experimental conditions. Geochimica et Cosmochimica Acta, v. 65, p. 47-62.

Huerta-Diaz, M.A., Tessier, A., and Carignan, R., 1998, Geochemistry of trace metals associated with reduced sulfur in freshwater sediments. Applied Geochemistry, v. 13, p. 213-233.

Icenhower, J., and London, D., 1996, Experimental partitioning of Rb, Cs, Sr, and Ba between alkali feldspar and peraluminous melt. American Mineralogist, v. 81, p. 719-734.

Kastner, M. and Siever, R., 1979, Low temperature feldspars in sedimentary rocks. American Journal of Science, v. 279, p. 435-479.

Kawabe, I., 1978, Lattice dynamical aspect of oxygen isotope partition function ratio for alpha quartz. Geochemical Journal, v. 13, p. 57-67.

Kharaka, Y. K. and Thordsen, J. J., 1992, Stable isotope geochemistry and origin of waters in sedimentary basins, *in* Clauer, N. and Chaudhuri, S., eds., Isotopic signatures and Sedimentary Records. Springer-Verlag Berlin Heidelberg, p. 411-466.

Kolata, D.R. and Nelson, W.J., 1990, Tectonic history of the Illinois Basin: *in* Leighton, M.W., Kolata, D.R., Oltz, D.F., and Eidel, J.J., eds., Interior Cratonic Basin. American Association of Petroleum Geologists Memoir 51, p. 263-285.

Kontak, D.J., and Smith, P.K., 1993, A metaturbidite-hosted lode gold deposit: The Beaver Dam deposit, Nova Scotia. I: Vein paragenesis and mineral chemistry. Canadian Mineralogist, v. 31, p. 471-522.

Krueger, H.W. and Woodward, H.H., 1972, Potassium-argon dating of sanidine-rich beds in the St. Peter Sandstone, Wisconsin. Geological Society of America Abstracts with Programs, v. 4, p. 568-569.

Kunk, M.J., Simonson, B.M., and Smoot, J.P., 1995, $^{40}Ar/^{39}Ar$ constrains on the age of K-Feldspar cementation in non-marine sediments of the Newark, Gettysburg, and Culpeper Basins. Abstracts With Programs-Geological Society of America, v. 27, No. 1, p. 62.

Lagache, M., 1984, The exchange equilibrium distribution of alkali and alkaline-earth elements between feldspar and hydrothermal solutions. *In* Brown, W.L. ed., Feldspars and Feldspathoids. D. Reidel Publishing Company, Boston, p. 247-280.

Lange, S., Chaudhuri, S., and Clauer, N., 1983; Strontium isotopic evidence for the origin of barites and sulfides from the Mississippi Valley-type ore deposits in Southeast Missouri. Economic Geology, v. 78, p. 1255-1261.

Larson, L.T., Miller, J.D., Nadeau, J.E., and Roedder, E., 1973, Two sources of error in low temperature inclusion homogenization determination, and corrections on publishsed temperatures for the East Tennessee and Laisvall deposits. Economic Geology, v. 68, p. 113-116.

Layer, P.W., Hall, C.M., and York, D., 1987, The derivation of $^{40}Ar/^{39}Ar$ age spectra of single grains of hornblende and biotite by laser step-heating. Geophysical Research Letters, v. 14, p. 757-760.

Leach, D.L., 1979, Temperature and salinity of the fluids responsible for minor occurrences of sphalerite in the Ozark region of Missouri. Economic Geology, v. 74, p. 931-937.

Leach, D.L., Nelson, R.C., and Williams, D., 1975, Fluid inclusion studies in the northern Arkansas zinc district. Economic Geology, v. 70, p. 1084-1091.

Leach, D.L. and Rowan, E.L., 1986, Genetic link between Ouachita foldbelt tectonism and the Mississippi Valley-type lead-zinc deposits of the Ozarks. Geology, v. 14, p. 931-935.

Lee, M. and Savin, S.M., 1985, Isolation of diagenetic overgrowths on quartz sand grains for oxygen isotopic analysis. Geochimica et Cosmochimica Acta, v. 49, p. 497-501.

Leeman, W.P. and Phelps, D.W., 1981, Partitioning of rare earths and other trace elements between sanidine and coexisting volcanic glass. Journal of Geophysical Research, v. 86, p. 1093-1099.

Leighton, M.W., 1990, Introduction to interior cratonic Basin: *in* Leighton, M.W., Kolata, D.R., Oltz, D.F., and Eidel, J.J., eds., Interior Cratonic Basins. American Association of Petroleum Geologists Memoir 51, p. 1-24.

Leighton, M.W. and Kolata, D.R., 1990, Selected interior cratonic basins and their place in the scheme of global tectonics: A synthesis: *in* Leighton, M.W., Kolata, D.R., Oltz, D.F., and Eidel, J.J., eds., Interior Cratonic Basins. American Association of Petroleum Geologists Memoir 51, p. 729-797.

Lev, S.M., McLennan, S.M., and Hanson, G.N., 1999, Mineralogic controls on REE mobility during black-shale diagenesis. Journal of Sedimentary Research, v. 69, p. 1071-1082.

Lo Bello, P., Feraud, G., Hall, C.M., York, D., Lavina, P., and Bernat, M., 1987, $^{40}Ar/^{39}Ar$ step-heating and laser fusion dating of a Quaternary pumice from

Neschers, Massif Central, France; the defeat of xenocrystic contamination. Chemical Geology, v. 66, p. 61-71.

Lohmann, K.C., and Walker, J.C.J., 1989, The $\delta^{18}O$ record of Phanerozoic abiotic marine calcite cements. Geophysical Research Letters, v. 16, p. 319-322.

Long, P.E., 1978, Experimental determination of partition coefficients for Rb, Sr, and Ba between alkali feldspar and silicate liquid. Geochimica et Cosmochimica Acta, v. 42, p. 833-846.

Long, K.R., Kelly, W.C., Ohle, E.L., and Lohman, N.K.C., 1986, Groung preparation and zinc mineralization in bedded and breccia ores of the Monte Cristo mine, north Arkansas. Economic Geology, v. 81, p. 809-830.

Lorens, R.B., 1981, Sr, Cd, Mn, and Co distribution coefficients in calcite as a function of calcite precipitation rate. Geochimica et Cosmochimica Acta, v. 45, p. 553-561.

Mackenzie, F.T., and Gees, R., 1971, Quartz: Synthesis at earth-surface conditions: Science, v. 173, p. 533-535.

Marshall, D.B., Woodward, H.H., and DePaolo, D.J., 1986, K-Ca-Ar systematics of authigenic sanidine from Waukau, Wisconsin, and the diffusivity of argon: Geology, v. 14, p. 936-938.

Matsuhisa, Y., Goldsmith, J.R., and Clayton, R.N., 1979, Oxygen isotopic fractionation in the system quartz-albite-anorthite-water. Geochimica et Cosmochimica Acta, v. 43, p. 1131-1140.

Matthews, A., and Beckinsale, D.R., 1979, Oxygen isotope equilibration systematics between quartz and water. American Mineralogist, v. 64, p. 232-240.

McBride, J.H., 1998, Understanding basement tectonics of an interior cratonic basin: southern Illinois Basin, USA. Tectonophysics, v. 293, p. 1-20.

McDougall, I., and Harrison, T.M., 1988, Geochronology and Thermochronology by the $^{40}Ar/^{39}Ar$ method. Oxford University Press, New York, 212 p.

McIntire, W.L., 1964, Trace element partition coefficients – a review of theory and applications to geology. Geochimica et Cosmochimica Acta, v. 27, p. 1209-1264.

McLimans, R.K., 1977, Geologic, fluid inclusion, and stable isotope studies of the Upper Mississippi Valley zinc-lead district, southwest Wisconsin. Unpublished Ph.D. thesis, University Park, Pennsylvania State University, 175 p.

McNeil, B., Shaw, H.F., and Rankin, A.H., 1995, Diagenesis of the Rotliegend Sandstones in the V-Fields, southern North Sea: a fluid inclusion study, *in* Cubitt, J.M., and England, W.A. eds., The Geochemistry of Reservoirs, p. 125-139.

Merrihue, C., and Turner, G., 1966, Potassium-argon dating by activation with fast neutrons. Journal of Geophysics Research, v. 71, p. 2852-2857.

Miller, J., 1988, Cathodoluminescence microscopy, *in* Tucker, M. ed., Techniques in Sedimentology, p. 174-190.

Milliken, K.L., Mack, L.E., and Land, L.S., 1994, Elemental mobility in sandstones during burial: whole-rock chemical and isotopic data, Frio formation, South Texas. Journal of Sedimentary Research, v. A64, p. 788-796.

Morse, J.W., and Bender, M.L., 1990, Partition coefficients in calcite: Examination of factors influemcing the validity of experimental results and their application to natural systems. Chemical Geology, v. 82, p. 265-277.

Mucci, A., and Morse, J., 1983, The incorporation of Mg^{2+} and Sr^{2+} into calcite

overgrowths: influences oof growth rate and solution composition. Geochimica et Cosmochimica Acta, v. 47, p. 217-233.

Murata, K.J., Rose, H.J. Jr., Carron, M.K., and Glass, J.J., 1957, Systematic variation of rare-earths in cerium-earth minerals. Geochimica et Cosmochimica Acta, v. 11, p. 141-161.

Musgrove, M.L., and Banner, J.L., 1993, Regional ground-water mixing and the origin of saline fluids: Midcontinent, United States. Science, v. 259, p. 1877-1882.

Nakai, S., Halliday, A.N., Kesler, S.E., and Jones, H.D., 1990, Rb-Sr dating of sphalerites from Tennessee and the genesis of Mississippi Valley type ore deposits. Nature, v. 346, p. 354-357.

Nakai, S., Halliday, A.N., Kesler, S.E., and Jones, H.D., Kyle, J.R., and Lane, T.E., 1993, Rb-Sr dating of sphalerites from Mississippi Valley-type (MVT) ore deposits. Geochimica et Cosmochimica Acta, v. 57, p. 417-427.

Nesbitt, H.W., 1980, characterization of mineral-formation water interaction in Carboniferous sandstones and shales of the Illinois Sedimentary Basin. American Journal of Science, v. 280, p. 607-630.

Noble, E.A., 1963, Formation of ore deposits by water of compaction. Economic Geology, v. 58, p. 1145-1156.

Oakes, C.S., Bodnar, R.J., and Simonson, J.M., 1990, The system NaCl-$CaCl_2$-H_2O. I. The ice liquidus at 1 atm total pressure. Geochimica et Cosmochimica Acta, v. 54, p. 603-610.

Odom, I.E., Willand, T.N., and Lassin, R.J., 1979, Paragenesis of diagenetic minerals in the St. Peter Sandstone (Ordovician), Wisconsin and Illinois. In Scholle, P.A.,

and Schluger, P.R. eds., Aspects of Diagenesis, p. 425-443.

Ohkouchi, N., Kawahata, H., Okada, M., Murayama, M., Matsumoto, E., Nakamura, T., and Taira, A., 1995, Benthic foraminifera cadmium record from the western Equatorial Pacific. Marine Geology, v. 127, p. 167-180.

Oliver, J., 1986, Fluids expelled tectonically from orogenic belts: their role in hydrocarbon migration and other geological phenomena. Geology, v. 14, p. 99-102.

O'Neil, J.R., and Taylor, H.P., Jr., 1967, The oxygen isotope and cation exchange chemistry of feldspars: American Mineralogist, v. 52, p. 1414-1437.

Onstott, T.C., Cohen, H., Miller. C., and Golden, J., 1996, Applications for UV laser microprobe to $^{40}Ar/^{39}Ar$ dating of fine-grained diagenetic minerals. American Geophysical Union Transactions, v. 77, No. 17, Supplementary, p. 92.

Osborne, M. and Haszeldine, S., 1993, Evidence for resetting of fluid inclusion temperatures from quartz cements in oilfields. Marine and Petroleum Geology, v. 10, p. 271-278.

Ottonello, G., 1997, Principles of Geochemistry. Columbia University Press, New York, 894 p.

Patterson, R.J., and Spoel, T., 1981, Laboratory measurements of the strontium distribution coefficient K_d^{Sr} for sediments from a shallow sand aquifer. Water Resources Reseearch, v. 17, p. 513-520.

Perny, B., Eberhardt, P., Ramseyer, K., Mullis, J., and Pankrath, R., 1992, Microdistribution of Al, Li, and Na in α quartz: possible causes and correlation with short-lived cathodoluminescence. American Mineralogist, v. 77, p. 534-544.

Person, M. and G. Garven, 1994, A sensitivity study of the driving forces on fluid flow during continental-rift basin evolution. Geological Society of American Bulletin, v. 106, p. 461-475.

Pettijohn, F.J., Potter, P.E., and Siever, R., 1987, Sand and Sandstone. Springer-Verlag, New York, 553 p.

Pitman, J.K. and C. Spötl, 1996, Origin and timing of carbonate cements in the St. Peter Sandstone, Illinois Basin: Evidence for a genetic link to Mississippi Valley-type mineralization. Society for Sedimentary Geology (SEPM) Special Publication 55, p. 187-203.

Pitman, J.K., Goldhaber, M.B., and Spötl, C., 1997, Regional diagenetic patterns in the St. Peter sandstone: Implications for brine migration in the Illinois Basin. U.S. Geological Survey Bulletin 2094-A, p. 1-17.

Plumlee, G.S., Leach, D.L., Hofstra, A.H., Landis, G.P., Rowan, E.L., and Viets, J.G., 1994, Chemical reaction path modeling of ore deposition in Mississippi Valley-type Pb-Zn deposits of the Ozark region, U.S. midcontinent. Economic Geology, v. 89, p. 1361-1383.

Podosek, F.A., and Huneke, J.C., 1973, Argon 40-argon 39 chronology of four calcium-rich achondrites. Geochimica et Cosmochimica Acta, v. 37, p. 887-904.

Potter, R.W., II, 1977, Pressure corrections for fluid-inclusion homogenization temperatures based on the volumetric properties of the system $NaCl-H_2O$. United States Geological Survey Journal of Research, v. 5, p. 603-607.

Pryor, W.A., 1972, Reservoir inhomogeneities of some recent sand bodies. Society of Petroleum Engineers Transactions, v. 253, p. 229-244.

Quinlan, G.M., 1987, Models of subsidence mechanisms in intracratonic basins and their applicability to North American examples, *in* C. Beaumont and A. J. Tankard eds., Sedimentary basins and basin-forming mechanisms. Canadian Society of Petroleum Geologists Memoir 12, p. 463-481.

Ramseyer, K., Baumann, J., Matter, A., and Mullis, J., 1988, Cathodoluminescence colors of α-quartz. Mineralogical Magazine, v. 52, p. 669-677.

Ramseyer, K., Fisscher, J., Matter, A., Eberhardt, P., and Geiss, J., 1989, A cathodoluminescence microscope for low intensity luminescence. Journal of Sedimentary Petrology, v. 59, p. 619-622.

Ramseyer, K., and Mullis, J., 1990, Factors influencing short-lived blue cathodoluminescence of α-quartz. American Mineralogist, v. 75, p. 791-800.

Ravenhurst, C.E., Reynolds, P.H., Zentilli, M., Krueger, H.W., and Blenkinsop, J., 1989, Formation of Carboniferous Pb-Zn and barite mineralisation from basin-derived fluids, Nova Scotia, Canada. Economic Geology, v. 84, p. 1471-1488.

Riciputi, L.R., and Paterson, B.A., 1994, High spatial-resolution measurement of O isotope ratios in silicates and carbonates by ion microprobe. American Mineralogist, v. 79, p. 1227-1230.

Riciputi, L.R., Machel, H.G., and Cole, D.R., 1994, An ion microprobe study of diagenetic carbonates in the Devonian Nisku Formation of Alberta, Canada. Journal of Sedimentary Research, v. A64, p. 115-127.

Riciputi, L.R., Paterson, B.A., and Ripperdan, R.L., 1998, Measurement of light stable isotope ratios by SIMS: Matrix effects for oxygen, carbon, and sulfur isotopes in minerals. International Journal of Mass Spectrometry and Ion Processes, v. 178, p.

81-112

Rimstidt, J.D., Balog, A., and Webb, J., 1998, Distribution of trace elements between carbonate minerals and aqueous solution. Geochimica et Cosmochimica Acta, v. 62, p. 1851-1863.

Robin, M. J.L., Sudicky, E.A., Gillham, R.W., and Kachanoski, R.G., 1991, Spatial variability of strontium distribution coefficients and their correlation with hydraulic conductivity in the Canadian Forces Base Borden Aquifer. Water Resources Research, v. 27, p. 2619-2632.

Roedder, E., 1971, Fluid inclusion evidence on the environment of formation of mineral deposits of the southern Appalachian Valley. Economic Geology, v. 66, p. 777-791.

Roedder, E., 1977, Fluid inclusion studies of ore deposits in the Viburnum Trend, southeast Missouri. Economic Geology, v. 72, p. 474-479.

Root, S., and Onasch, C.M., 1999, Structure and tectonic evolution of the transitional region between the central Appalachian foreland and interior cratonic basins. Tectonophysics, v. 305, p. 205-223.

Rowan, E.L. and Leach, D.L., 1989, Constraints from fluid inclusions on sulfide precipitation mechanisms and ore fluid migration in the Viburnum Trend lead district, Missouri. Economic Geology, v. 84, p. 1948-1965.

Rowan, E.L., and Goldhaber, M.B., 1995, Duration of mineralization and fluid flow history of the Upper Mississippi Valley zinc-lead district. Geology, v. 23, p. 609-612.

Sangster, D.F., Nowlan, G.S., and McCracken, A.D., 1994, Thermal comparison of

Mississippi Valley-type lead-zinc deposits and their host rocks using fluid inclusion and conodont color alteration index data. Economic Geology, v. 89, p. 493-514.

Schmidt, R.A., 1962, Temperature of mineral formation in the Miani-Picher district as indicated by liquid inclusions. Economic Geology, v. 57, p. 1-20.

Schmitt, R.A., Smith, R.H., and Olehy, D.A., 1964, Rare-earth yttrium and scandium abundances in meteoritic and terrestrial matter. Geochimica et Cosmochimica Acta, v. 28, p. 67-86.

Seyedolali, A., Boggs, S. Jr., and Krinsley, D., 1992, Trace element composition of quartz as a provenance indicator. Geological Society of America Abstracts with Programs, v. 24, No. 5, p. 80.

Sholkovitz, E. and Shen, G.T., 1995, The incorportion of rare earth elements in modern coral. Geochimica et Cosmochimica Acta, v. 59, p. 2749-2756.

Singer, A. and Muller, G., 1979, Diagenesis in argillaceous sediments: *in* Larson, G., and Chilingar, G.V., eds., Diagenesis in sediments and sedimentary rocks, v. 2, p. 115-212.

Sloss, L.L., 1988, Tectonic evolution of the craton in Phanerozoic time, in L.L. Sloss ed., Sedimentary cover- North American craton. Geology of North America, v. D-2, p. 25-51.

Smith, J.V., 1975, Some chemical properties of feldspars. Mineralogical Society of America Short Course Note 2; Feldspar Mineralogy, p. 18-29.

Spangenberg, J.E., Fontbote, L., and Macko, S.A., 1999, An evaluation of the inorganic and organic geochemistry of the San Vicente Mississippi Valley-type zinc-lead

district, Central Peru: Implications for ore fluid composition, mixing processes, and sulfate reduction. Economic Geology, v. 94, p. 1067-1092.

Spirakis, C.S., 1995, Problems with applying topographically driven flow to genesis of the Upper Mississippi Valley Zinc-Lead district and to fluid flow in the Illinois Basin. U.S. Geological Survey Bulletin, 2094-C, p. 1-12.

Spötl, C., Kralic, M., and Kunk, M.J., 1996, Authigenic feldspar as an indicator of paleo-rock/water interactions in Permian carbonates of the Northern calcareous Alps, Austria. Journal of Sedimentary Research, v. 66, p. 139-146.

Srinivasan, K., Riciputi, L.R., and Walker, K.R., 1994, REE geochemistry of Cambro-Ordovician Platform carbonates: implications for sources of diagenetic fluids. Geological Society of America – Abstracts with Programs, v. 26, No. 7, p. 130.

Sternbeck, J., Sohlenius, G., and Hallberg, R.O., 2000, Sedimentary trace elements as proxies to depositional changes induced by a Holocene fresh-brackish water transition. Aquatic Geochemistry, v. 6, p. 325-345.

Stix, J., and Gorton, M.P., 1990, Variations in trace element partition coefficients in sanidine in the Cerro Toledo Rhyolite, Jemez Mountains, New Mexico: Effects of composition, temperature, and volatiles. Geochimica et Cosmochimica Acta, v. 54, 2697-2708.

Sverjensky, D.A., 1981, The origin of a Mississippi Valley-type deposit in Viburnum Trend, southeast Missouri. Economic Geology, v. 6, p. 1848-1872.

Sverjensky, D.A., 1984, Oil field brines as ore-forming solutions. Economic Geology, v. 79, p. 23-27.

Sverjensky, D.A. and G. Garven, 1992, Tracing great fluid migrations. Nature, v. 356, p.

481-482.

Taylor, M., Kesler, S.E., Cloke, P.L., and Kelly, W.C., 1983, Fluid inclusion evidence for fluid mixing, Mascot-Jefferson City zinc district, Tennessee. Economic Geology, v. 78, p. 1425-1439.

Temmam, M., Paquette, J., and Vali, H., 2000, Mn and Zn incorporation into calcite as a function of chloride aqueous concentration. Geochimica et Cosmochimica Acta, v. 64, p. 2417-2430.

Tesoriero, A., and Pankow, J., 1996, Solid solution partition of Sr^{2+}, Ba^{2+}, and Cd^{2+} to calcite. Geochimica et Cosmochimica Acta, v. 60, p. 1053-1063.

Tunner, G., 1971a, Argon 40 – argon 39 dating: The optimization of irradiation parameters. Earth and Planetary Science Letters, v. 10, p. 227-234.

Tunner, G., 1971b, ^{40}Ar-^{39}Ar ages from the lunar maria. Earth and Planetary Science Letters, v. 11, p. 169-191.

Veizer, J., 1983, Chemical diagenesis of carbonates: Theory and application of trace element technique. In Arthur, M.A., Anderson, T.F., Kaplan, I.R., Veizer, J., and Land, L.S. eds., Stable Isotopes in Sedimentary Geology. Society of Sedimentary Geology (SEPM) Short Course 10, p. 3-1 – 3-100.

Viets, J.G. and Leach, D.L., 1990, Genetic implications of regional and temporal trends in ore fluid geochemistry of Mississippi Valley-type deposits in the Ozark region. Economic Geology, v. 85, p. 842-861.

Wadleigh, M.A., Longstaffe, F.J., Frape, S.K., McNutt, R.H., and McKenna, C., 1990, Diagenetic evolution of Cambro-Ordovician clastic sedimentary rocks, Southwestern Ontario. American Association of Petroleum Geologists Bulletin,

v. 74, p. 1312.

Walgenwitz, Z., Pagel, M., Meyer, A., Maluski, H., and Monie, P., 1990, Thermo-chronological approach to reservoir diagenesis in the offshore Angola Basin: a fluid inclusion, $^{40}Ar/^{39}Ar$ and K-Ar investigation. American Association of Petroleum Geologists Bulletin, v. 74, p. 547-563.

Warnock, A.C., Zeitler, P.K., and Van de Kamp, P.C., 1996, New $^{40}Ar/^{39}Ar$ ages on authigenic K-feldspar from the Fountain Formation near Eldorado Springs, Colorado. Geological Society of America Abstracts with Programs, v. 28, No. 7, p. 279.

Watson, E.B., 1996, Surface enrichment and trace-element uptake during crystal growth. Geochimica et Cosmochimica Acta, v. 60, p. 5013-5020.

Watt, G.R., Wright, P., Galloway, S., and McLean, C., 1997, Cathodoluminescence and trace element zoning in quartz phenocrysts and xenocrysts. Geochimica et Cosmochimica Acta, v. 61, p. 4337-4348.

Whitney, G. and Northrop, H.R., 1987, Diagenesis and fluid flow in the San Juan Basin, New Mexico - Regional zonation in the mineralogy and stable isotope composition of clay minerals in sandstone: American Journal of Science, v. 287, p. 353-382.

Williams, L.B., Hervig, R.L., and Bjorlykke, K., 1997, New evidence for the origin of quartz cements in hydrocarbon reservoirs revealed by oxygen isotope microanalyses. Geochimica et Cosmochimica Acta, v. 61, p. 2529-2538.

Williams, L.B., Hervig, R.L., and Dutton, S.P., 1997, Constraints on paleofluid compositions in the Travis Peak Formation, East Texas: evidence from

microanalyses of oxygen isotopes in diagenetic quartz. Society for Sedimentary Geology (SEPM) Special Publication 57, p. 269-280.

Worden, R.H., Coleman, M.L., and Matray, J-M., 1999, Basin scale evolution of formation waters: A diagenetic and formation water study of the Triassic Chaunoy Formation, Paris Basin. Geochimica et Cosmochimica Acta, v. 63, p. 2513-2528.

York, D., Hall, C.M., Yanase, Y., Hanes, J.A. and Kenyon, W.J., 1981, $^{40}Ar/^{39}Ar$ dating of terrestrial minerals with a continuous laser. Geophysical Research Letters, v. 8, p. 1136-1138.

Zhang, L., Liu, J., Zhou, H., and Chen, Z., 1989, Oxygen isotope fractionation in the quartz-water-salt system. Economic Geology, v. 84, p. 1643-1650.

Zimmerman, R.K., and Kesler, S.E., 1981, Fluid inclusion evidence for solution mixing, Sweetwater (Mississippi Valley-type) district, Tennessee. Economic Geology, v. 76, p. 134-142.

Appendix

Appendix 1 Record of analyses performed on Mount Simon Sandstone samples (marked with * if analyzed by that method)

Borehole ID	Depth (ft)	Depth (m)	Thin Section	Fluid Inclusion	Cathodoluminescence	$\delta^{18}O_{qtz}$	$\delta^{18}O_{Kfs}$	Trace Element	$^{40}Ar/^{39}Ar$
UPH -3 (Illinois)	1331	406	*	*					
	1368.4	417	*						
	1402.2	427							
	1874.2	571	*	*					
	2078.5	634	*	*		*		*	
	2131.1	650							
	2147	654	*		*	*	*	*	
	2176.5	663	*						
C3707 (Illinois)	1434.9	437							
	1449	442	*						
	1497.8	457	*				*	*	*
	1530	466	*						
C7466 (Illinois)	2577	785							
	2606	794	*	*			*		*
	2632	802	*	*		*			
C4389 (Illinois)	2360	719	*	*	*	*		*	
	2422	738							
	2558	780	*	*	*	*		*	
	2634	803	*	*	*	*	*	*	
C3904 (Illinois)	3281	1000							
	3283.3	1001							
	3290	1003	*	*	*		*		
	3312	1009	*	*	*	*		*	

BR-1 (Illinois)	3928.6	1197	*	*	*	*		*	
	3987.6	1215							
	5195.3	1584							
	4275.8	1303							
	4351.2	1326							
	4376	1334							
C13638 (Illinois)	4124.5	1257							
	4159.5	1268	*	*			*		*
	4182.7	1275	*	*					
	4187	1276							
	4215	1285	*	*	*	*		*	
C8948 (Illinois)	5152.8	1571	*	*					
	5167	1575							
	5170	1576	*						
	5199	1585	*						
	5201	1585	*						
C4831 (Illinois)	8464	2580							
	8468	2581	*	*					
	8469	2581	*	*	*	*	*	*	*
C415 (Indiana)	3895	1187							
	3934	1199	*						
	3953	1205	*	*					
C675 (Indiana)	4298	1310	*	*					
	4313	1315	*				*		*
	4331.5	1320							
	4346	1325	*	*					

C435 (Indiana)	2869	874							
	3074.5	937							
	3428	1045							
	3449	1051	*	*					
	3661	1116	*	*	*	*		*	
C250 (Indiana)	3351.5	1022	*	*	*	*		*	
	3456	1053							
	3521	1073	*	*	*	*	*	*	*
C437 (Indiana)	2860	872							
	2885	879							
	2908	886							
	2915	888	*	*			*		*
	2988	911	*	*					
C189 (Indiana)	5466.5	1666							
	5646.5	1721	*	*	*		*	*	*
	5777	1761							
	5826	1776	*	*	*	*		*	
CMS1 (Wisconsin)	outcrop		*	*			*		
CMS3 (Wisconsin)	outcrop		*	*			*	*	

Vita

Zhensheng Chen graduated from Nanjing University in 1989 with a M.S. in Geology. He worked as an Assistant Research Fellow and an Associate Research Fellow in the Chinese Academy of Geological Sciences, participating in six research projects on stable isotope geochemistry of fluid-rock interactions and mineral ore deposits. In 1996, he started a Ph.D. program in Geological Sciences at the University of Tennessee under the supervision of Dr. Claudia I. Mora. His career goal is to explore high-resolution, low-detection-limit analytical techniques and their applications to geochemistry, biochemistry, and environmental geology.